PREFACE

The method of photosensitization has been used to a considerable extent in recent years for the generation of free radicals and for the study of their subsequent reactions.

The present investigation is concerned with the mercury photosensitized decomposition of neopentane. The initial step in the reaction involves the formation of neopentyl radicals, and the technique therefore provides a convenient means of studying the unimolecular decomposition of these radicals. Widely different values of the activation energies for the decomposition of neopentyl radicals have been reported; one object of the present work has therefore been to obtain a reliable value.

A further object of the work has been to study the kinetics of the reactions of methyl radicals, which are produced in the process. In particular, a study has been made of hydrogen abstraction from neopentane by methyl radicals, and of the pressure dependence of the combination of methyl radicals.

ACKNOWLEDGEMENTS

This research was conducted under the direction of Professor K. J. Laidler, whose patience and constant readiness for valuable discussions is most gratefully acknowledged. I am also grateful for the interest shown and the assistance rendered by Professor Laidler in the shaping of this thesis.

With gratitude the author wishes to thank Drs. H. P. Schuchmann, M. M. Papic and J. Esser and Mrs. Mary Simon for many helpful suggestions concerning experimental problems and many useful discussions during the past few years.

TABLE OF CONTENTS

LIST OF FIGURES

LIST OF TABLES

ABSTRACT

The mercury-photosensitized decomposition of neopentane was investigated from 230°C to 335°C, and at pressures from 3 to 280 mm Hg. The following were identified as primary products and their initial rates of formation measured over a range of conditions: H_2, CH_4, C_2H_6, i-C_4H_8, neohexane and dineopentyl. The results are explained in terms of mechanism in which the primary step involves the split of neopentane into the neopentyl radical and H atom; neopentyl radicals then undergo further reactions including a split into i-C_4H_8 + CH_3. Estimates are made of the free-radical concentrations at various temperatures and pressures. A simplified steady-state treatment is worked out and is shown to explain the pressure dependence of the rates of formation of the various primary products.

A fall-off in the methyl radical combination was observed at low pressures. Comparison of this process with the CH_3 + neopentane hydrogen abstraction yields for the latter an activation energy of 11.5 kcal/mole and a frequency factor of 4.9×10^{11} cc $mole^{-1}$ s^{-1}. The relative importance of CH_3 + neopentyl and neopentyl + neopentyl is compared. The decomposition of the neopentyl radical into CH_3 + i-C_4H_8 shows a fall-off at low pressures; the limiting activation energy at high pressures is 29.0 kcal/mole, while that at low pressures is 17.1 kcal/mole. The former value leads

to 6.7 kcal/mole for the heat of formation of the neopentyl radical at 25°C, to 21.3 kcal/mole for the heat of its dissociation into i-C_4H_8 + CH_3 and to 98.5 kcal/mole for the heat of dissociation of neopentane into neopentyl + H. Entropy values are also calculated.

The following were identified as secondary products of the mercury-photosensitized decomposition of neopentane, and their maximal rates measured over a range of conditions: C_2H_4, C_3H_6, C_3H_8, i-C_4H_{10}, 2,2,3,3-tetramethylbutane and 2,2,4,4-tetramethylpentane. A mechanism is proposed which explains the kinetics of formation of these products. It involves the reaction of H atom with i-C_4H_8 formed as primary product; this leads to the formation of C_4H_9 which reacts further; one of its products is C_3H_6 which also reacts with H atoms.

CHAPTER I

INTRODUCTION

In systems where atoms and radicals are present, unimolecular, bimolecular and termolecular reactions occur.

Unimolecular reactions include the decomposition of a radical to give a H atom and an olefin, e.g.,

$$R \rightarrow H + Ol_1$$

or to give a radical and an olefin, e.g.,

$$R \rightarrow R' + Ol_2$$

The main factor governing such reactions is the bond dissociation energy of the decomposing radical.

A common type of bimolecular reaction is hydrogen abstraction from a molecule,

$$RH + X \rightarrow R + XH$$

where X can be an atom or a radical. Another type of bimolecular reaction is the combination or disproportionation of two radicals,

$$R + R \rightarrow R_2$$

$$R + R \rightarrow RH + Ol$$

In cases where olefin is present in addition to atoms and radicals, the addition of an atom or a radical to the double bond can be observed,

$$Ol + H \rightarrow R^*$$

where R^* is a radical having excess of energy.

In bimolecular reactions such as combinations and additions to the double bond two species produce one product, which carries away some excess of energy. This excess of energy is sufficient for the product to decompose unless it can lose its energy by collision or by distributing it among its internal degrees of freedom. In combination reactions in which atoms or small radicals are taking part, there is little possibility for the redistribution of energy, and reaction can take place only if the energized molecule is stabilized by another molecule. The reaction can then be said to occur by the termolecular mechanism

$$2R + M \rightarrow R_2 + M$$

In the addition of an atom or a radical to the double bond the resulting radical carries away a large excess of energy, and both C-C and C-H bond rupture can occur unless the radical is stabilized by collision with a molecule.

In the mercury-photosensitized decomposition of saturated hydrocarbons a hydrogen atom and a radical is formed in the initial act of the decomposition. In the case of neopentane the radical formed is the neopentyl radical. At higher temperatures the radical will decompose and produce the CH_3 radical and i-C_4H_8. The presence of H atoms and i-C_4H_8 leads to the formation of excited C_4H_9 radicals.

Thus in this system H atoms and neopentyl, CH_3 and excited C_4H_9 radicals will be present. It is therefore expected that all types of reactions mentioned above will take place in the system.

In the mercury-photosensitized decomposition of alkanes, the energy required for the decomposition is supplied by a low pressure mercury lamp. A direct collision of a photon with a molecule is ineffective unless light of short wave length, i.e., of high energy, is used. The presence of mercury vapor increases the efficiency. Light of 2537 A wave length is absorbed by an atom in the Hg (^1S_o) state, transforming it into the Hg ($^3P_1$) excited state. On collision with a molecule, the Hg ($^3P_1$) atom may be deactivated to Hg (^1S_o), with energy transferred to the molecule. According to the spin conservation rule, a possible way of decomposition is direct C-H bond scission, without an excited molecule being formed. An alkyl radical is thus formed directly in the initial act of decomposition. The collision of Hg ($^3P_1$) atom with a molecule has little temperature coefficient, so that an alkyl radical can be produced over a wide range of temperatures. The main aspects of the mercury-photosensitized decompositions of hydrocarbons were discussed by Steacie (1), Calvert and Pitts (2), Cvetanovic (3) and Gunning and Strausz (4).

This method is of great value in the study of the reactions of alkyl radicals. For example, the photosensitized

decompositions of methylether and ethane (5,6,7,8) have been studied, in order to obtain information on the decomposition of methoxymethyl and ethyl radicals respectively. Also, some information concerning hydrogen abstraction and combination reactions of radicals was obtained from these studies. In these investigations, the importance of light homogeneity with respect to the vapor pressure of mercury was realized; a homogeneous system is required to obtain reliable information. If a high vapor pressure of mercury is used, the light is absorbed at one end of reaction vessel, and in these regions high concentrations of alkyl radicals are present. The combination reactions of radicals will then predominate over hydrogen abstractions, and the results will be unreliable. The partial pressure of mercury must therefore be kept below a minimum value.

The vapor pressure of mercury affects also the degree of conversion in photosensitized decompositions; i.e., with the vapor pressure controlled, the conversion can be kept below a certain level, and complications due to secondary reactions can be avoided. An example of experiments at very low conversions is an investigation on the photosensitized decomposition of propane (9,10); that secondary reactions were eliminated was shown from the time-yield relations of the products (the concentrations of olefines as products were very low and quenching of H atoms by the olefines was insignificant). In this study, two

kinds of alkyl radicals (n-propyl and i-propyl) were formed in the initial act of decomposition and a complicated set of reactions of alkyl radicals is expected. The elimination of secondary reactions is therefore necessary in order to avoid difficulties in interpretation of data.

The neopentane molecule contains only one kind of C-H bond, and only one kind of alkyl radical will be formed in the initial act of decomposition. Another advantage is that there is only one way of the alkyl radical produced to decompose, namely into the CH_3 and $i\text{-}C_4H_8$. These facts mean that less restrictions is imposed on the degree of conversion; some secondary reactions may also occur without complicating the interpretation of the results.

Previous Investigations on the Photosensitized Decomposition of Neopentane

In an early study Darwent and Steacie (11) investigated the photosensitized decomposition of neopentane at pressures between 50 and 400 mm Hg, and between 25° and 200°C, in the presence and absence of hydrogen. They observed the reaction rate to be very low in the early stages of the experiment, and to increase with time to a much higher and approximately constant value. The reaction rate was expressed as the amount of non-condensables (H_2 + CH_4) produced during a certain period of time. The marked acceleration of the reaction in the later stages they attributed to the accumulation of hydrogen and/or dineopentyl, which were the main products in the decomposition study. Experiments in the presence of hydrogen showed that the rate is greatly accelerated by the addition of small amounts of hydrogen.

Experiments were carried out in which the reaction was stopped at a point where the rate has already increased; the non-condensable gases were then pumped off from liquid air and the reaction allowed to proceed. These studies showed that the rate of production of non-condensable gases in the second portion was equal to the final rate in the first portion of the experiment. From this observation it was concluded that dineopentyl was also responsible for acceleration of the rate. This conclusion could have been confirmed in experiments in which a certain amount of dineopentyl is

added to neopentane, as in experiments in the presence of hydrogen. However, this additional confirmation was not made.

Darwent and Steacie proposed the following mechanism for the decomposition:

$$\text{neo-}C_5H_{12} + Hg(^3P_1) \rightarrow \text{neo-}C_5H_{12}^* + Hg(^1S_o)$$

$$\text{neo-}C_5H_{12} + Hg(^3P_1) \rightarrow \text{neo-}C_5H_{11} + H + Hg(^1S_o)$$

$$\text{neo-}C_5H_{12} + H \rightarrow \text{neo-}C_5H_{11} + H_2$$

$$2\ \text{neo-}C_5H_{11} \rightarrow C_{10}H_{22}$$

$$\text{neo-}C_5H_{11} + H \rightarrow \text{neo-}C_5H_{12}^*$$

$$\text{neo-}C_5H_{12}^* + M \rightarrow \text{neo-}C_5H_{12} + M^*$$

$$\text{neo-}C_5H_{12}^* \rightarrow CH_3 + \text{t-}C_4H_9$$

It was believed that the initial act proceeds by both the direct C-H bond scission and the excited molecule formation, and the deactivation of the excited molecule is responsible for the extremely small quantum yield of hydrogen production (0.004 at 25°C). Comparison of the value with the then available quantum yields for some other hydrocarbons indicated that neopentane resembles methane in its behaviour, so that the symmetry of the hydrocarbon molecule plays an important role in its mercury-photosensitized decomposition; this is probably due to the long life of the excited molecule formed in the initial quenching act. However, the possibility of formation of an excited molecule in the initial act is ruled

out on the basis of the spin conservation rule and of several later experimental observations.

In view of the composition of non-condensable gases (e.g., the CH_4 content at 25°C and 103.3 mm Hg is 10.9%; that at 412.3 mm Hg is 3.8%) it is expected that the reaction of H atoms with neo-C_5H_{11} radicals plays a very important role in the inefficiency. The methane and also C_2 hydrocarbons found must arise from CH_3 radicals. It is unlikely that the CH_3 radicals can be produced at 25°C by decomposition of neo-C_5H_{11} radicals. Atomic cracking is the only possibility for production of CH_3 radicals. The observed content of CH_4 in non-condensable gases proves also that at such high pressures as 412 mm Hg the atomic cracking occurs despite the fact that it is expected to be negligible with respect to deactivation of excited neopentane molecules.

The mercury saturator in this study was kept at a temperature of 20°C. On the basis of a latter observation of Loucks and Laidler (5) concerning the inhomogeneity of light in relation to the pressure of mercury, it would seem likely that these experiments were carried out under conditions of light inhomogeneity, i.e., reaction occurred only at one side of the reaction vessel where high concentrations of H atoms and neo-C_5H_{11} radicals were present; combination reaction of H atoms and neo-C_5H_{11} radicals could therefore occur to a great extent. This is probably largely responsible for the extremely low quenching efficiency.

Another likely reason for the inefficiency is the presence in the reactant of some unsaturated hydrocarbons, which are able to scavenge H atoms. The neo-C_5H_{12} used was prepared by Grignard reaction between t-butyl chloride and methyl magnesium chloride, and there is some possibility that i-C_4H_8 is produced by H atom abstraction from t-C_4H_9 by CH_3 radicals.

Holroyd and Klein (12) investigated the identity of radicals produced from various hydrocarbons by mercury photosensitization. For the detection of the radicals they used labelled $C_2^{14}H_4$. The ethene added to the hydrocarbons scavenged H atoms present producing $C_2^{14}H_5$ radicals. In the case of neo-C_5H_{12}, the analysis of $C_4^{14}H_{10}$, which also arises from $C_2^{14}H_5$ radicals, was in the presence of large amounts of neopentane, which masked the butane region. Despite these difficulties, Holroyd and Klein realized that the quantum yield must be much higher than was determined by Steacie and Darwent (11). They also concluded that the back reaction, i.e.,

$$H + \text{neo-}C_5H_{11} \rightarrow \text{neo-}C_5H_{12}^*$$

must be important in the absence of scavengers.

The quantum yield of neopentane was reinvestigated by Gunning and his co-workers (12). The substrate used in this study was very carefully purified, and it is believed that no unsaturated hydrocarbons are present as impurities.

At a temperature of 25°C they found hydrogen and dineopentyl as major products. They detected also as a minor heavy product the mixture of cis and trans forms of 2,2,5,5-tetramethyl hexene-3.

Absorbed light intensity was measured by propane actinometry taking $\phi_{H_2} = 0.50$ at constant $\Delta H_2/\Delta t$ region at a propane pressure of 1000 torr. Under steady illumination the quantum yield for hydrogen production was 0.60 at a substrate pressure of 800 mm Hg. For the rotating sector runs the quantum yield rises with increasing pressure of reactant from 0.367 at 102 mm Hg, and appears to level off at 0.76 for a pressure of 1012 mm Hg. The exposure time in these experiments was 120 minutes, and an increase of the time caused the quantum yield to fall off fairly linearly. The relation between the yield and pressure was shown by plotting $1/\phi_{H_2}$ vs. 1/P. The function was linear and the value of ϕ_{H_2} obtained from extrapolation to $P = \infty$ was 0.87. The following initial steps were suggested for the mechanism (R = t-butyl):

$$RCH_3 + Hg(^3P_1) \rightarrow RCH_2 + H + Hg(^1S_o)$$

$$RCH_3 + H \rightarrow RCH_2 + H_2$$

$$2\ RCH_2 \rightarrow C_{10}H_{22}$$

$$RCH_2 + H \rightarrow RCH_3$$

A significant difference between the quantum yields of hydrogen and dineopentyl was observed, and it was realized that the heavy dineopentyl product is undergoing decomposition,

as indicated by the presence of the minor C-10 olefin detected. For the consumption of dineopentyl the following mechanism was assumed:

$$H + RCH_2CH_2R \rightarrow H_2 + RCHCH_2R$$

$$RCH_2 + RCH_2CH_2R \rightarrow RCH_3 + RCHCH_2R$$

$$RCH_2CH_2R + Hg(^3P_1) \rightarrow RCHCH_2R + H + Hg(^1S_o)$$

$$RCH_2 + RCHCH_2R \rightarrow RCH_3 + RCH{=}CHR$$

$$RCH_2 + RCHCH_2R \rightarrow (RCH_2)_2CHR$$

$$RCH{=}CHR + H \rightarrow RCHCH_2R$$

In the last reaction H atoms are scavenged by the olefin, resulting in a decrease of $\emptyset_{H_2}$.

On the basis of all these observations the authors concluded that neopentane shows no exceptional behaviour in the primary reaction with $Hg(^3P_1)$ atoms and closely resembles ethane, the primary quantum yield being close to unity.

Sato and Tsunashima (13) have investigated the mercury photosensitized decomposition of neopentane over the temperature range of 25° to 500°C. The main products below 250°C were hydrogen, i-C_4H_{10}, ethane and neohexane. Above 250°C the amounts of methane, i-C_4H_8, ethane and propylene markedly increased with increase of temperature. Propane was a minor product in all runs. It was observed that the amounts of i-C_4H_{10} and neohexane decreased with increase of temperature above 250°C. The curve relating the yield of hydrogen

produced and the temperature had an abnormal shape; the amount increased with temperature to a maximum at about 200°C, and later decreased with increase of temperature. For the formation of hydrogen and methane the following mechanism was proposed:

$$\text{Hg}^* + \text{neo-}C_5H_{12} \longrightarrow \text{Hg} + \text{neo-}C_5H_{12}$$

$$\text{Hg}^* + \text{neo-}C_5H_{12} \longrightarrow \text{Hg} + \text{neo-}C_5H_{11} + H$$

$$H + \text{neo-}C_5H_{12} \rightarrow \text{neo-}C_5H_{11} + H_2$$

$$H + \text{neo-}C_5H_{11} \rightarrow CH_3 + \text{t-}C_4H_9$$

$$CH_3 + \text{neo-}C_5H_{12} \rightarrow CH_4 + \text{neo-}C_5H_{11}$$

The apparent activation energy for hydrogen production was found to be 4.2 kcal/mole, similar to that of Darwent and Steacie (11). The authors also accepted the idea of physical quenching of excited Hg atoms by neopentane as the main reason for the low quantum yield of hydrogen.

Small amounts of propane were found below 150°C, and were attributed to atomic cracking of tert-butyl radicals produced by atomic cracking of neopentyl radicals:

$$H + \text{t-}C_4H_9 \rightarrow CH_3 + C_3H_7$$

$$C_3H_7 + \text{neo-}C_5H_{12} \rightarrow C_3H_8 + \text{neo-}C_5H_{11}$$

It was assumed that neo-C_5H_{11} radicals react at low temperatures, mostly by combination reactions:

$$2\ \text{neo-}C_5H_{11} \rightarrow C_{10}H_{22}$$

$$\text{neo-}C_5H_{11} + CH_3 \rightarrow C_6H_{14}$$

The increase of the rates of methane and $i\text{-}C_4H_8$ formation at temperatures above 200°C was attributed to the reaction

$$\text{neo-}C_5H_{11} \rightarrow CH_3 + i\text{-}C_4H_8$$

The amounts of hydrogen and $i\text{-}C_4H_8$ were not linear with time up to one minute below 300°C, while methane increased even at 400°C. This was explained by a much larger quenching cross section for hydrogen as compared with methane, and to the following reaction of $i\text{-}C_4H_8$:

$$H + i\text{-}C_4H_8 \rightarrow t\text{-}C_4H_9$$

To explain the marked increase of hydrogen at 500°C the next reaction is proposed

$$t\text{-}C_4H_9 \rightarrow i\text{-}C_4H_8 + H$$

At higher temperatures propylene was also observed and was believed to arise from the reaction

$$t\text{-}C_4H_9 \rightarrow i\text{-}C_4H_9 \rightarrow CH_3 + C_3H_6$$

For the evaluation of the activation energy for the decomposition of $\text{neo-}C_5H_{11}$ radicals the initial rates for methane and $i\text{-}C_4H_8$ production were used. For the decomposition of $\text{neo-}C_5H_{11}$ radicals an activation energy of 17 ± 2 kcal/mole was obtained. In the case of methane, the relation was not linear at low temperatures.

There is no mention of the temperature of the mercury saturator. However, the curvature at low temperatures of the plot of the logarithm of the rate of methane formation against the reciprocal of the temperature is caused by CH_3 radicals arising from atomic cracking, which seems to be important; also, in this work the experiments were probably carried out under conditions of light inhomogeneity. The activation energy obtained for the decomposition of the neo-C_5H_{11} radicals is out of the region of activation energies of alkyl radicals decompositions; this is probably due to the fact that the light was absorbed only at one side of the reaction vessel. Combination of CH_3 radicals is thus favored with respect to the hydrogen abstraction, and smaller amounts of methane are produced. Under such conditions combination of CH_3 with neo-C_5H_{11} radicals is also favored and more neohexane is formed. The evident decrease of methane production with increase of pressure is experimental confirmation of extensive atomic cracking in the system, and thus of the inhomogeneity of light absorption.

It is now well established (12) that there is no reason to suspect that there is some exceptional behavior of neopentane molecule in the initial quenching act with an excited atom of mercury. The quantum yield for hydrogen production is close to unity (12).

The decomposition study of Sato and Tsunashima (13) still accepts the idea of an extremely low quantum yield for

hydrogen production. Some of the reactions proposed here do not explain well the formation of certain products. There is no differentiation between the primary and secondary products.

In order to get more information about the mechanism it will be necessary to pay attention also to minor products and to find out the origin of their formation.

The photosensitized decomposition of neopentane was not used very successfully by Sato and Tsunashima for the study of the reactions of alkyl radicals. The activation energy for the decomposition of neo-C_5H_{11} radicals (14) is low. Also, no attempt was made to investigate other reactions of alkyl radicals occurring in the decomposition of neo-C_5H_{12}.

Neo-C_5H_{12} is quite a simple molecule compared with some lighter hydrocarbons. Despite this, not many investigations have dealt with it. A probable reason is the experimental difficulty of analytical separation of the most important primary product i-C_4H_8 and the secondary product i-C_4H_{10} from the substrate. Some restrictions are also expected concerning the pressure region used because of the vapor pressure of neopentane.

Other Studies on the Decomposition of Neopentane

The vacuum ultraviolet photolysis of neopentane was studied by Lias and Ausloos (15) at 1470 Å and 1236 Å. Using a mixture of neo-C_5H_{12}, neo-C_5D_{12} and NO, they found that all of the methane was either CH_4 or CD_4, so that it must have arisen from the molecular process

$$\text{neo-}C_5H_{12}^* \rightarrow CH_4 + (CH_3)_2C{=}CH_2$$

Mixed methanes are formed only in the absence of the radical scavenger, and indicate the presence of the radical reactions. In the presence of NO the yield of i-C_4H_8 was always larger than that of CH_4, and the following additional mode was postulated:

$$\text{neo-}C_5H_{12}^* \rightarrow H + CH_3 + (CH_3)_2C{=}CH_2$$

The propylene found in the photolysis of mixtures of neo-C_5H_{12} + neo-C_5D_{12} was only of C_3H_6 and C_3D_6 composition, indicating the occurrence of the alternative dissociative process:

$$\text{neo-}C_5H_{12}^* \rightarrow 2CH_3 + CH_3CH{=}CH_2$$

The CH_3 radical is the major radical produced in this system; this was confirmed by the presence of ethane as a major product in the absence of the free radical scavenger.

Anderson and Benson (16) have investigated the pyrolysis of neopentane in the presence of HCl. The products of the HCl-catalyzed reaction, CH_4 and i-C_4H_8, were identical

with those from the uncatalyzed pyrolysis. In both cases, there were very small amounts of C_2H_4 and C_2H_6. The amount of hydrogen was negligible. Engel and co-workers (17) proposed a very simple chain for the neopentane decomposition:

$$\text{Chain} \begin{cases} \text{neo-}C_5H_{12} \xrightarrow{i} (CH_3)_3C + CH_3 \\ \text{neo-}C_5H_{12} + CH_3 \xrightarrow{2} CH_4 + (CH_3)_3CCH_2 \\ (CH_3)_3CCH_2 \xrightarrow{3} (CH_3)_2C{=}CH_2 + CH_3 \\ 2\ CH_3 \xrightarrow{t} C_2H_6 \end{cases}$$

The concentration of neo-C_5H_{11} radicals is expected to be much lower than that of CH_3, so that only termination involving CH_3 radicals is important. In the presence of HCl the slow step 2 is replaced by:

$$CH_3 + HCl \underset{2a'}{\overset{2a}{\rightleftharpoons}} CH_4 + Cl$$

$$Cl + \text{neo-}C_5H_{12} \rightleftharpoons HCl + \text{neo-}C_5H_{11}$$

The HCl present produced an 8-fold acceleration of the rate. From the results these workers calculated $k_3 = 10^{3.3\pm0.3}$ sec.$^{-1}$ at 762°K. They estimated that log $A_3 = 13\pm1$ and $E_3 = 34\pm3.5$ kcal/mole, and for the reverse reaction $A_{-3} = 10^{7\pm1}$ liter/mole sec., $E_{-3} = 15\pm3.5$ kcal/mole. They tentatively concluded that thermodynamic and kinetic considerations favor the lower values, e.g., log $A_3 = 12.5$, $E_3 = 32$ kcal/mole, log $(A_{-3}) = 6$ and $E_{-3} = 13$ kcal/mole.

The pyrolysis of neo-C_5H_{12} was reinvestigated by Niclause and co-workers (18). The overall kinetic mechanism for the pyrolysis is:

$$\text{neo-}C_5H_{12} \rightarrow (CH_3)_3C + CH_3$$

$$(CH_3)_3C \rightarrow i\text{-}C_4H_8 + H$$

$$H + \text{neo-}C_5H_{12} \rightarrow H_2 + \text{neo-}C_5H_{11}$$

$$(CH_3)_3C + \text{neo-}C_5H_{12} \rightarrow i\text{-}C_4H_8 + \text{neo-}C_5H_{11}$$

$$\text{neo-}C_5H_{11} \rightarrow i\text{-}C_4H_8 + CH_3$$

$$CH_3 + \text{neo-}C_5H_{12} \rightarrow CH_4 + \text{neo-}C_5H_{11}$$

$$2\ CH_3 \rightarrow C_2H_6$$

As major products were analyzed methane and i-C_4H_8. Also, small amounts of hydrogen, ethane and 2 methyl-butene-1 and traces of i-C_4H_{10} were found. From the results the following rate constant for the decomposition of neo-C_5H_{12} is obtained:

$$k = 10^{16.8}\ \exp(-82/RT)\ \text{sec.}^{-1}$$

The initial rate constant of the overall reaction (order 3/2) is approximately:

$$k_o = 10^{13}\exp\left(-\frac{50{,}000}{RT}\right)\ \text{mole}^{-1/2}\text{ml}^{1/2}\text{s}^{-1}\ .$$

Tsang (19) studied the thermal decomposition of neo-C_5H_{12} in a single-pulse shock tube. The main reaction product was i-C_4H_8, and the ratio of CH_4 to i-C_4H_8 was about 0.6. Small amounts of ethane and propylene were also found. The ratio of the propylene to the i-C_4H_8 was less than 0.05.

From this study the rate constant for the decomposition of neo-C_5H_{12} into CH_3 and t-C_4H_9 radicals at 1100°K and 4 atm is:

$$k = 10^{16.1}\exp(-78.2/RT)\,sec^{-1}.$$

CHAPTER II

EXPERIMENTAL

Materials

The neopentane used was obtained from Phillips Petroleum Company with stated research grade purity 99.92% and was further purified, after thorough degassing, by distillation from methylene chloride slush (-97°C) to n-pentane slush (-132°C). The first and final third of the sample was rejected and only the middle third was stored and used in the investigation. Gas-chromatographic analysis of the purified sample showed no impurities in front of the neopentane peak, and only a very small peak (probably C_5) was observed on the tail of the neopentane peak. This peak changed only very little after one hour's irradiation at 335°C.

The 2,2,5,5-tetramethyl hexane (dineopentyl) and 2,2,4,4-tetramethyl pentane were obtained from the American Petroleum Institute as API Standard Samples and 2,2,3,3-tetramethyl butane was obtained from the Matheson-Coleman Co. These compounds were used for calibration of chromatograph without further purification. The 2,2-dimethyl butane (neohexane) was obtained from the Aldrich Chemical Company, and was subjected to purification by distillation before being used for calibrations of the chromatograph.

Apparatus

The investigations were carried out in a static system. The main parts of the apparatus are shown in Figure 1.

A cylindrical quartz reaction vessel was used; it had plane parallel windows at both sides, was about 9 cm in length and 5 cm in diameter, and its volume was 170 cc. The reaction vessel was placed in a cylindrical copper collar 14 cm in length; this was constructed from two half cylinders so that by joining them together the reaction vessel was inside the cylinder. In the walls of the cylinder were bored holes for thermocouples. The reaction vessel, before placed in the collar, was wrapped with asbestos paper. Also, the surface of the collar was covered with asbestos paper before being wound with resistance wire; the windings of the wire were placed along the whole length of the collar. The first layer of the windings was covered by asbestos paper and so isolated from the second, which was placed on in the same way as the first, and was again wrapped by asbestos and asbestos strings and placed in a box filled with asbestos flakes. In order to minimize temperature fluctuations the whole box was packed in glass wool.

The temperature in the reaction vessel was controlled by a thermoelectric temperature controller which was activated by means of a thermocouple placed in the wall of the collar and reaching the middle of the reaction vessel.

FIGURE 1

A schematic diagram of the apparatus

R.V.	Reaction vessel
F.	U.V. filter
L.	U.V. lamp
C.	Thermocouple
V.	Variac
T.	Trap
M.	Manometer
S.	Stopcock
D.	Mercury diffusion pump
T.P.	Toepler pump
Mc.	McLeod gauge
B.	Storage bulb

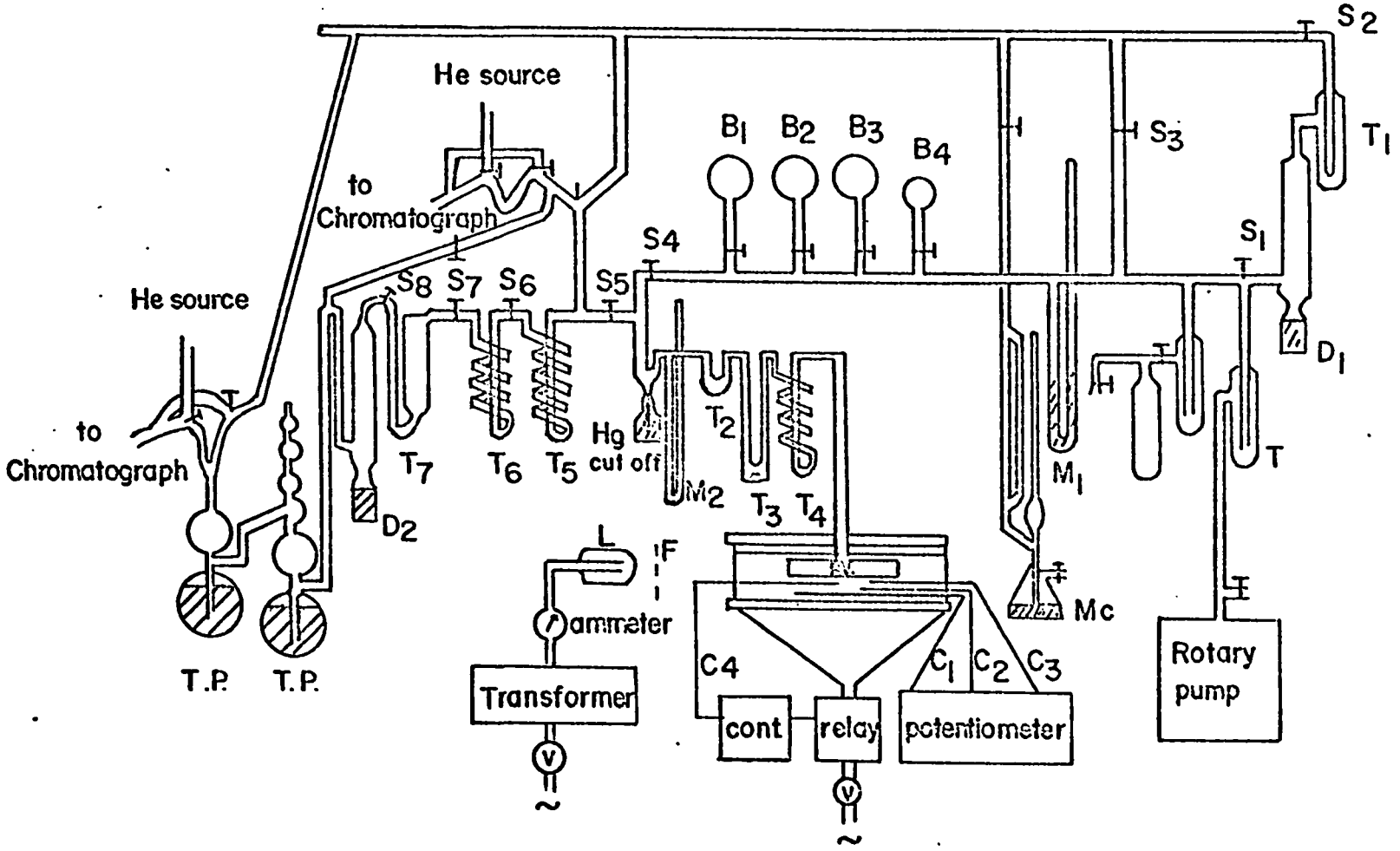
He source
to Chromatograph
He source
to Chromatograph
T.P.
T.P.
D2
T7
T6
T5
S8
S7
S6
S5
S4
Hg cut off
M2
T2
T3
T4
B1
B2
B3
B4
S3
S2
T1
S1
D1
T
M1
Mc
L
F
ammeter
Transformer
C4
C1
C2
C3
cont
relay
potentiometer
Rotary pump

The temperature of the reaction vessel was measured by means of a chromel-alumel thermocouple ($0^{\circ}C$ reference), connected to a Croydon Type P-3 potentiometer. Three thermocouples were used; they gave temperature at both sides and at the middle of the reaction vessel.

The lamp used was a low-pressure lamp emitting the characteristic line spectrum of mercury vapor with peak emission in the ultraviolet at 2537 A. The lamp was maintained at 25 cm from the window of the reaction vessel. The lamp was operating at room temperature and before each experiment was warmed up for 20 minutes. In order to eliminate the mercury 1849 A line a Corning glass color filter C.S. No. 9-54, which was non-transparent for the wavelengths shorter than 2000 A, was placed between the incident window of the reaction vessel and the source of light.

The concentration of mercury in the reaction vessel was controlled by the temperature of a spiral trap in the lead of the reaction vessel. The concentration of mercury was assumed to correspond to the equilibrium vapor pressure of mercury at the temperature of the spiral trap. In this work the temperature of the spiral trap was $-15.3^{\circ}C$.

The entire system could be evacuated to less than 10^{-5} mm Hg by means of an Edwards diffusion pump, which was in series with a liquid nitrogen trap and a Welch rotary pump. The residual pressure was measured with a McLeod gauge. All stopcocks were lubricated with silicone grease.

Procedure

A sample of neopentane, stored in a bulb covered by aluminum wrap, was admitted to the manifold which, like the whole apparatus, was evacuated to a pressure of 10^{-5} mm Hg. The sample was then trapped in a U-tube in the lead to the reaction vessel. The reaction system was then separated from the other part of the apparatus by closing the mercury cut-off, and the neopentane was allowed to expand into the reaction zone. On its way to the reaction vessel the neopentane was saturated with mercury vapor in the mercury saturator, which was kept at $0^{\circ}C$. The vapor pressure of mercury in the reaction system was controlled by the temperature of the spiral trap, which was placed after the mercury saturator and was kept at $-15.3^{\circ}C$.

Special attention was paid to the vapor pressure of mercury. At all times when the experiments were not being carried on, the mercury saturator was kept at the temperature of liquid nitrogen ($-196^{\circ}C$) in order to condense the main part of the mercury remaining in the reaction vessel and so to avoid an excess of mercury during the experiments.

The lamp used was switched on at least 20 minutes before each experiment. The reaction was started with the removal of the shutter placed between the lamp and the window of the reaction vessel, and was stopped by switching off the lamp. The reaction products and the remaining neopentane were trapped from the reaction zone into the U-tube which

was immersed in liquid nitrogen and then underwent the analysis.

Analysis

The products of reaction were separated into three fractions: (1) non-condensables, (2) condensables at -196°C (liquid nitrogen), (3) condensables at -97°C (methylene chloride slush). In order to prevent losses of C_2 hydrocarbons, the solid nitrogen trap (at -210°C) was used in series with the liquid nitrogen trap. The non-condensable products, which comprised hydrogen and methane, were collected using the Toepler pump (the pumping lasted 30 minutes). The fraction (2) condensables comprised ethane, i-C_4H_8 and 2,2-dimethyl butane (neohexane) as primary products, and ethylene, propylene, propane and i-C_4H_{10} as secondary products. Fraction (3) comprised 2,2,5,5-tetramethyl hexane (dineopentyl) as primary product and 2,2,3,3-tetramethyl butane and 2,2,4,4-tetramethyl pentane as secondary products. In analyses of the high boiling products contained in fraction (3), special precautions were taken; for example, in order to prevent loss of products, the tubing in the lead to the reaction vessel was carefully heated by a small flame.

The volume of the non-condensables was first measured in the gas burette; they were then analyzed chromatographically using a 6 m long column filled with 80-100 mesh Porapak Q operating at 0°C. The fraction (2) was analyzed

on an 8.5 m long column of 30% Squalane on 60-80 mesh Chromosorb P operating at 30°C. By the use of this column the main analytical problem could be solved, i.e., good separation of i-C_4H_8 and i-C_4H_{10} was achieved, and both these products had a shorter retention time than neopentane so that neither of them was covered by the peak of the reactant. In the case of the product neohexane, the height measurement could not yield a good calibration curve so that only the area of the peak was measured. As far as other products are concerned the measurement of height gave good calibration curves. For ethylene and propane accurate analyses were obtained only in these experiments where sufficient amounts of these products were formed, i.e., in high-conversion experiments. The fraction (3) was analyzed on an 0.5 m long column of 30% Squalane on 60-80 mesh Chromosorb P. For all these products only the peak area was measured. All columns used were 1/4 inch in diameter.

The gas chromatograph used was assembled from commercially available units. The detector used was of a thermistor type and was maintained at 30°C. The detector was supplied from 6 batteries of 1.5 V (Mallory - M 900) connected in series. The output used was 8 V d.c. and the current through the filament of the detector was 200 mA. The signal from the detector was put through a 10 mV Leeds and Northrup Speedomax Type G recorder.

A good baseline was obtained by installing Edwards pressure controllers in both the reference flow and the sensing flow of the chromatograph. Since the thermal conductivity detector measures the differential conductivity between a carrier gas and a mixture of solute in the carrier gas, it is obvious that the greatest sensitivity will be obtained when the carrier and the solute have widely differing conductivities. Since most products have low conductivities, a carrier gas of high conductivity should be used. Helium was chosen as carrier gas in all cases. However, the determination of hydrogen in helium sometimes poses a problem, because the thermal conductivity of hydrogen is higher than that of helium and a negative peak should result. In actual fact, at low concentrations the thermal conductivity of hydrogen appears to be lower than that of helium. It therefore gives a positive peak like those for other products. Fortunately, the amounts of hydrogen produced in the present study were small and the response peak was sufficiently linear and reproducible.

CHAPTER III

PRIMARY REACTIONS

RESULTS AND OBSERVATIONS

In this study a compromise had to be made between the temperature of the mercury saturator and the light homogeneity in the reaction vessel. It was originally intended that the temperature of the mercury saturator should be -32°C, but the highest reactant pressure that could then be used was 108 mm Hg. At 0°C it was possible to use a maximum reactant pressure of 530 mm Hg; however, the region of light inhomogeneity was approached. As a compromise the work was done at a saturator temperature of -15.3°C at which the vapor pressure of neopentane is 280 mm Hg.

At this temperature of the mercury saturator, several runs were done to find the maximum temperature of the reaction system at which the rate became independent of the pressure. It was found that the highest temperature of the reaction system at which the rate of methane formation attains a constant value, is 310°C. It was originally intended that this temperature should be the highest used in the study, but it was later found necessary to work up to 335°C. At a temperature of 230°C no measurable amount of ethane was formed; at 256°C an accurate rate of ethane formation could be measured only at higher pressures. In order to obtain more

complete information concerning the pressure dependence of the combination of CH_3 radicals, and to obtain some parameters for the hydrogen abstraction by CH_3 radicals, the experiments were carried out also at a temperature of 335°C. Unfortunately, at this temperature the region of constant rate of methane production was not reached.

As primary products were analyzed: hydrogen, methane, ethane, i-C_4H_8, neohexane (2,2-dimethyl butane) and dineopentyl (2,2,5,5-tetramethyl hexane). Over the whole temperature region only the amounts of H_2, CH_4, i-C_4H_8 and neohexane were measured. As was mentioned above, no measurable amounts of ethane were found at a temperature of 230°C. Dineopentyl was observed only at the temperatures of 230°C and 256°C; at 230°C only an approximate rate of production could be obtained. At the temperature of 286°C dineopentyl was detected only in small amounts at high conversions.

The highest pressure used is 280 mm Hg, which is the vapor pressure of neopentane at the temperature of the mercury saturator (-15.3°C). In the low-pressure region the accuracy of the analysis was limited. At temperatures of 230°C and 256°C, the experiments were not carried out at pressures below 16 and 10 mm Hg respectively, because of inaccurate analysis. At higher temperatures sufficient amounts of methane, ethane and i-C_4H_8 were also produced at pressures below 10 mm Hg, so that accurate analyses were obtained. The chromatograph used in this work was not

sensitive enough to hydrogen, so that this product could not be analyzed at low pressures.

In Figure 2 are shown the yield-time curves for all primary products at 286°C, except for dineopentyl which was studied at a temperature of 256°C. It is seen that the curves are linear only at very low conversions, and that later the effect of secondary reactions is evident. This means that to get an accurate initial rate, attention has to be paid to the linear region, i.e., to the low-conversion experiments. The rates of production of primary products are listed in Table I.

Production of Hydrogen

Typical hydrogen yield-time curves are shown in Figures 3 and 4. At low conversions the curves are linear, while at high conversions deviations from linearity are observed. The length of the linear region decreases with increase of temperature, as is shown in Figures 3 and 4, because of increase of the concentration of i-C_4H_8 with increase of temperature, i.e., because of more extensive removal of H atoms by i-C_4H_8. The initial rates were obtained from the slopes in the linear region.

The chromatograph used had not sufficient sensitivity to hydrogen, so that the evaluation of initial rates was inaccurate at pressures below 10 mm Hg at temperatures

FIGURE 2

Yield-time curves for primary products at a temperature of 286°C and a pressure of 112 mm Hg.

A methane

B $i\text{-}C_4H_8$

C dineopentyl*

D hydrogen

E neohexane

F ethane

*Taken at temperature of 256°C

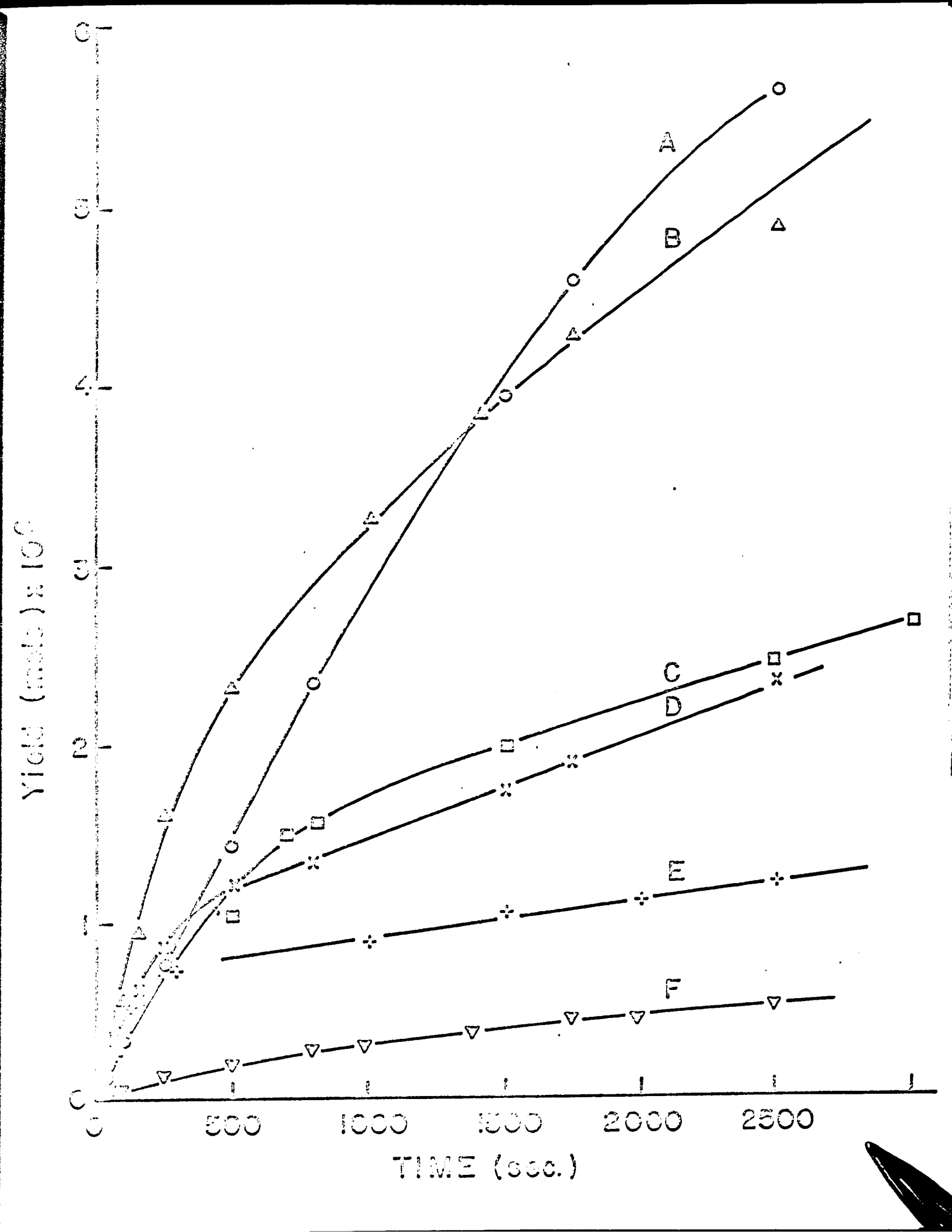
Yield (mole) x 10^6
0
2
4
6
8
0
500
1000
1500
2000
2500
TIME (sec.)
A
B
C
D
E
F

TABLE I

Rates of production of hydrogen, methane, ethane and i-C_4H_8 at different pressures and temperatures

Temperature °C	Pressure mm Hg	$v_3 \times 10^{12}$	$v_4 \times 10^{12}$ mole cc^{-1}	$v_6 \times 10^{12}$ sec^{-1}	$v_8 \times 10^{12}$
230	18	22.5	0.145	3.1	n.m.
230	36	27.4	0.375	4.12	n.m.
230	52	29.5	0.675	4.36	n.m.
230	70	32.9	0.74	5.30	n.m.
230	104	37.5	1.20	5.88	n.m.
230	136	37.3	1.78	6.03	n.m.
230	170	38.7	2.08	6.45	n.m.
230	206	38.1	2.08	6.71	n.m.
230	240	38.1	2.17	6.65	n.m.
230	260	38.7	2.11	6.84	n.m.
230	280	37.6	2.25	6.85	n.m.
256	6	n.d.	0.475	4.05	0.765
256	10	10.5	0.58	5.42	0.91
256	17	17.5	1.18	8.01	0.93
256	27	20.1	1.37	8.83	0.94

TABLE I (cont'd)

Temperature °C	Pressure mm Hg	$v_3 \times 10^{12}$	$v_4 \times 10^{12}$ mole cc^{-1}	$v_6 \times 10^{12}$ sec^{-1}	$v_8 \times 10^{12}$
256	40	22.1	2.53	10.2	0.895
256	57	28.4	3.82	14.0	0.89
256	77	31.4	4.7	15.3	0.91
256	110	35.0	6.6	20.2	0.893
256	152	37.3	8.5	21.5	0.89
256	190	37.3	10.8	21.8	0.90
256	225	36.5	10.7	22.4	0.67
256	261	36.1	10.7	22.8	0.57
256	275	36.5	10.7	22.4	0.51
286	4	n.d.	0.8	8.5	1.91
286	6	n.d.	1.3	15.6	2.94
286	9	8.5	2.05	18.0	3.51
286	17	17.1	3.51	23.1	3.72
286	27	20.2	5.7	26.1	3.69
286	40	23.6	9.3	42.0	3.69
286	50	28.1	10.8	43.9	3.72

TABLE I (cont'd)

Temperature °C	Pressure mm Hg	$v_3 \times 10^{12}$	$v_4 \times 10^{12}$ mole cc^{-1}	$v_6 \times 10^{12}$ sec^{-1}	$v_8 \times 10^{12}$
286	77	30.5	17.4	48.8	3.75
286	112	33.0	26.4	61.3	3.70
286	150	35.8	36.5	75.0	3.72
286	190	35.2	39.4	80.3	3.69
286	230	35.7	41.2	80.1	3.34
286	262	37.0	41.8	80.1	2.59
286	280	35.9	41.2	80.9	2.05
310	3	n.d.	1.5	20.1	2.25
310	5	n.d.	2.5	23.0	3.80
310	7	n.d.	4.1	32.1	6.00
310	9.5	n.d.	6.1	31.3	8.60
310	12	n.d.	7.4	40.4	9.77
310	16	14.0	9.1	45.2	11.5
310	24	19.5	14.3	56.2	11.25
310	40	25.5	23.2	74.4	11.7
310	54	31.2	33.9	80.9	11.3

TABLE I (cont'd)

Temperature °C	Pressure mm Hg	$v_3 \times 10^{12}$	$v_4 \times 10^{12}$ mole cc^{-1}	$v_6 \times 10^{12}$ sec^{-1}	$v_8 \times 10^{12}$
310	75	34.6	54.5	100.5	11.6
310	115	37.8	68.6	120.4	11.5
310	153	38.5	88.4	141.0	11.7
310	195	37.3	108.2	152.0	10.5
310	232	37.9	115.0	163.0	10.1
310	260	38.5	116.0	174.9	8.7
310	280	39.3	116.0	177.0	7.1
335	3	n.d.	3.6	26.2	4.8
335	5	n.d.	6.0	31.9	6.6
335	6.5	n.d.	6.5	40.0	7.5
335	9	n.d.	7.6	50.5	9.2
335	12	n.d.	12.8	56.2	12.9
335	18	n.d.	18.7	63.5	14.7
335	28	23.3	27.4	75.2	21.1
335	40	27.1	41.2	99.2	24.7

TABLE I (cont'd)

Temperature °C	Pressure mm Hg	$v_3 \times 10^{12}$	$v_4 \times 10^{12}$ mole cc^{-1}	$v_6 \times 10^{12}$ sec^{-1}	$v_8 \times 10^{12}$
335	56	35.2	75.7	128.0	26.0
335	81	37.6	93.8	171.5	25.9
335	115	39.8	158.6	230.2	26.5
335	151	40.5	182.5	250.4	26.4
335	192	39.4	230.0	288.0	25.1
335	245	38.5	272.7	343.0	24.4
335	280	40.1	306.0	389.0	20.2

n.m. - not measurable

n.d. - not determined

v_3 - rate of production of hydrogen

v_4 - rate of production of methane

v_6 - rate of production of iso-butene

v_8 - rate of production of ethane

FIGURE 3

Yield-time curves for production of hydrogen at 256°C and at different pressures.

A 225 mm Hg

B 110 mm Hg

C 27 mm Hg

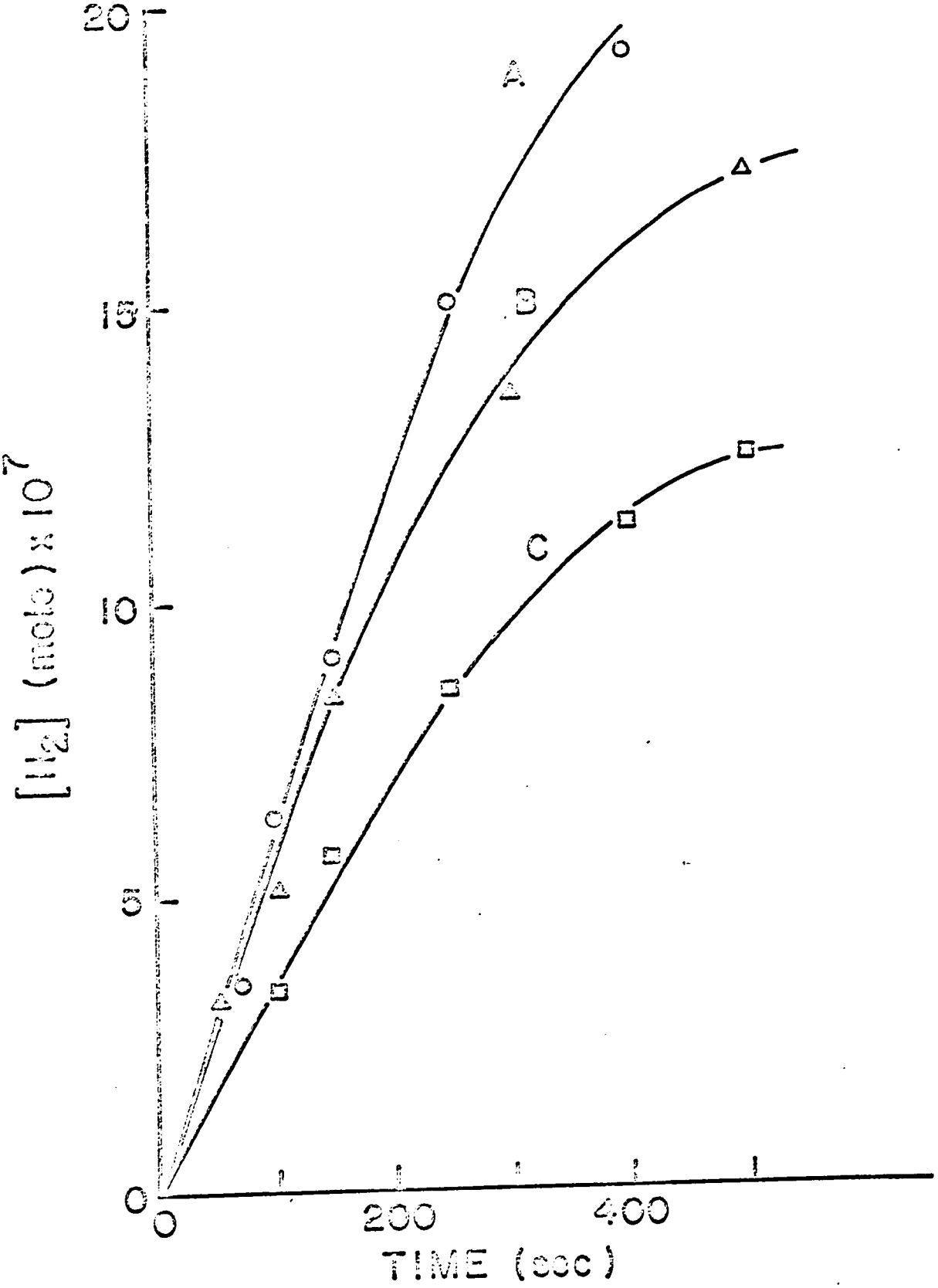
20
15
10
5
0
0
200
400
TIME (sec)
[H2] (mole) x 10^7
A
B
C

FIGURE 4

Yield-time curves for production of hydrogen at 286°C and at different pressures.

A 230 mm Hg

B 112 mm Hg

C 40 mm Hg

20
15
10
5
0
0
200
400
TIME (sec)
$[H_2]$ (mole) x 10^7
A
B
C

of 230° and 256°C, and at pressures below 25 mm Hg at temperatures of 310°C and 335°C.

The relation between the initial rate and pressure is shown in Figure 5. The initial rate increases with pressure and becomes constant at pressures above 100 mm Hg. The rate of hydrogen production shows no temperature dependence within the experimental errors.

A double logarithmic plot of the initial rate against the pressure is shown in Figure 6. The reaction order with respect to reactant changes from 1.0 at low pressures to zero at high pressures.

Production of Methane

Typical methane yield-time curves are shown in Figure 7. The yields are found to be linear with respect to time, indicating that true initial rates were measured. The effect of secondary reactions is evident only at very high conversions. The initial rates were obtained from slopes of the straight lines, the slopes being divided by the volume of the reaction vessel. The rates for different temperatures and pressures are listed in Table I.

The plots of the rates against the pressure are shown in Figure 8. The rates increase with pressure, attaining constant values. At the temperature of 230°C the rates are constant at pressures of above 120 mm Hg, at 256°C above

FIGURE 5

The plot of rate of hydrogen production against pressure at different temperatures.

ooo	335°C
▫▫▫	310°C
xxx	286°C
ΔΔΔ	256°C
▽▽▽	230°C

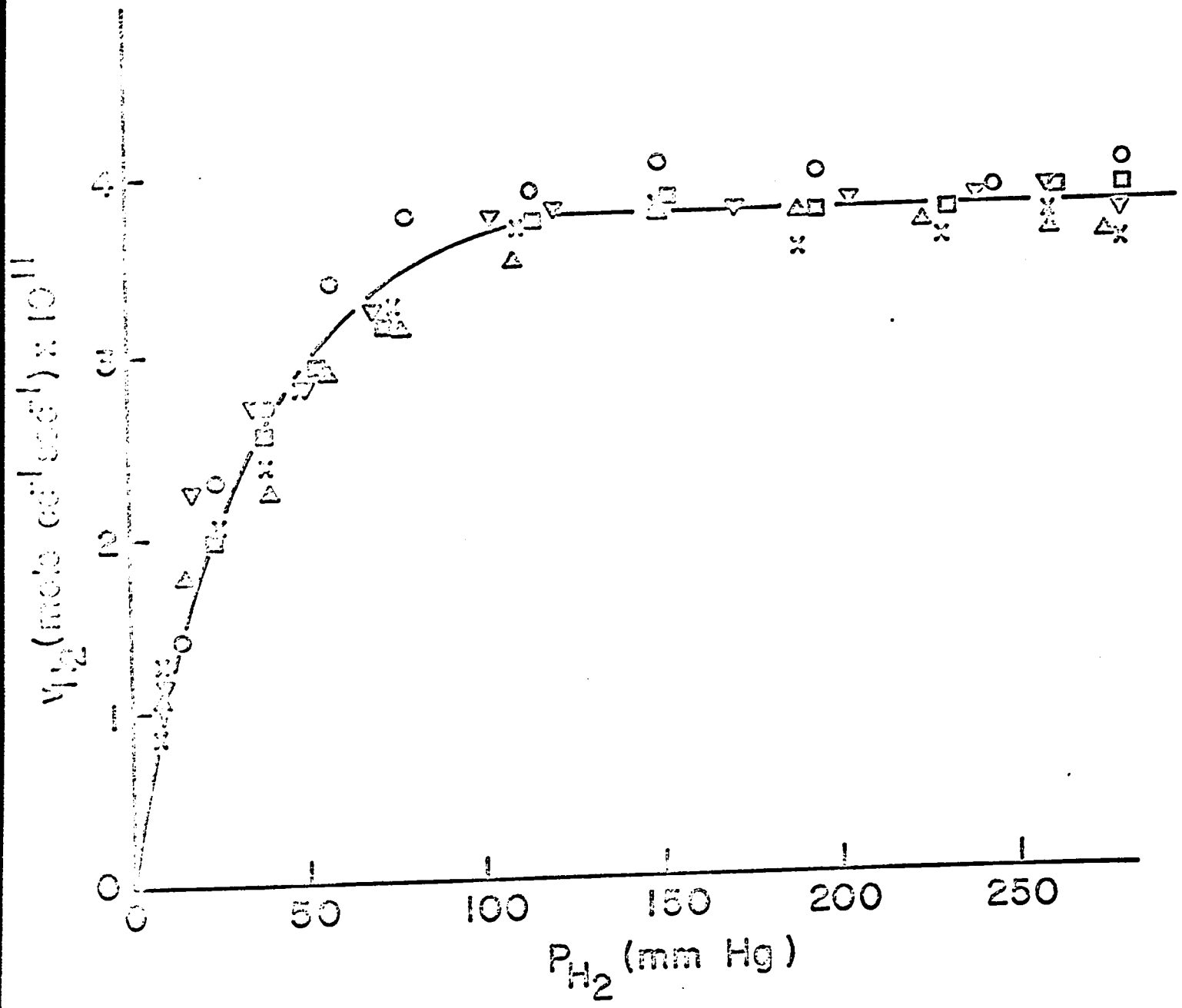
V_{H_2} (moles cm^{-2} sec^{-1}) x 10^{11}
0
2
4
0
50
100
150
200
250
P_{H_2} (mm Hg)

FIGURE 6

Order plot for hydrogen production.

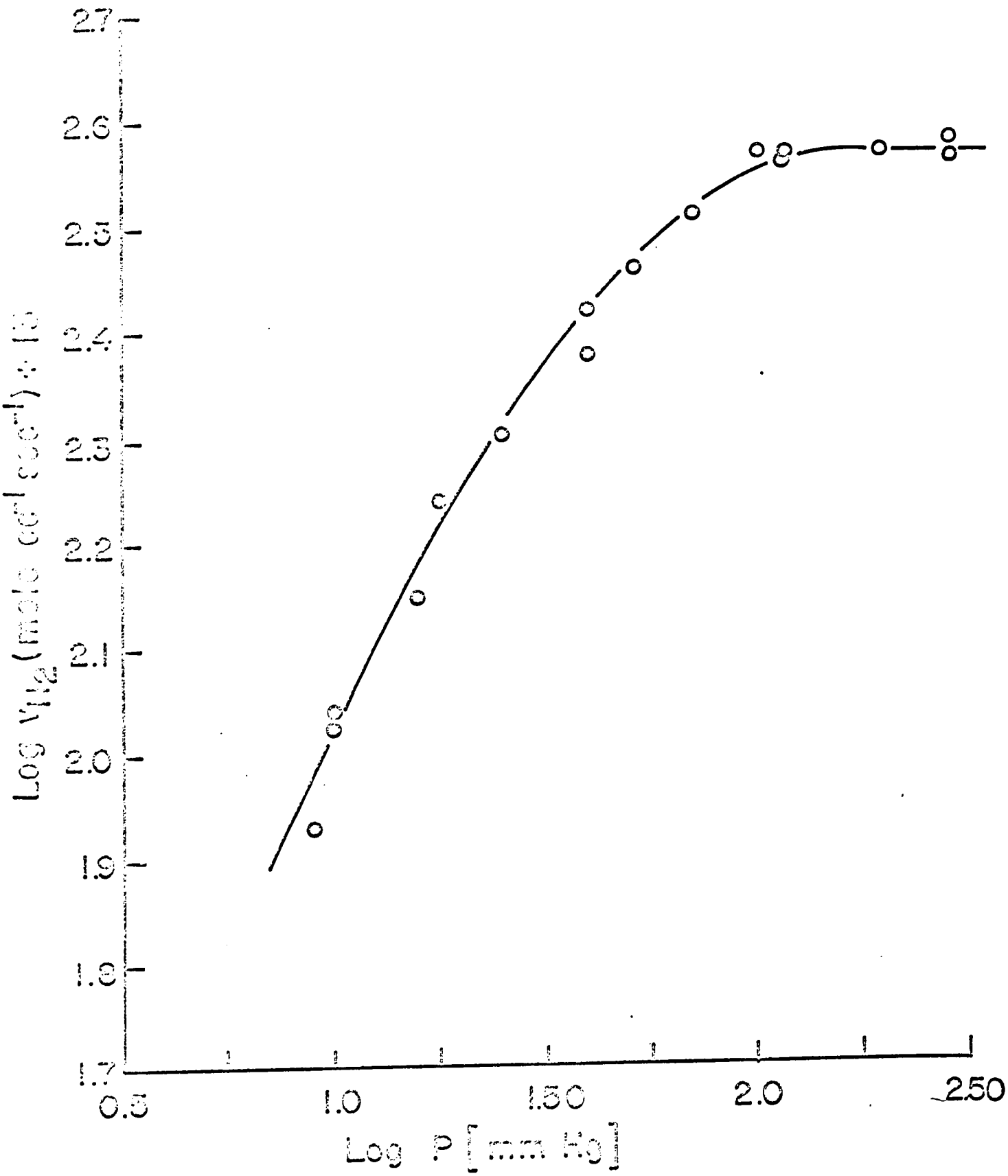
Log v_{H_2} (mole cm^{-1} sec^{-1}) x 10
2.7
2.6
2.5
2.4
2.3
2.2
2.1
2.0
1.9
1.8
1.7
0.5
1.0
1.50
2.0
2.50
Log P [mm Hg]

FIGURE 7

Typical yield-time curves for methane at different temperatures and pressures.

A	232 mm Hg	310°C
B	230 mm Hg	286°C
C	40 mm Hg	310°C
D	225 mm Hg	256°C
E	40 mm Hg	286°C
F	40 mm Hg	256°C

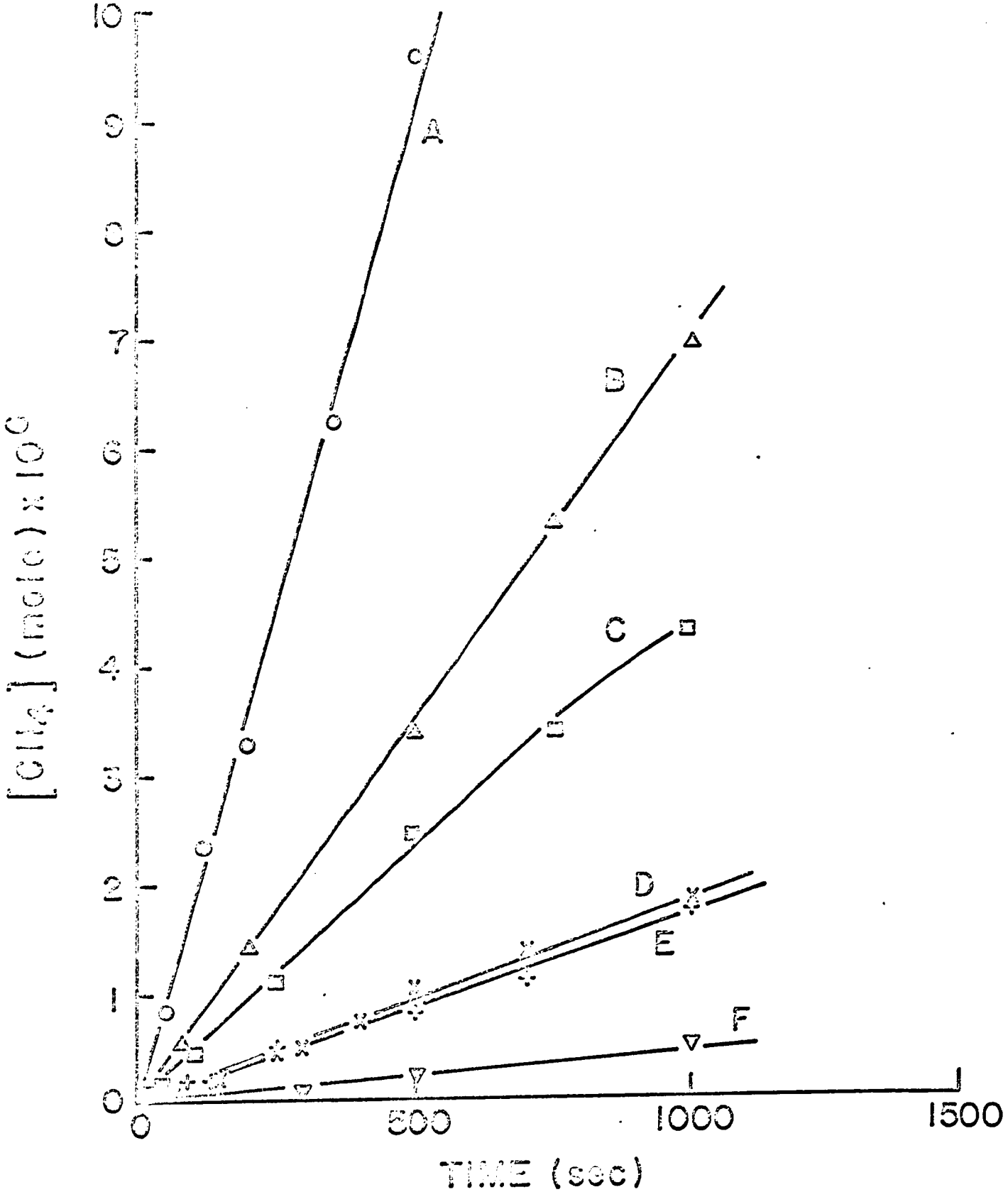
[CH4] (mole) x 10^6
TIME (sec)
0
1
2
3
4
5
6
7
8
9
10
500
1000
1500
A
B
C
D
E
F

FIGURE 8

Rates of methane formation plotted against pressure at different temperatures.

A 310°C

B 286°C

C 256°C

D 230°C

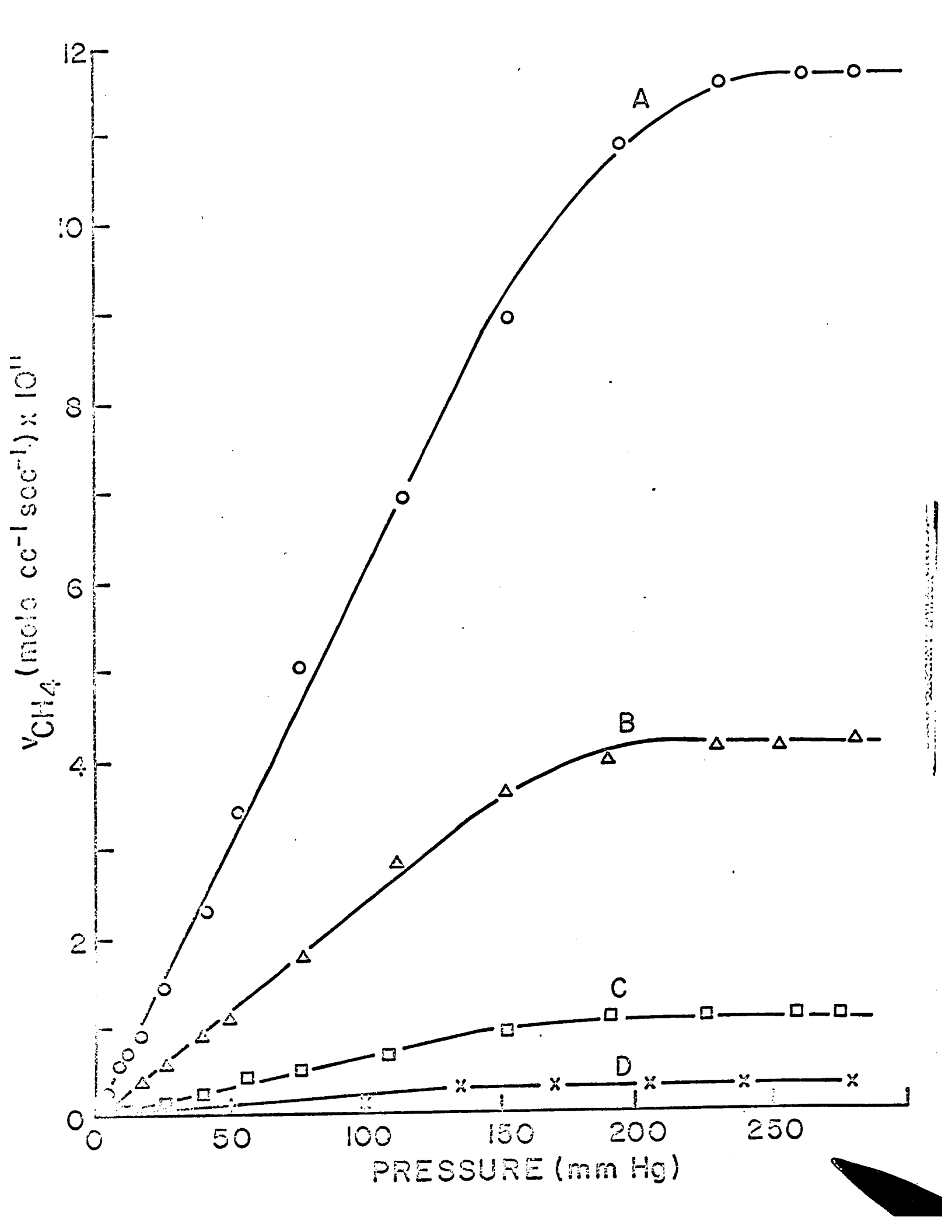
12
10
8
6
4
2
0
0
50
100
150
200
250
A
B
C
D
PRESSURE (mm Hg)
v_{CH_4} (mole cc^{-1} sec^{-1}) x 10^{11}

150 mm Hg, at 286°C above 190 and at 310°C above 230 mm Hg. At the temperature of 335°C, the region of constant rate was not attained and the results for this temperature are not shown in Figure 8.

Double logarithmic plots of rate against pressure are shown in Figure 9. The reaction order with respect to pressure of reactant changes from 1.0 at low pressures to zero at high pressures.

A plot of the logarithm of the rate against the reciprocal of the temperature is shown in Figure 10. The rates are taken at 280 mm Hg and resulting activation energy is 28.8 kcal/mole.

Production of Ethane

A typical ethane yield-time relation is shown in Figure 11. The yield is at first a linear function of time, and later it deviates from linearity. The initial rates were obtained from the slopes in the linear region. At low pressures, where the linear region was not large, the lines were extrapolated to higher conversions and the slope of this line divided by volume of the reaction vessel was taken as the initial rate. The values of the rates for different temperatures and pressures are listed in Table I.

At 230°C no measurable amount of ethane was detected. At 256°C sufficient amounts of ethane were formed only at higher pressures, despite the fact that the chromatograph had a high enough sensitivity to ethane.

FIGURE 9

Order plots for methane at different temperatures.

A 335°C

B 310°C

C 286°C

D 256°C

E 230°C

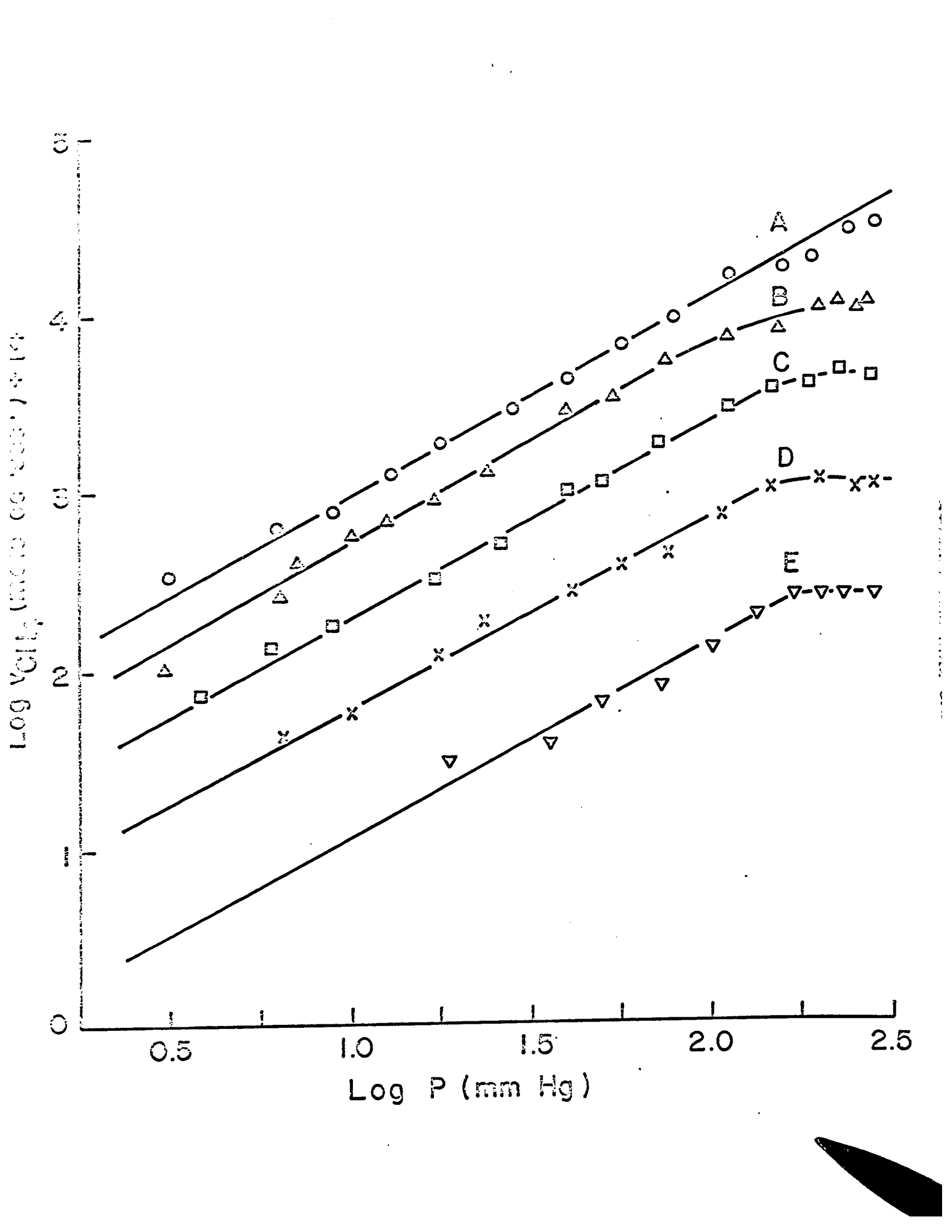
A
B
C
D
E
0.5
1.0
1.5
2.0
2.5
Log P (mm Hg)

FIGURE 10

Logarithm of the rate of methane production (at 280 mm Hg) against the reciprocal of the temperature.

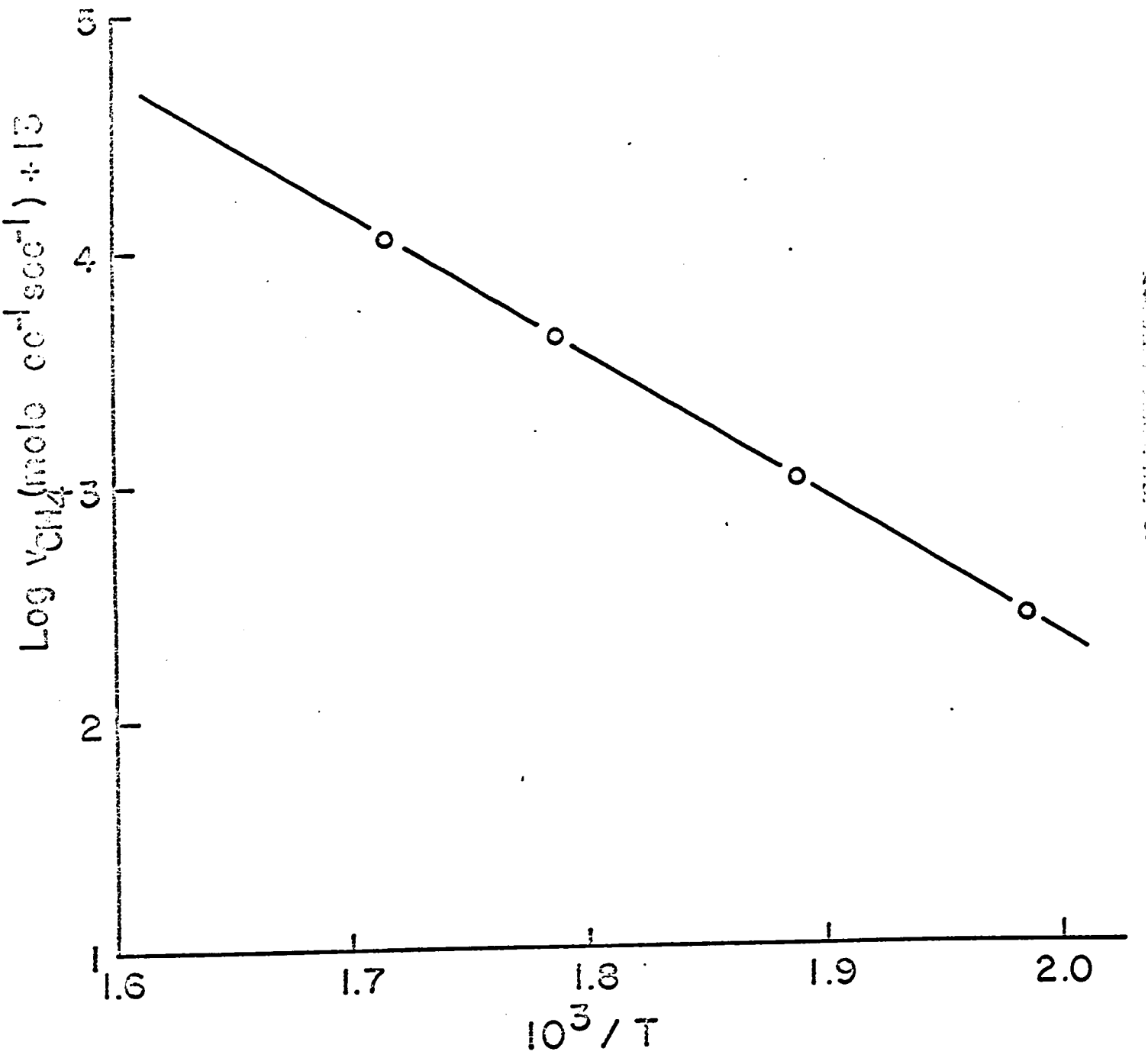
Log v_{CH_4}(mole cc^{-1}sec^{-1}) + 13
5
4
3
2
1
1.6
1.7
1.8
1.9
2.0
10^3 / T

FIGURE 11

Ethane yield-time relation.

A	310°C	115 mm Hg
B	310°C	9.5 mm Hg
C	310°C	280 mm Hg
D	286°C	112 mm Hg
E	286°C	6 mm Hg

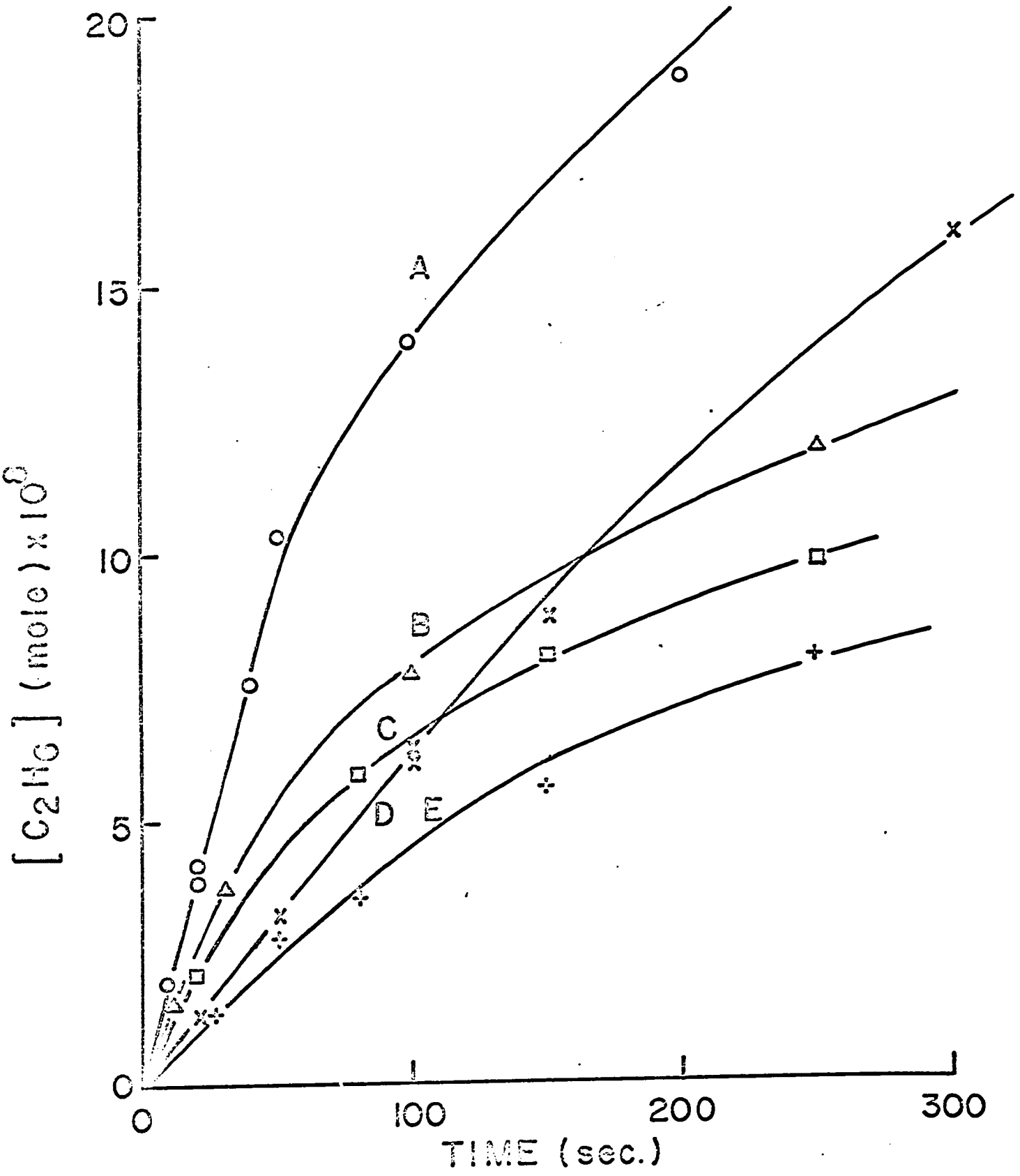
20
15
10
5
0
0
100
200
300
TIME (sec.)
[C2H6] (mole) x 10^8
A
B
C
D
E

The relation between the rates and the pressures is shown in Figure 12. The rate increases with increase of pressure, until the region of constant rate is attained and another increase of pressure causes the rate to decrease. Some aspects of this observation will be discussed later.

A double logarithmic plot of the rate against the pressure of reactant is shown in Figure 13, which shows only results at temperatures of 310°C and 335°C, where it was possible to extend the measurements of the rates to low pressures. The reaction order for ethane with respect to pressure of reactant changes from 1.0 at low pressures to zero at high pressures.

The relation between the logarithm of the initial rate against the reciprocal of temperature is shown in Figure 14. The rates were taken at pressures of 110 mm Hg. The activation energy from the slope attains a value of 28.8 kcal/mole.

Production of Iso-Butene

A typical i-C_4H_8 yield-time relation is shown in Figure 15. The relation is linear at low conversions, but later deviates from linearity due to secondary reactions which i-C_4H_8 undergoes. The initial rates were obtained from the slopes in the linear region. The rates at different temperatures are listed in Table I.

FIGURE 12

Rate of ethane production against pressure.

A 335°C

B 310°C

C 286°C

D 256°C

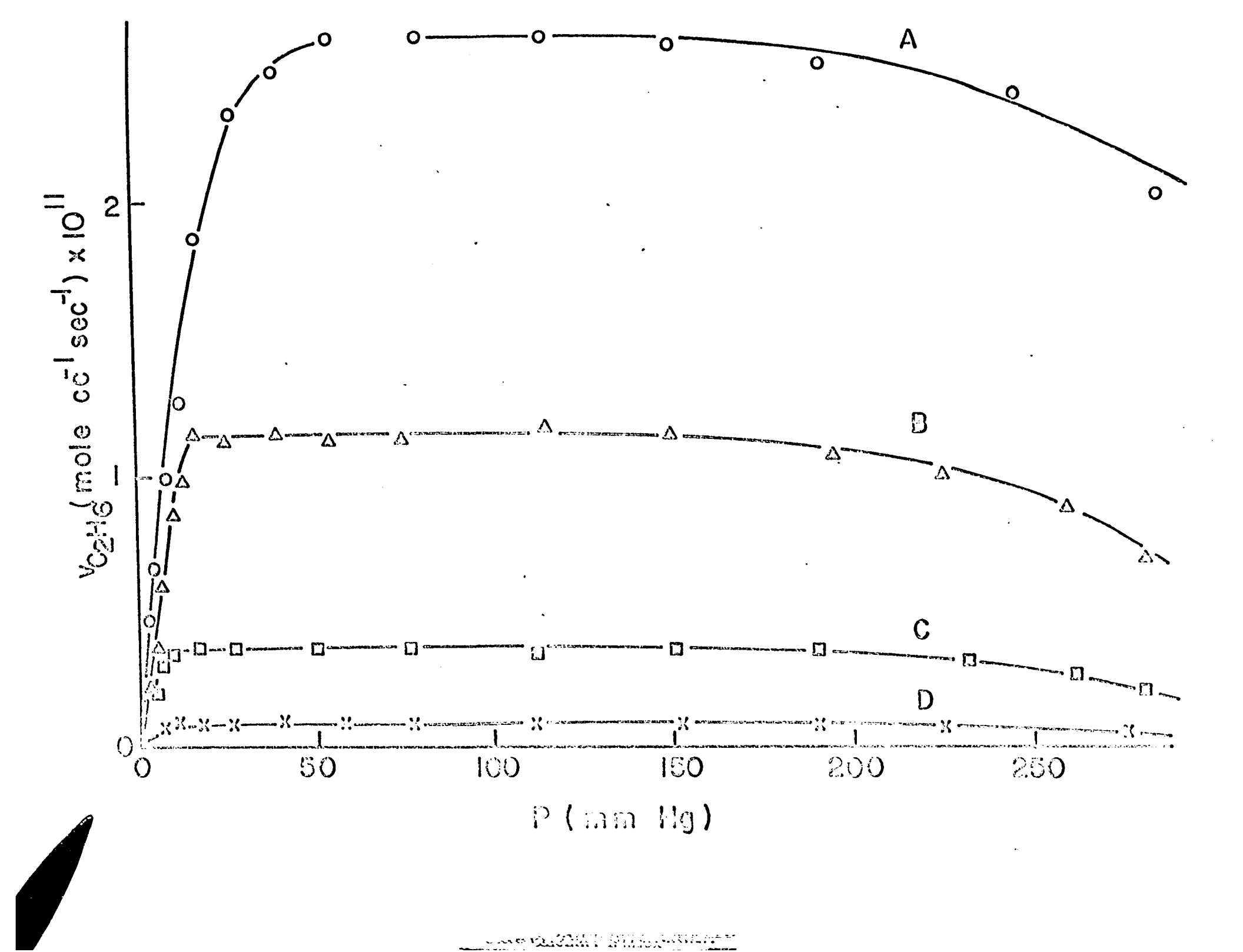
A
B
C
D
2
1
0
0
50
100
150
200
250
P (mm Hg)
$v_{C_2H_6}$ (mole cc^{-1} sec^{-1}) x 10^{11}

FIGURE 13

Order plots for ethane.

A 335°C

B 310°C

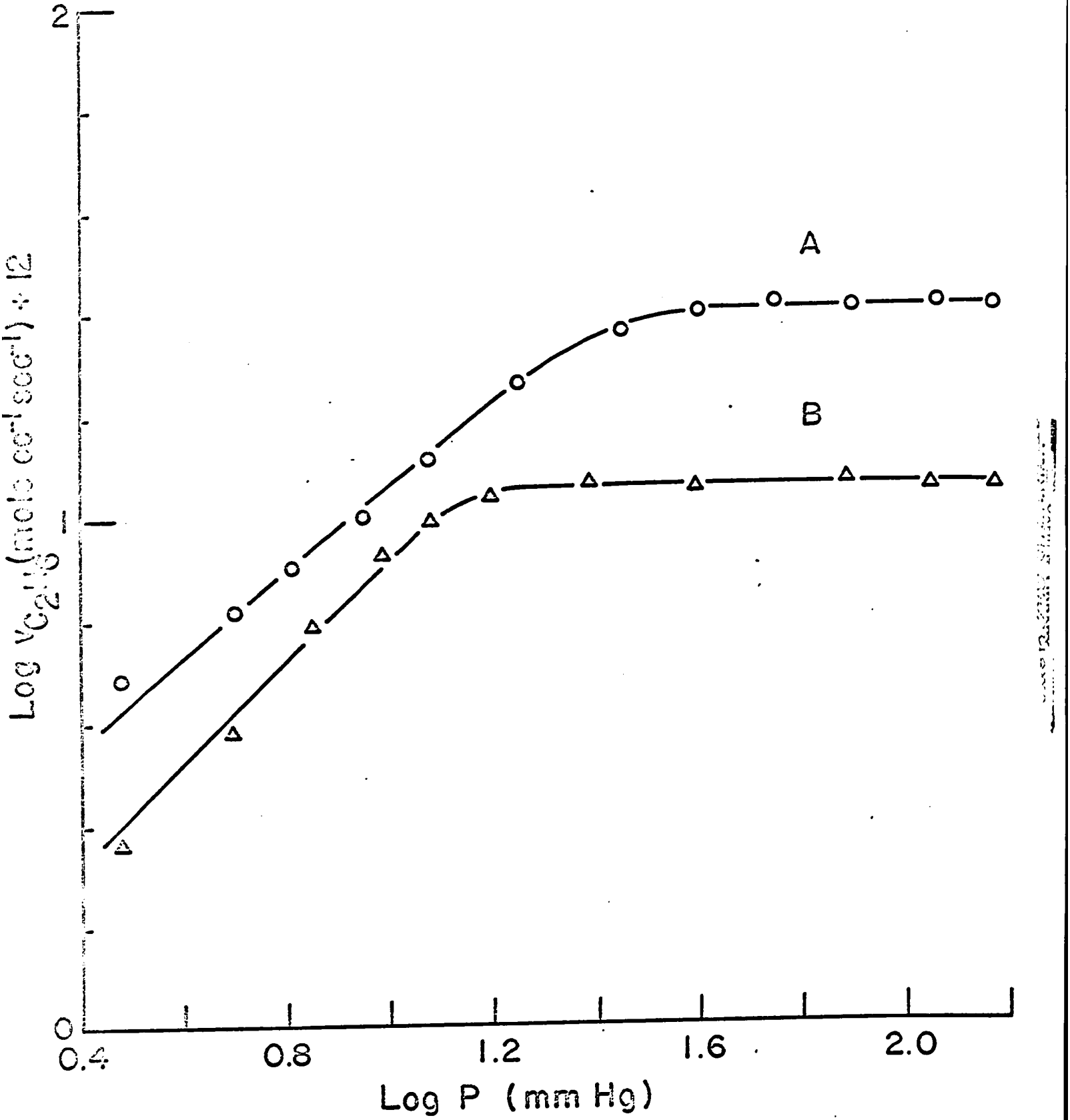
2
0
0.4
0.8
1.2
1.6
2.0
A
B
Log P (mm Hg)

FIGURE 14

The logarithm of the rate of ethane production against reciprocal of temperature.

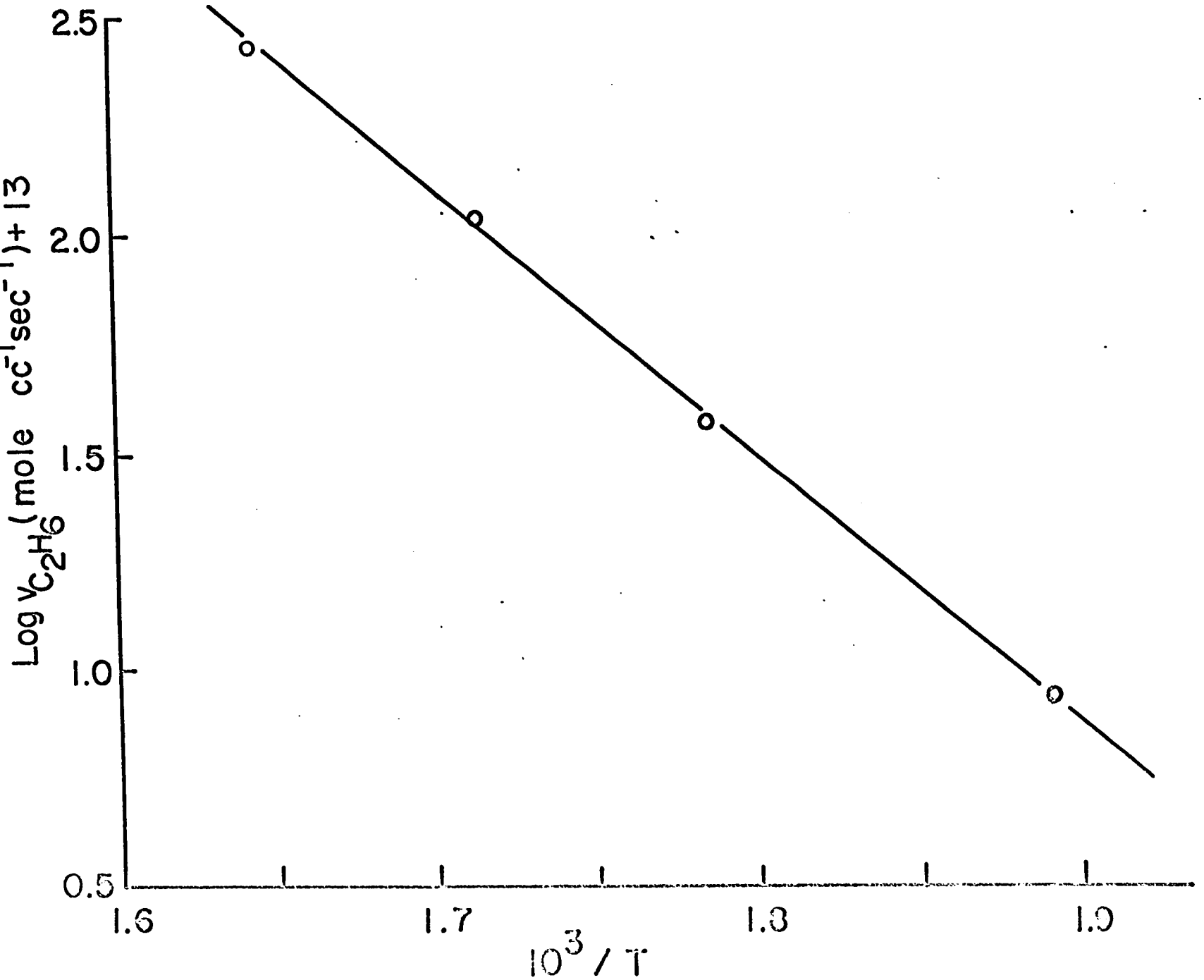
2.5
2.0
1.5
1.0
0.5
Log $v_{C_2H_6}$ (mole cc^{-1}sec^{-1})+ 13
1.6
1.7
1.8
1.9
10^3 / T

FIGURE 15

Yield of iso-butene against time.

A	310°C	232 mm Hg
B	286°C	230 mm Hg
C	310°C	40 mm Hg
D	286°C	40 mm Hg

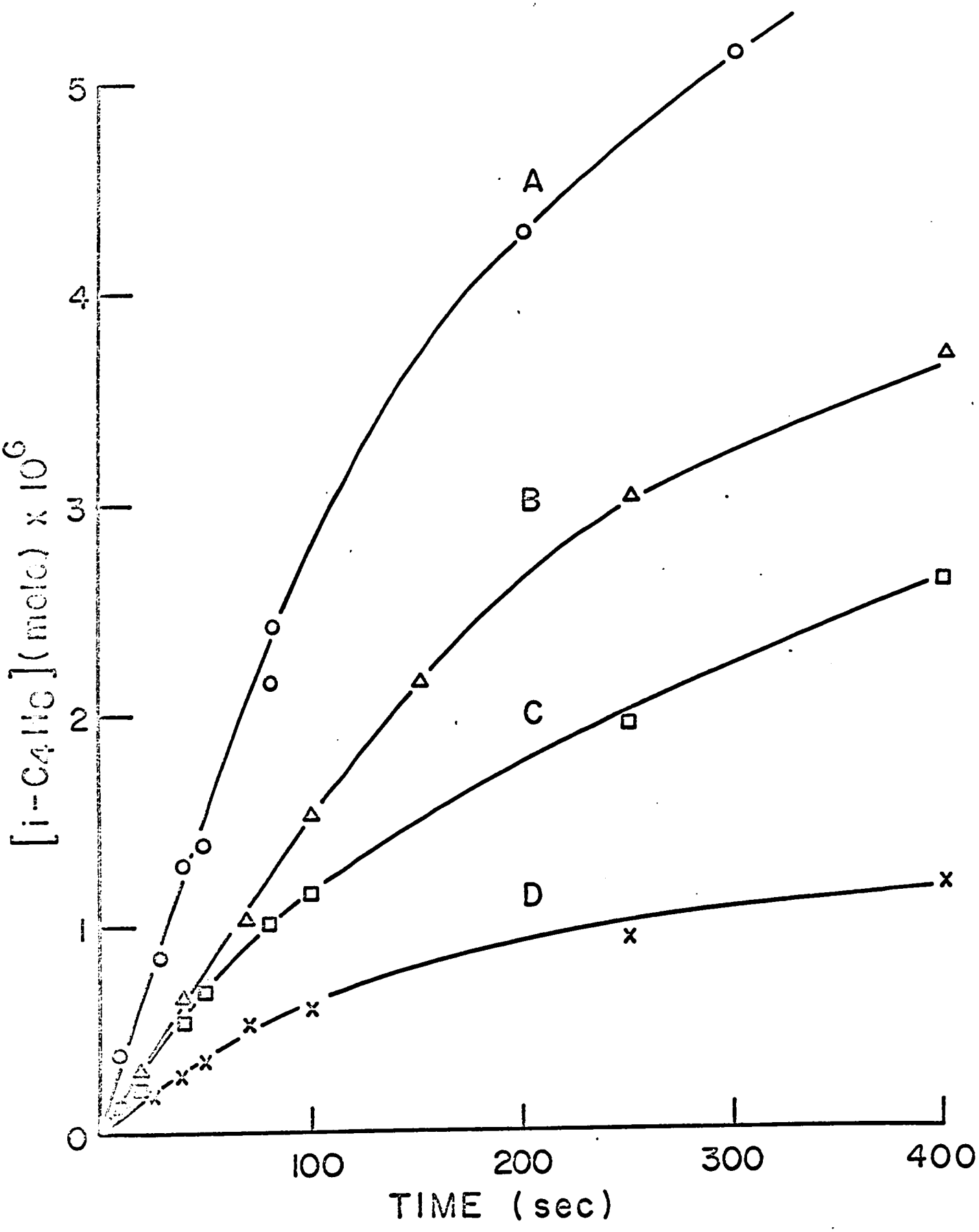
5
4
3
2
1
0
A
B
C
D
100
200
300
400
TIME (sec)
[i-C4H8](mole) x 10^6

A plot of the rates against pressure at different temperatures is shown in Figure 16. The rate increases with pressure and later attains a constant value. At a temperature of 230°C the rate is constant at pressures above 75 mm Hg, at 256°C above 140 mm Hg and at 286°C above 200 mm Hg. At temperatures of 310°C and 335°C the region of constant rate was not reached.

A double logarithmic plot of the rate against pressure at different temperatures is shown in Figure 17. The reaction order with respect to reactant changes from 0.5 at low pressures to zero at high pressures.

A plot of the logarithm of the rate against the reciprocal of the temperature is shown in Figure 18. The rates are taken at pressures of 280 mm Hg. The activation energy calculated from the slope is 27.5 kcal/mole.

Production of Neohexane

A typical yield-time relation is shown in Figure 19. As in the case of the other products the yield is linear with time at low concentrations; later it deviates from linearity due to secondary reactions.

The yield-time relation at pressures of 77 mm Hg and higher follows approximately the same curve. At pressures of 40 mm Hg and lower the yields are smaller, but at lower conversions the curves approach the yield-time curve for higher pressures. Unfortunately, at pressures below 20 mm Hg

FIGURE 16

The rate of iso-butene production against pressure.

A 310°C

B 286°C

C 256°C

D 230°C

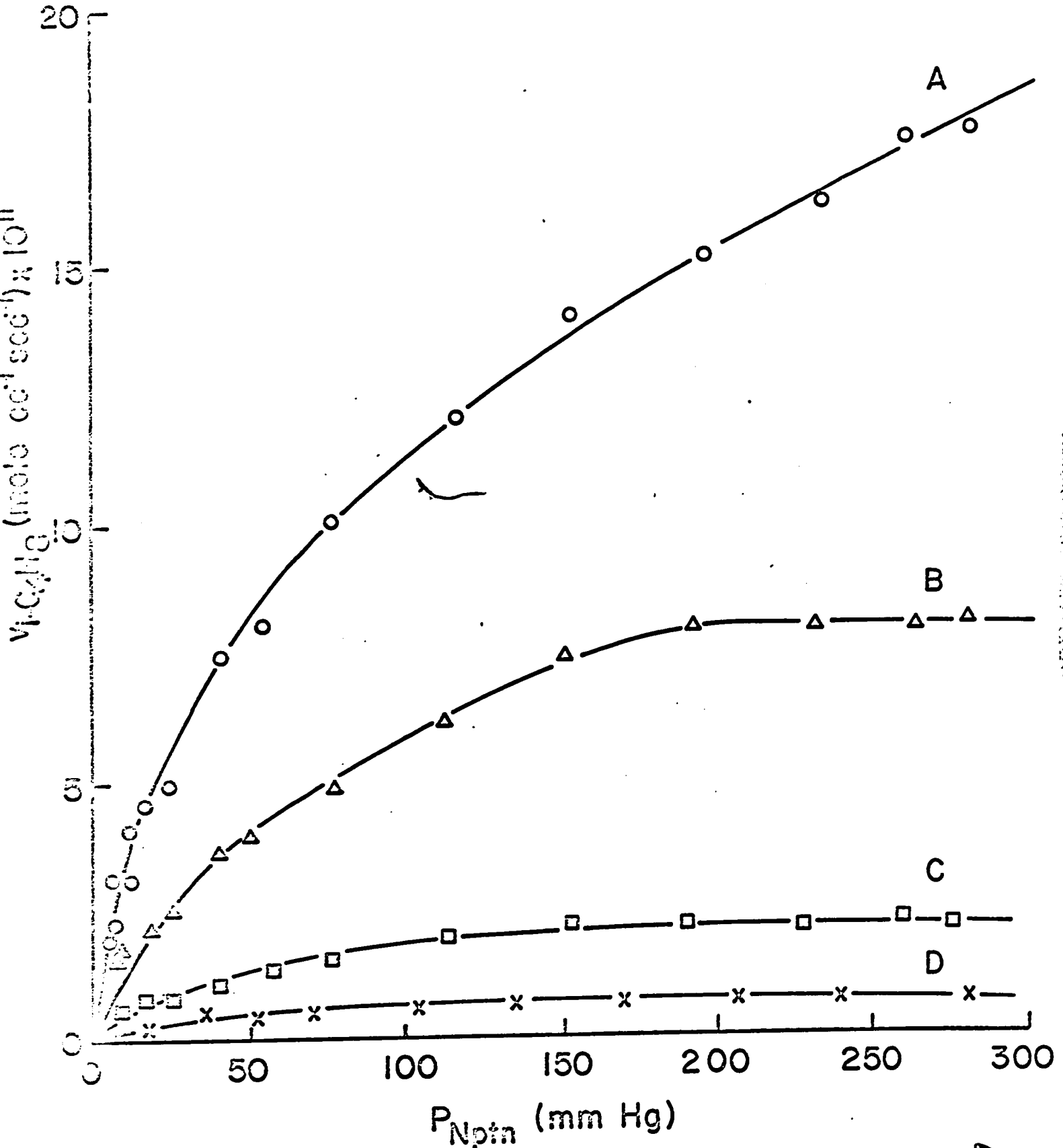
20
15
10
5
0
A
B
C
D
0
50
100
150
200
250
300
P_{Nptn} (mm Hg)
$V_{1\text{-}C_4H_8}$ (mole cc^{-1} sec^{-1}) x 10^{11}

FIGURE 17

Order plot of iso-butene.

A 335°C

B 310°C

C 286°C

D 256°C

E 230°C

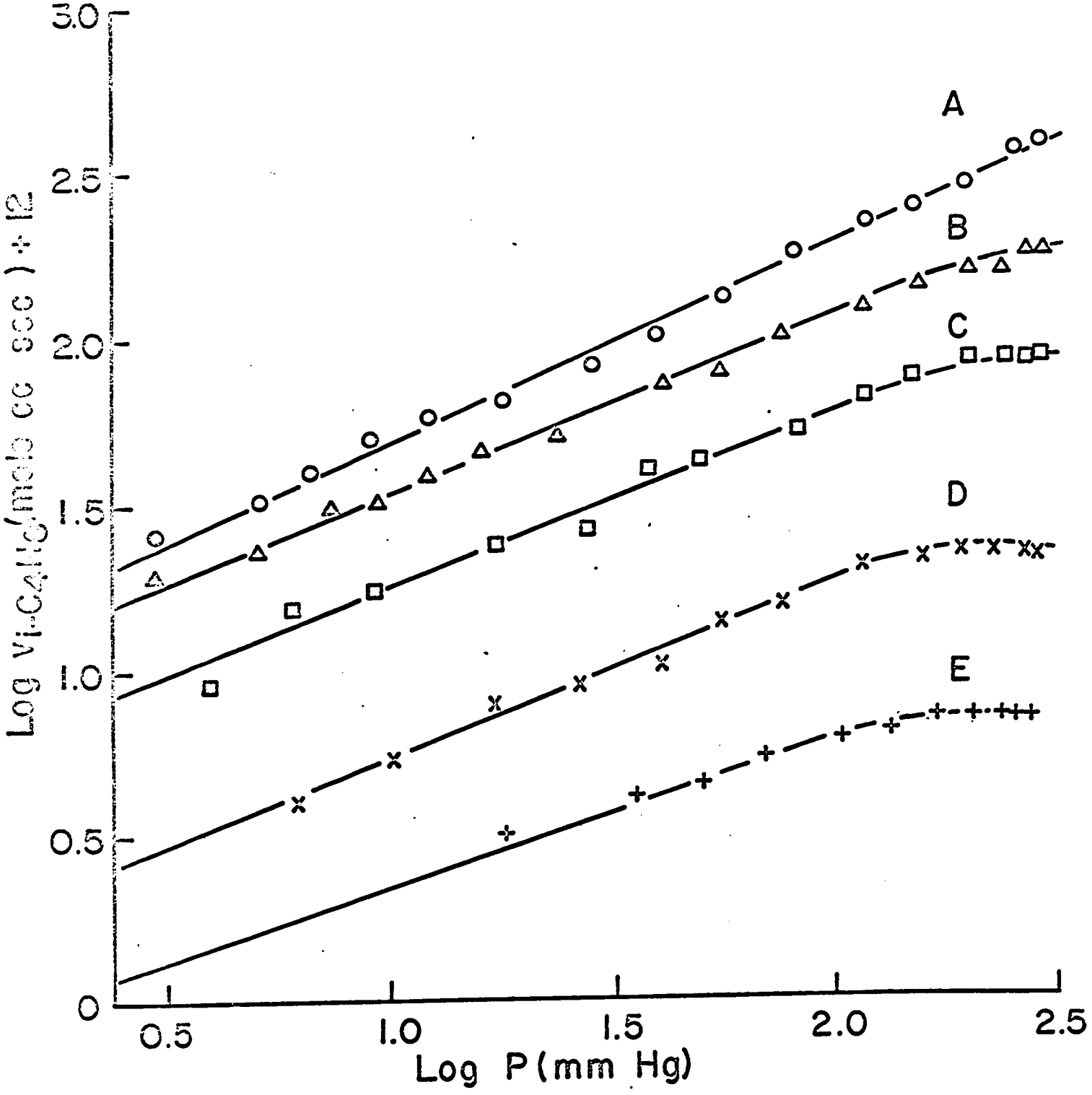
3.0
2.5
2.0
1.5
1.0
0.5
0
0.5
1.0
1.5
2.0
2.5
Log P (mm Hg)
A
B
C
D
E

FIGURE 18

The logarithm of the rate of i-C_4H_8 production against the reciprocal of the temperature.

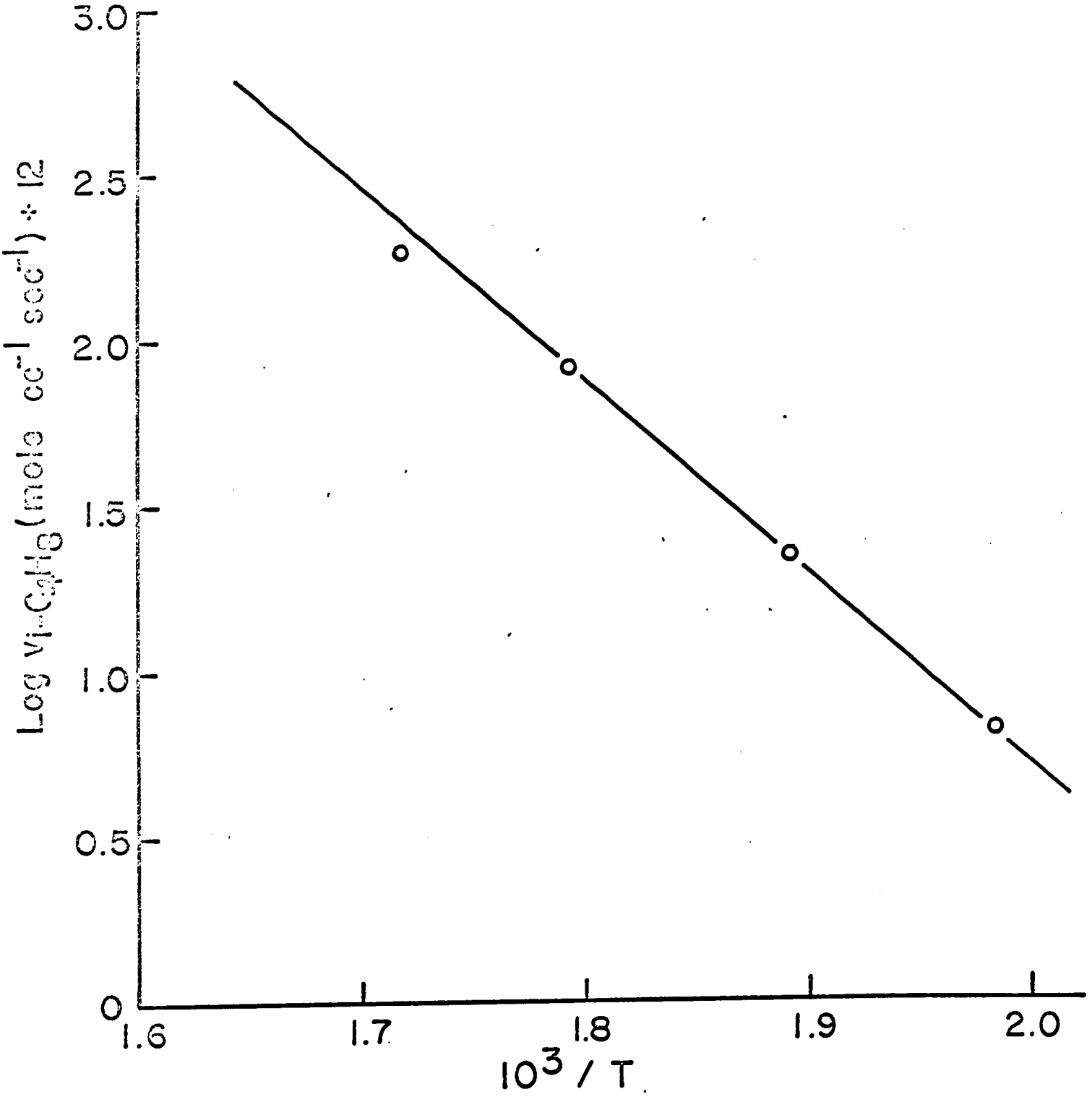
3.0
2.5
2.0
1.5
1.0
0.5
0
Log v_i--C_4H_8 (mole cc^{-1} sec^{-1}) + 12
1.6
1.7
1.8
1.9
2.0
10^3 / T

FIGURE 19

Yield-time curves for production of neohexane at 286°C and at different pressures.

A	x x x	280 mm Hg
	□ □	230 mm Hg
	+ + +	190 mm Hg
	▽ ▽ ▽	112 mm Hg
	o o o	77 mm Hg
B	Δ Δ Δ	40 mm Hg
C		17 mm Hg

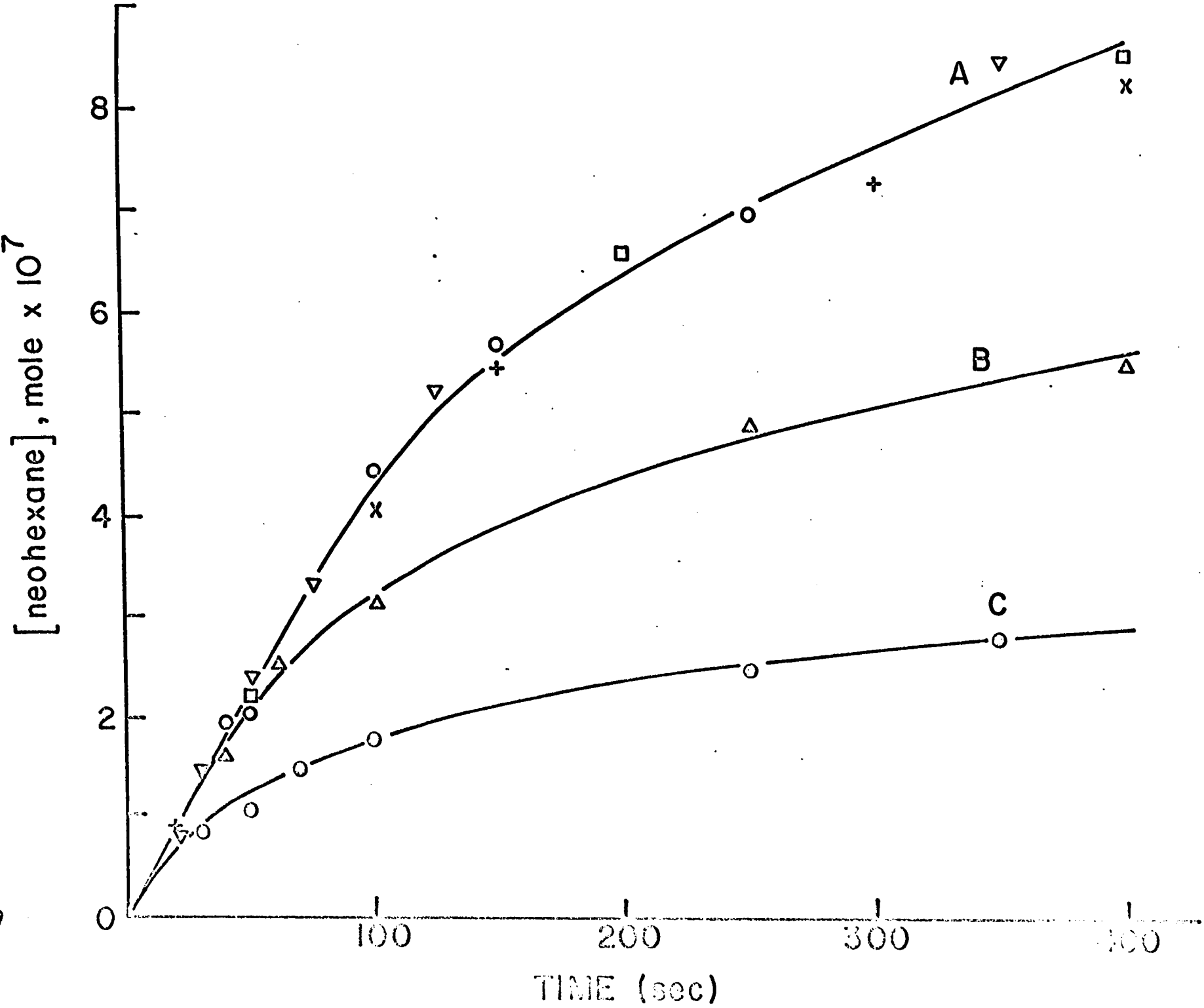
[neohexane], mole x 10^7
0
2
4
6
8
100
200
300
TIME (sec)
A
B
C

and at low conversions analyses were very inaccurate because of insufficient sensitivity of the chromatograph to neohexane.

The initial rate was obtained from the slope in the linear region. In this case the rates were not evaluated for each pressure used, but the average rate was taken from the slope of the linear region. In later calculation, where the rate of neohexane was used, it was assumed that also at low pressures, where the evaluation of the rate was not possible, the rate is the same. This is in agreement with expectations concerning the combination of alkyl radicals.

With increase of temperature, the rate increased until the temperature of 310°C is reached. Another increase of temperature causes only little change of the rate. Some other aspects of the observation will be discussed later. The average rates for different temperatures are listed in Table II.

Production of Dineopentyl

A typical dineopentyl yield-time relation is shown in Figure 20. Dineopentyl is a high boiling hydrocarbon (b.p. 140°C) and so there are difficulties in measuring its yield. In this case only the peak area was measured, and even in calibration considerable scattering was observed. Some uncertainties arise also from complications concerning the trapping of such a high-boiling product. It was not possible to measure the yield at low conversions, so that

TABLE II

The initial rates of neohexane production at different temperatures

Temperature ^{o}C	Rate mole $cc^{-1} sec^{-1} \times 10^{11}$
230	0.45
256	1.15
286	2.66
310	3.39
335	3.38

FIGURE 20

Yield-time curves for production of dineopentyl at 230°C and at different pressures.

A	o o o	54 mm Hg
	x x x	136 mm Hg
B	Δ Δ Δ	40 mm Hg

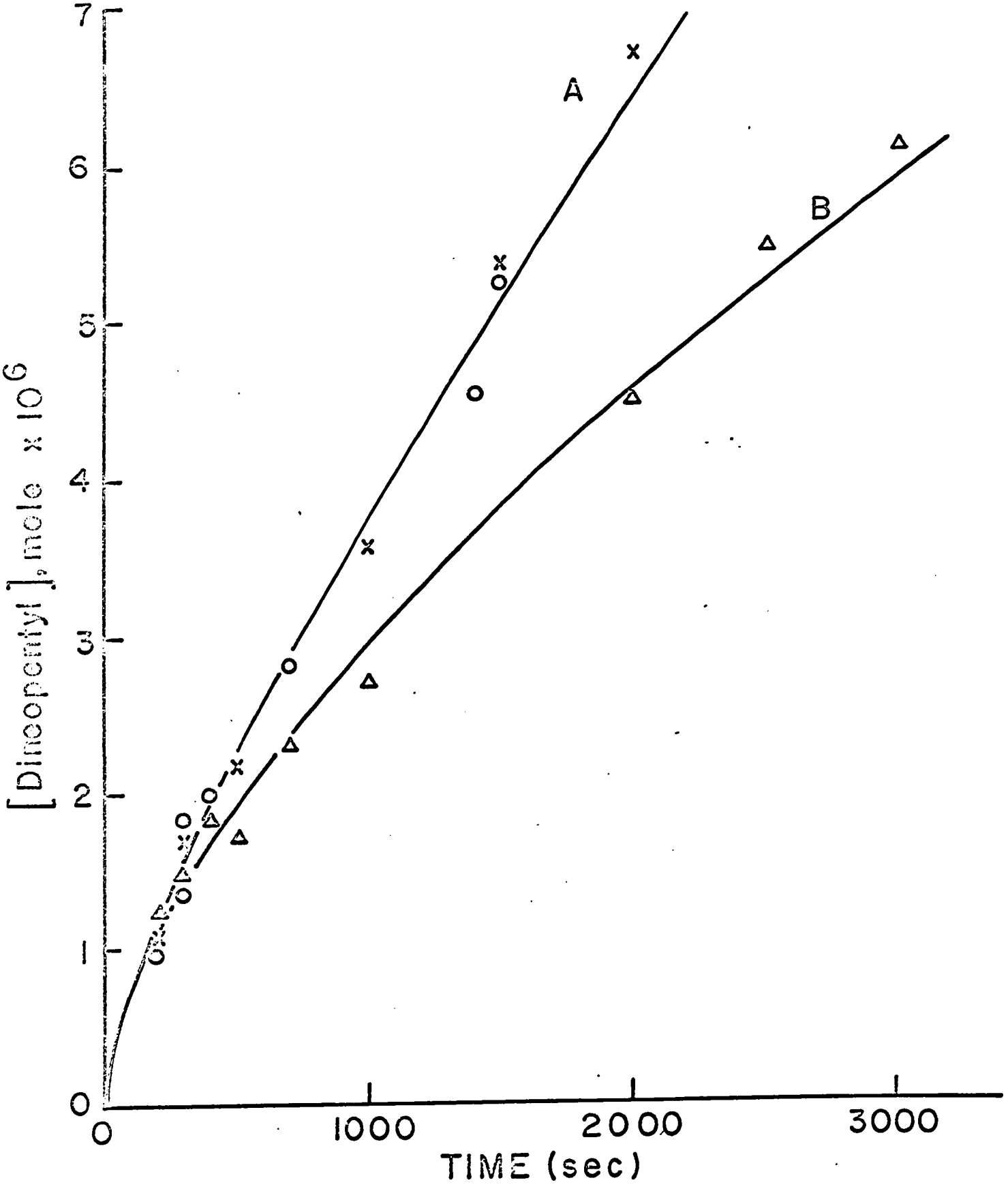
7
6
5
4
3
2
1
0
[Dimeopentyl], mole x 10^6
A
B
0
1000
2000
3000
TIME (sec)

the extrapolation of the yield-time curve had to be done to zero contact time. The inaccuracy increased in experiments at pressures below 40 mm Hg, because of small yield of the product.

Only at temperatures of 230°C and 256°C was it possible to measure the yield. At the temperature of 286°C, little product was detected even at high conversion. At temperatures of 310°C and 335°C, under no conditions was dineopentyl detected.

As is seen from Figure 20, at pressures higher than 40 mm Hg the yields at different pressures follow approximately the same curve. At pressures of 40 mm Hg, the yields are smaller, but at lower conversions the curve approaches that for higher pressures.

The initial rate was calculated only for a temperature of 230°C, from the slope of the extrapolated line. The value obtained is 3.72×10^{-11} mole/cc sec and should be considered as approximate.

KINETICS AND MECHANISM

In the present section the primary reactions of the mercury-photosensitized decomposition of neopentane are considered. The initial process is the excitation of an atom of mercury by collision with a photon of light. A mercury atom absorbs 2537 Å radiation from a low pressure mercury lamp, and then loses its energy on collision with a neopentane molecule; this decomposes by scission of a C-H bond with the production of an alkyl radical and a hydrogen atom.

The hydrogen atoms produced in this act react mostly in metathetical reactions with the formation of hydrogen molecules. When olefin is present, either as an impurity or product of a reaction, hydrogen atoms are removed and highly energized radicals are produced. The combination of hydrogen atoms with radicals also occurs in these systems.

Alkyl radicals produced in the initial act can undergo hydrogen abstraction, recombination and disproportionation reactions. The neopentyl radical cannot disproportionate, because of the absence of a hydrogen atom on the β carbon. The decomposition of neopentyl radicals is evident at temperatures of 286°C and higher.

As was said before, the primary products are: hydrogen, methane, ethane, iso-butene, neohexane and

dineopentyl. In further discussion the symbol Nptn is used for neopentane and Nptl for the neopentyl radical. On the basis of the analysis of products, the following mechanism for primary reactions is proposed:

1	$Hg + h\nu$	$\rightarrow Hg^*$
2	$Hg^* + Nptn$	$\rightarrow Nptl + H + Hg$
3	$Nptn + H$	$\rightarrow Nptl + H_2$
4	$Nptn + CH_3$	$\rightarrow Nptl + CH_4$
5	$Nptn + Nptl$	$\rightarrow Nptl + Nptn$
6	$Nptl$	$\rightarrow i\text{-}C_4H_8 + CH_3$
7	$Nptl + CH_3$	$\rightarrow C_6H_{14}$ (2,2'-dimethylbutane)
8	$2\ CH_3$	$\rightarrow C_2H_6$
9	$2\ Nptl$	$\rightarrow C_{10}H_{22}$ (2,2,5,5-tetramethylhexane)
10	$Nptl + H$	$\rightarrow CH_3 + t\text{-}C_4H_9$
11	$Nptl + H$	$\rightarrow Nptn$
12	$CH_3 + H$	$\rightarrow CH_4$
13	$i\text{-}C_4H_8 + H$	$\rightarrow C_4H_9^*$

As was shown, e.g., in Figure 2, yield-time relations for all primary products except for methane are linear only at low conversions. Later deviations from linearity are observed and they are attributed to secondary reactions which have their origin in reaction 13. Recently, Papic and Laidler

studied the photosensitized decomposition of propane (9). In their work the yield-time relation was linear over the whole time region despite the fact that an olefin was present as product. This is due to the fact that the experiments were carried out up to much lower conversions than was possible in the present work, so that insufficient amounts of olefines were produced for the quenching of hydrogen atoms to be evident.

Hydrogen atoms are produced in the initial quenching act (reaction 2); which is believed to be the only source of hydrogen atoms. The proposed mechanism is in agreement with the expectation that the initial decomposition is C-H bond rupture. Most of the hydrogen atoms undergo reaction 3. Reaction of H atoms with Nptl radicals (reactions 10 and 11) also probably occurs. The quenching of hydrogen atoms by i-C_4H_8 in reaction 13 is evident only after enough i-C_4H_8 has been produced. Reaction 13 is the basis of several secondary products, and further discussion will be given in the next chapter.

Nptl radicals are formed with H atoms in the initial quenching reaction 2. Additional sources of Nptl radicals are hydrogen abstraction reactions 3 and 4. Nptl radicals can combine in reaction 9 to form dineopentyl and also combine with CH_3 radicals by reaction 7, resulting in the formation of neohexane. Most of the Nptl radicals at higher

temperatures (286°C and higher) decompose into i-C_4H_8 and CH_3 radicals in reaction 6. As far as the reaction of Nptl radicals with H atoms is concerned, it is expected that reaction 10 predominates over 11 at low pressures, whereas the stabilization of excited Nptn molecule (reaction 11) is more important at higher pressures. More detailed discussion of Nptl radicals reactions will be given in the next section of the chapter.

As was said, the origin of the CH_3 radicals is reaction 6, although at lower pressures some additional amounts are also formed in reaction 10 (atomic cracking). Methyl radicals react in the combination reaction 7 with Nptl radicals, producing neohexane; they produce ethane in the combination reaction 8. With increase of temperature and pressure reaction 4, hydrogen abstraction by CH_3 radicals, becomes more important with respect to reaction 7 and 8.

Steady-State Treatment

Reactions 5 and 12 in the proposed mechanism are included only for completeness and will not be considered in the steady-state treatment. The steady-state equations for H atoms, CH_3 radicals and Nptl radicals are:

$$I_a\phi = v_3 + v_{10} + v_{11} + v_{13} \qquad \text{I}$$

$$v_6 + v_{10} = v_4 + v_7 + 2v_8 \qquad \text{II}$$

$$v_3 + v_4 + I_a\phi = v_6 + v_7 + 2v_9 + v_{10} + v_{11} \qquad \text{III}$$

where I_a is intensity of light used and ϕ the quantum yield of hydrogen. The steady-state concentrations of the radicals can be obtained from the above equations by expressing rates in the usual way; for example, equation I is

$$I_a\phi = k_3[Nptn][H] + k[H][Nptl] + k_{13}[H][i\text{-}C_4H_8]$$

where $k = k_{10} + k_{11}$. Reaction 13 is responsible for the formation of the secondary products. As will be shown in the next chapter, all secondary products have some induction period in yield-time relations, and their rates of production are assumed to be negligible at zero contact time; this means that v_{13} can be neglected in equation I. The steady-state concentration of H atoms is then

$$[H] = \frac{I_a\phi}{k_3[Nptn] + k[Nptl]} \qquad \text{IV}$$

Similarly, equation II can be expressed as

$$k_6[Nptl] + k_{10}[H][Nptl] = k_4[CH_3][Nptn] + k_7[CH_3][Nptl] + 2k_8[CH_3]^2$$

From the experimental observations it is seen that at 230°C only unmeasurable amounts of ethane are produced; even at temperature of 310°C less than 20% of the total amount of CH_3 radicals are used in reaction 8, so that v_8 in equation II is neglected. The steady-state concentration of CH_3 radicals is then

$$[CH_3] = \frac{k_6[Nptl] + k_{10}[H][Nptl]}{k_4[Nptn] + k_7[Nptl]} \qquad \text{V}$$

In order to obtain the approximate steady-state concentration of Nptl radicals, to equation III is added equation II, in which v_8 is neglected. We then obtain:

$$I_a\phi + v_3 = 2v_7 + 2v_9 + v_{11}$$

Reaction 11 is negligible at low pressures and it is assumed that also at high pressures this reaction is not very important; the increase of pressure causes H atoms to react more in hydrogen-abstraction reaction than in the combination reaction 11, and v_{11} is therefore also neglected. The final equation is thus

$$I_a\phi + k_3[H][Nptn] = 2k_7[CH_3][Nptl] + 2k_9[Nptl]^2$$

and the approximate steady-state concentration of Nptl radicals is

$$[Nptl] = 1/2\left[\frac{k_7^2}{k_9^2}[CH_3]^2 + \frac{2I_a\phi}{k_9} + \frac{2k_3}{k_9}[H][Nptn]\right]^{1/2} - \frac{k_7}{2k_9}[CH_3]; \qquad VI$$

At the higher temperatures used in the study dineopentyl was not detected, so that v_9 in equation III can be neglected. To express the approximate steady-state concentration at these temperatures, it is more convenient to use in equation III instead of $I_a\phi$ the expression from equation I in which v_{13} is neglected; then

$$2v_3 + v_4 = v_6 + v_7$$

and

$$2k_3[H][Nptn] + k_4[CH_3][Nptn] = k_6[Nptl] + k_7[CH_3][Nptl]$$

From this equation, the approximate steady-state concentration of Nptl radicals at higher temperatures is

$$[\text{Nptl}] = \frac{[\text{Nptn}](2k_3[\text{H}] + k_4[\text{CH}_3])}{k_6 + k_7[\text{CH}_3]} \qquad \text{VII}$$

The approximate steady-state concentration of H atoms, CH_3 radicals and Nptl radicals at different temperatures and pressures are summarized in Table III. The concentrations of H atoms were obtained from the expression

$$[\text{H}] = v_3/k_3[\text{Nptn}]$$

k_3 was evaluated using the values $E_3 = 9.7$ kcal/mole and for $A_3 = 10^{14}$ cc/mole sec.

The concentrations of CH_3 radicals were calculated from the relation

$$[\text{CH}_3] = v_4/k_4[\text{Nptn}]$$

For k_4 were used values obtained in the present study.

To evaluate the concentration of Nptl radicals, there was only one procedure, i.e., to use v_6 and then $[\text{Nptl}] = v_6/k_6$, where for k_6 were taken values from present study.

Complicated expressions are obtained for the dependence of the rates of formation of the products on the pressure of Nptn; simple orders are therefore not found. The situation is simplified by taking into account the calculated approximate concentrations of the radicals. Some approximations

TABLE III

The approximate concentrations of H atoms, CH_3 and Nptl radicals, and the concentrations of Nptn*

Temperature °C	Pressure mm Hg	H	CH_3	Nptl	Nptn
335	280	1.29×10^{-6}	11.2×10^{-13}	1.31×10^{-12}	7.39×10^{-6}
335	115	2.7×10^{-16}	12.9×10^{-13}	1.35×10^{-12}	3.0×10^{-6}
335	12	-	10.3×10^{-13}	1.72×10^{-12}	3.4×10^{-7}
310	280	1.72×10^{-16}	6.2×10^{-13}	2.22×10^{-12}	7.70×10^{-6}
310	115	4.06×10^{-16}	8.44×10^{-13}	1.85×10^{-12}	3.14×10^{-6}
310	9.5	-	9.72×10^{-13}	2.22×10^{-12}	2.61×10^{-7}
286	280	1.10×10^{-16}	3.22×10^{-13}	2.40×10^{-12}	8.03×10^{-6}
286	112	2.14×10^{-16}	4.91×10^{-13}	2.21×10^{-12}	3.21×10^{-6}
286	9.0	6.80×10^{-16}	4.86×10^{-13}	3.00×10^{-12}	2.58×10^{-7}
256	275	3.48×10^{-16}	1.47×10^{-13}	3.41×10^{-12}	8.33×10^{-6}
256	110	8.41×10^{-16}	2.39×10^{-13}	2.97×10^{-12}	3.32×10^{-6}
256	10	27.60×10^{-16}	2.21×10^{-13}	2.79×10^{-12}	3.02×10^{-7}
230	280	5.46×10^{-16}	6.10×10^{-14}	3.12×10^{-12}	8.93×10^{-6}
230	104	14.5×10^{-16}	7.4×10^{-14}	3.0×10^{-12}	3.31×10^{-6}
230	18	45.0×10^{-16}	5.8×10^{-14}	4.11×10^{-12}	5.1×10^{-7}

*The concentrations are given in mole/cc.

can then be used to avoid the complications, as was done by Papic (20).

Production of Hydrogen

Hydrogen is formed in reaction 3, the metathetical reaction of H atoms with the parent molecule. A typical yield-time relation is shown in Figures 3 and 4. It is seen that the yield at low conversions is a linear function of time. The later deviation from linearity is caused by quenching of H atoms by i-C_4H_8, formed in reaction 6. A yield-time relation for i-C_4H_8 in Figure 15 shows that the deviation from linearity is evident when the concentration of i-C_4H_8 is in the region of 0.5 - 2.0x10^{-8} mole/cc. It is supposed that at this concentration of i-C_4H_8 the extensive quenching of H atoms, reaction 13, begins to be important.

Figure 5 shows the relation between the rate of hydrogen formation and the pressure of Nptn. The rate is constant at pressures above 100 mm Hg. The rate is also independent of temperature. These results can be related to the origin of the hydrogen molecule, i.e., quenching of Nptn molecule by excited Hg atoms, a quenching reaction that is expected to be temperature independent. This observation also suggests that there is no other source of H atoms in the temperature region used.

The reaction order for hydrogen production with respect to pressure of Nptn was observed to change from 1.0

at low pressures to zero at high pressures. Using equation IV for the steady-state concentration of H atoms, the rate of hydrogen production can be expressed as

$$v_3 = \frac{k_3[\text{Nptn}] \times I_a\phi}{k_3[\text{Nptn}] + k[\text{Nptl}]} = \frac{I_a\phi}{1 + \frac{k[\text{Nptl}]}{k_3[\text{Nptn}]}}$$

At high pressures the following approximate expression is obtained,

$$v_3 = I_a\phi$$

This proves the independence of v_3 on pressure at higher pressures, in agreement with the experimental observations.

At low pressures the approximate expression for v_3 is:

$$v_3 = \frac{I_a\phi \; k_3[\text{Nptn}]}{k[\text{Nptl}]}$$

If the approximate concentrations of Nptl radicals in Table III are considered it is seen that the change of pressure from 280 mm Hg to about 10 mm Hg results in very little change of concentration of Nptl radicals. The same change of pressure causes more than a 10-fold change of Nptn concentration. It is assumed that the change of v_3 at low pressures is much more affected by the change of concentration of Nptn.

Production of Methane and Ethane

A comparison of the yield-time relations of the products shows that the yield of ethane is linear only at low conversions and later deviates from linearity, due to secondary reactions. In reaction 13 some other radicals are formed, i.e., mostly t-C_4H_9, so that a certain competition for CH_3 radicals must be expected between the combination reaction 8 and the combination reaction of CH_3 radicals with C_4H_9 radicals; this will result in a deviation of ethane yield from linearity with respect to time.

As far as methane is concerned, the yield-time relation is linear, and only at very high conversions is the effect of secondary reactions evident.

The rate for ethane production v_8 predominates over that for methane v_4 at low pressures. With the use of the approximate concentration of CH_3 radicals from Table III it is possible to obtain the ratio v_8/v_4 from the following relation:

$$v_8/v_4 = \frac{k_8[CH_3]^2}{k_4[CH_3][Nptn]}$$

At pressures of about 10 mm Hg, this ratio is in the region of 1 - 2 depending on temperature, in agreement with the experimental observation. The activation energy of a combination reaction is assumed to be zero, so that at least at low pressures this reaction is much more likely to occur than

reaction 4. With increase of pressure reaction 4 is becoming more important. It seems that the turning point is between 10 - 20 mm Hg.

It is shown in Figure 9 that the reaction order for production of methane changes from 1.0 at low pressures to zero at high pressures. With the use of equation V for the steady-state concentration of CH_3 radicals, the rate of production of methane can be expressed as

$$v_4 = k_4[Nptn][CH_3] = \frac{k_4[Nptn][Nptl](k_6+k_{10}[H])}{k_4[Nptn] + k_7[Nptl]} = \frac{[Nptl](k_6+k_{10}[H])}{1 + \frac{k_7[Nptl]}{k_4[Nptn]}}$$

At low pressures the approximate steady-state expression for v_4 is

$$v_4 = \frac{k_4}{k_7}[Nptn](k_6 + k_{10}[H])$$

In the present case, as is seen from Table III, the approximate concentration of H atoms shows about a three-fold change when the pressure of Nptn decreases from 110 mm Hg to about 10 mm Hg. The same change of pressure results in more than a ten-fold change of concentration of Nptn. It is assumed that at low pressures the rate v_4 is much more effected by change of concentration of Nptn than by the change of concentration of H atoms.

At high pressures reaction 10, i.e., atomic cracking, can be neglected as a second source of CH_3 radicals, and the approximate rate v_4 for high pressure is

$$v_4 = k_6[\text{Nptl}]$$

This is the same as the rate of decomposition of Nptl radicals. This means that at high pressure the rate v_4 is approaching the rate v_6, i.e., CH_3 radicals produced in reaction 6 are used mostly in the hydrogen abstraction reaction 4. This is also in agreement with the expectation that at high pressures the reaction 6, i.e., the decomposition of Nptl radicals, is the only source of CH_3 radicals. The conclusion from the present results is that this is the situation at high temperatures; for example, at 335°C and a pressure of 280 mm Hg more than 70% of the CH_3 radicals produced are used in reaction 4.

The rates of methane production at different temperaturesand pressures are shown in Figure 8. The rate at first increases with pressure, later attaining a constant value. The region of constant rate was not attained at 335°C. The Arrhenius plot, from the values of v_4 taken at a pressure of 280 mm Hg for temperatures from 230°C to 310°C, is shown in Figure 10. The activation energy from the slope is 28.8 kcal/mole.

The order of ethane production with respect to Nptn is observed to be 1.0 at low pressures, changing to zero at high pressures (Figure 13). A similar interpretation of v_8 to that for v_4 gives a very complicated expression and will not be presented here.

Several workers have studied the rate of ethane production, i.e., the combination of CH_3 radicals with respect

to pressure. Kistiakowsky and Roberts (21) and Dodd and Steacie (22) found in a study of the photolysis of gaseous acetone at temperatures from 150 to 250°C that the effect becomes appreciable at pressures below 10 mm Hg. Toby and Weiss (23) studied the combination of CH_3 radicals in the photolysis of azomethane at pressures of 3 to 60 mm Hg and in the temperature range of 25°C to 180°C. They observed a significant fall-off of the rate coefficient at pressures below 10 mm Hg. Loucks (7) examined the reaction at temperatures from 200°C to 300°C and observed the beginning of fall-off at a pressure of 100 mm Hg.

The most extensive study of the combination of CH_3 radicals with respect to pressure was done by Grotewold and co-workers (24,25) who photolyzed mixtures of azomethane and azoethane, and of azomethane and azopropane. They used the cross-combination ratio of CH_3 radicals with higher radicals for characterization of the effect of pressure, on the assumption that the combinations of CH_3 radicals with higher radicals will be pressure independent over the pressure region used in the study, and that the increase of the ratio at low pressures is caused only by decrease of the rate coefficient of ethane formation. The authors observed that the pressure fall-off at 15°C, 60°C and 100°C was at pressures about 100 times lower than one would expect from previous determinations.

The pressure dependence of the combination of CH_3 radicals from the present study is shown in Figure 12, where the rate of ethane formation is related to pressure. From the figure it is seen that a significant decrease of v_8 occurs at temperatures of 335°C at pressures of less than 35 mm Hg. At a temperature of 310°C the decrease is observed below about 15 mm Hg and at 286°C below 10 mm Hg. Results at a temperature of 256°C are not taken into account for reasons mentioned previously. The conclusion can be drawn that an increase of temperature of about 25°C results in about a 2-fold increase in the pressure at which the rate of ethane formation begins to decrease.

The curves in Figure 12 have an interesting shape; the rate at first increases with increase of pressure, and reaches a constant value. Further increase of pressure causes the rate to decrease. This may mean that the combination reaction of CH_3 radicals is suppressed by increase of pressure, which favors hydrogen abstraction by CH_3 radicals.

An alternative explanation for the observation is that there is a second source of CH_3 radicals, the atomic cracking in reaction 10. The excited Nptn molecule must be an intermediate, and reactions 10 and 11 should be written in the following way:

$$H + Nptl \xrightarrow{a} Nptn^*$$

$$Nptn^{*} + Nptn \xrightarrow{b} 2\ Nptn$$

$$Nptn^{*} \xrightarrow{c} CH_3 + i\text{-}C_4H_8$$

At higher pressures, reaction b predominates over c, so that the amount of CH_3 radicals from the source decreases. Because of restrictions mentioned previously, it was not possible to extend the experiments to higher pressures so as to get more information about the behavior.

The effect of pressure on the combination reaction of CH_3 radicals is usually studied by relating the combination reaction with the hydrogen abstraction reaction by CH_3 radicals. This approach enables us to get some information about the rate constant of the metathetical reaction, as for example, in the study of Loucks (26). In this approach it is assumed that hydrogen abstraction by CH_3 radicals is independent of pressure. It is also believed that, under the condition of the study, the amounts of methane and ethane arising from heterogeneous effects are negligible. The rates for CH_3 radical-combination and hydrogen abstraction reactions are:

$$v_4 = k_4[CH_3][Nptn]$$

$$v_8 = k_8[CH_3]^2$$

From these equations it follows that

$$\frac{k_8^{1/2}}{k_4} = \frac{v_8^{1/2}}{v_4}\ [Nptn]$$

A double logarithmic plot of $k_8^{1/2}/k_4$ against the concentration of reactant is shown in Figure 21. The slope in the pressure-dependent region changes from about 0.5 at low pressures to zero at high pressures, indicating that the reaction is in the third order region.

A plot of the logarithm of $k_8^{1/2}/k_4$ against the reciprocal of the temperature is shown in Figure 22. The values of the ratio are average values taken from Figure 21 at pressure of 110 mm Hg. From the slope it is calculated that

$$E_8^{1/2} - E_4 = -11.5 \text{ kcal/mole}$$

If $E_8 = 0$, then $E_4 = 11.5$ kcal/mole.

A value of 10.4 has been tabulated (27) as an average value. Kerr and Timlin (28) compared this value with the activation energy for hydrogen abstraction by CH_3 radicals from $(CH_3)_4Si$ and they concluded that it is probably too low. In their work they found 12.0 kcal/mole for E_4, in good agreement with the value obtained from Polanyi's theoretical equation, $E = 0.49\ (D_{CH} - 74.3)$ with $D_{C-H} = 99$ kcal/mole. The value obtained in the present study supports this conclusion of the authors.

From the intercept in Figure 22, and using for A_8 the value of 2.2×10^{13} cc mole^{-1} sec^{-1} (31), the frequency factor for the abstraction reaction is

$$A_4 = 4.9 \times 10^{11} \text{ cc mole}^{-1} \text{ sec}^{-1}$$

FIGURE 21

Log-log plot of $k_8^{1/2}/k_4$ against pressure of Nptn.

A 335°C

B 310°C

C 286°C

D 256°C

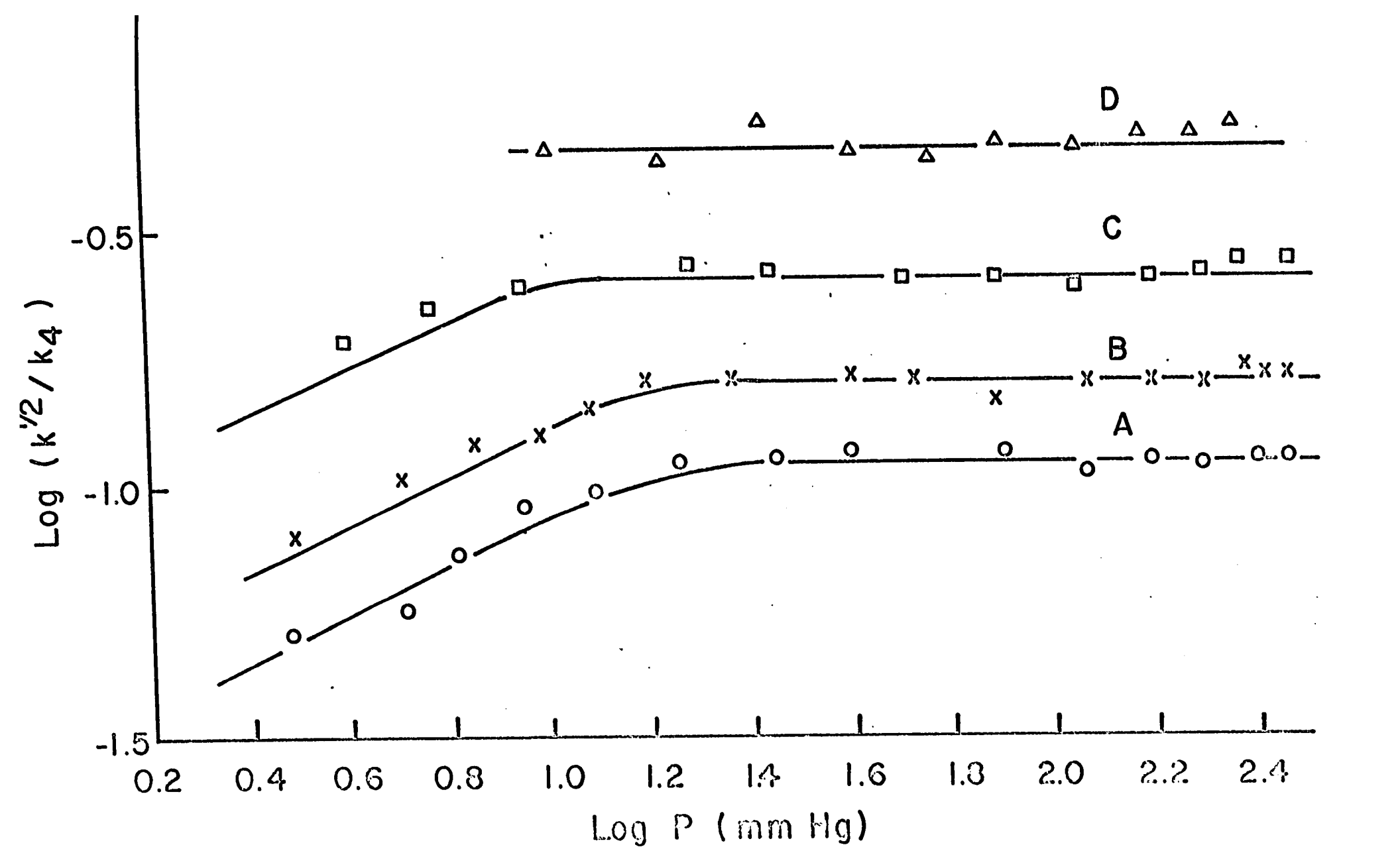
D
C
B
A
-0.5
-1.0
-1.5
Log (k'^1/2 / k4)
0.2
0.4
0.6
0.8
1.0
1.2
1.4
1.6
1.8
2.0
2.2
2.4
Log P (mm Hg)

FIGURE 22

Plot of logarithm of $k_8^{1/2}/k_4$ against reciprocal of temperature.

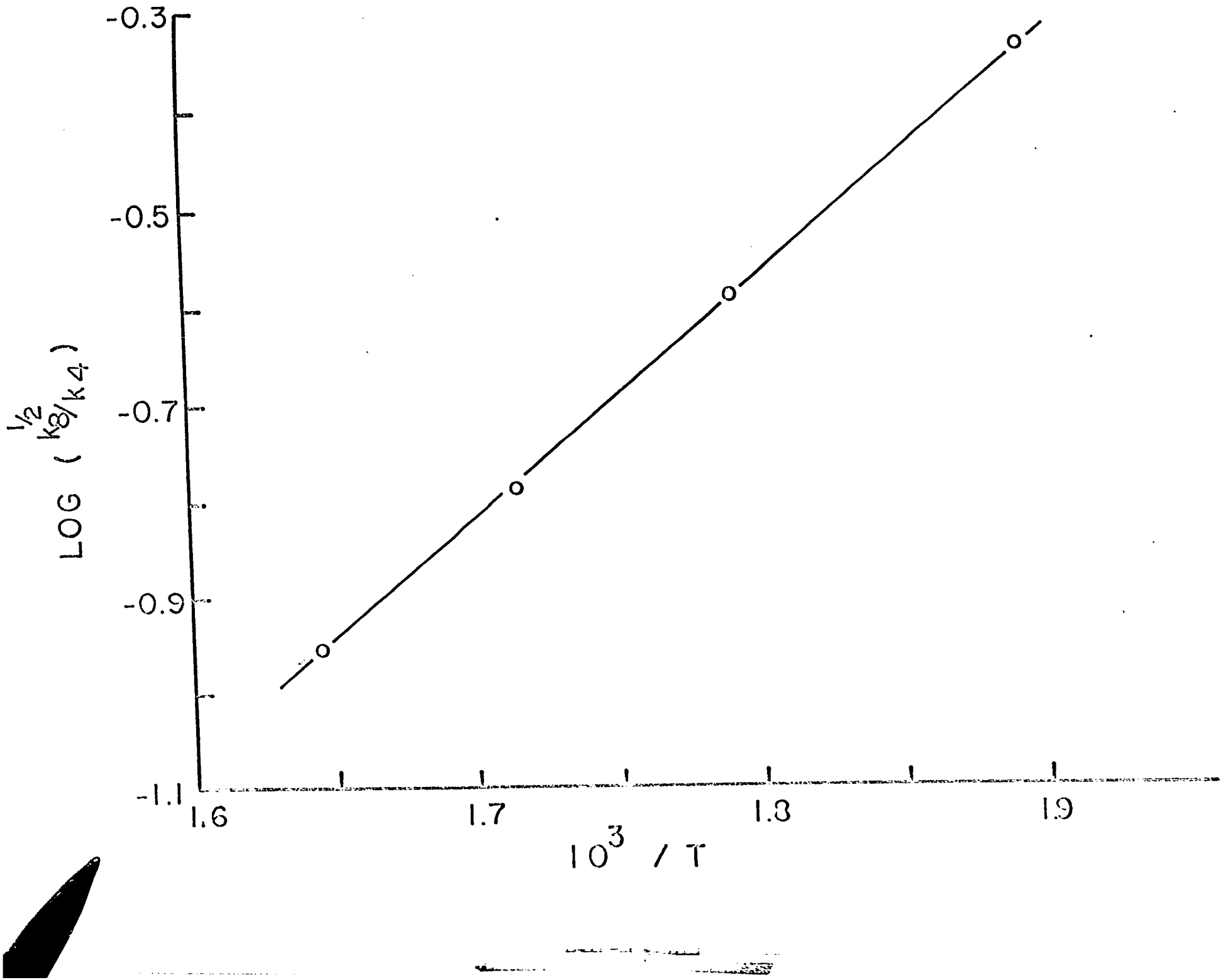
-0.3
-0.5
-0.7
-0.9
-1.1
LOG (k8/k4)^1/2
1.6
1.7
1.8
1.9
10^3 / T

and the rate constant is

$$k_4 = 4.9 \times 10^{11} \exp^{-11.5/RT} \text{ cc mole}^{-1}\text{sec}^{-1}$$

Production of Iso-Butene

Iso-butene is produced in the decomposition reaction of Nptl radicals. A yield-time relation for i-C_4H_8 production is shown in Figure 15. The yield is linear with time at low conversions and later deviates from linearity because of secondary reactions. Iso-C_4H_8 serves here as a quencher of H atoms, and the quenching results in the formation of C_4H_9 radicals, which give rise to secondary products. From Figure 15 it is seen that the deviation from linearity occurs when the concentration of i-C_4H_8 is in the range of 0.5 - 2.0×10^{-8} mole/cc. The lower limit is for low pressures; at higher pressures a high concentration of i-C_4H_8 is necessary for the deviation to be evident, because of suppression of the scavenging reaction by increasing the concentration of reactant.

The rate of i-C_4H_8 production in relation to the pressure of Nptn is shown in Figure 16. A double logarithmic plot of v_6 against pressure (Figure 17) shows that the reaction order changes from about 0.5 at low pressures to zero at high pressures. The rate of i-C_4H_8 production is expressed as $v_6 = k_6[\text{Nptl}]$. With the use of the expression for the steady-state concentration of Nptl radicals given by equation VI, the expression for v_6 has the following form:

$$v_6 = \frac{k_6}{2}\left[\frac{k_7^2}{k_9^2}[CH_3]^2 + \frac{2I_a\phi}{k_9} + \frac{2k_3}{k_9}[H][Nptn]\right]^{1/2} - \frac{k_6 k_7 [CH_3]}{2k_9}$$

The predominant term in brackets is $2k_3/k_9[H][Nptn]$ and the concentration of H atoms at lower pressures changes much less with change of pressure than the concentration of neopentane; the dependence of v_6 on $[Nptn]^{1/2}$ can be understood on this basis. At higher pressures [H] becomes inversely proportional to [Nptn]; the kinetics of formation of $i\text{-}C_4H_8$ are therefore zero order.

At the higher temperatures used in the present study, no dineopentyl was detected. The steady-state concentration of Nptl radicals for this case is expressed by equation VII. The rate of $i\text{-}C_4H_8$ production is

$$v_6 = k_6 \times [Nptn] \frac{(2k_3[H] + k_4[CH_3])}{k_6 + k_7[CH_3]}$$

according to which the reaction order of $i\text{-}C_4H_8$ production with respect to pressure of Nptn should change from 0.5 at low temperatures to 1.0 at high temperatures, over the range of pressure in which the rate constant k_6 is observed to be pressure-dependent.

A plot of the logarithm of v_6 for different temperatures, and at a pressure of 280 mm Hg, against the reciprocal of the temperature, is shown in Figure 18. The activation energy from the slope is 27.5 kcal/mole. Only at 230°C, 256°C and 286°C was the region of constant rate v_6 reached, so that in this case the activation energy obtained is less reliable.

REACTIONS OF NEOPENTYL RADICALS

In this part are considered only those reactions which gave products which it was possible to analyze. These include the combination reactions of two Nptl radicals, the combination of Nptl radicals with CH_3 radicals, and the decomposition of Nptl radicals.

Combination Reactions of Neopentyl Radicals

In the mechanism proposed for the primary reactions of the mercury-photosensitized decomposition of Nptn, Nptl radicals combine in reactions 7 and 9.

The dineopentyl produced in reaction 9 was found only at temperatures of 230°C and 256°C (and at 286°C in high conversion experiments), but only at 230°C was it possible to obtain the approximate initial rate. Some quantitative information concerning the amounts of Nptl radicals disappearing in reaction 9 can be obtained on the basis of the material balance. For the Nptl radicals, neglecting reactions 10 and 11, it follows that

$$2v_3 + v_4 = 2v_9 + v_6 + v_7 = 2v_9 + v_4 + 2v_7 + 2v_8$$

The ratios

$$\frac{2v_9 + v_6 + v_7}{2v_3 + v_4} \quad \text{and} \quad \frac{2v_9 + 2v_8 + v_4 + 2v_7}{2v_3 + v_4}$$

should therefore be equal to unity at all temperatures used in this study. For the reason mentioned above, the rate v_9 will not be included and the ratio

$$\frac{v_6 + v_7}{2v_3 + v_4}$$

will therefore express the fraction of Nptl radicals removed by reaction 6 and 7. The results are summarized in Table IV. On the basis of these results the conclusion can be drawn that at the temperature of 230°C approximately 85% of the Nptl radicals formed are removed by the combination reaction 9. At the temperature of 256°C the percentage is about 55, and at 286°C the ratio is close to 1.0, indicating that the combination of Nptl radicals in reaction 9 occurs only to a very small extent.

A comparison of the combination reactions 7 and 9 shows a striking difference as far as the effect of temperature is concerned. In the case of reaction 7 the rate of formation of neohexane increases with increase of temperature in the temperature region where an evident decrease of dineopentyl production was observed. The rate of neohexane production increases until the temperature of 310°C is reached. A further increase of temperature to 335°C causes a slight decrease of the rate, and it is expected that further increase of temperature will decrease the rate of neohexane production. Qualitatively similar phenomena were observed by Sato and Tsunashima (13). The observation can be explained on the basis of different thermal stabilities of dineopentyl and neohexane. It is believed that dineopentyl is much less stable than neohexane, and being formed in combination

TABLE IV

Experimental Results for Combination of Neopentyl Radicals

Temperature °C	Pressure mm Hg	$v_3\ 10^{12}$	$v_4\ 10^{12}$	$v_7\ 10^{12}$	$v_6\ 10^{12}$	$\frac{v_6 + v_7}{2v_3 + v_4}$
			mole cc^{-1} sec^{-1}			
230	36	27.5	0.37	4.5	4.12	0.155
230	104	37.5	1.20	4.5	5.88	0.139
230	240	38.1	2.47	4.5	6.93	0.141
256	27	20.1	1.37	11.5	8.73	0.480
256	110	35.0	6.60	11.5	21.2	0.430
256	225	36.5	10.70	11.5	22.4	0.410
286	50	28.6	10.80	26.6	43.9	1.03
286	112	33.1	26.40	26.6	61.3	1.01
286	230	35.7	41.20	26.6	80.3	0.96

reaction it can consequently decompose much more easily than the latter. The decomposition becomes faster with increase of temperature. On the basis of this discussion, and taking into account the experimental observation, it is concluded that the stability of neohexane is markedly affected at temperatures above 310°C.

In view of the approximate concentrations of CH_3 and Nptl radicals in Table III the concentration of CH_3 radicals is seen to rapidly increase with increase of temperature; at the same time the concentration of Nptl radicals slightly decreases. This effect favors the combination of CH_3 radicals with Nptl radicals with respect to combination of two Nptl radicals.

It is also expected that there is some difference in the duration of collisions between two Nptl radicals and that of CH_3 radicals with Nptl radicals. If the time of combination of two Nptl radicals is greater there is a higher probability for a Nptl radical to decompose during the collision of two Nptl radicals, than during the collision of CH_3 radicals with Nptl radicals.

The increase of temperature from 310° to 335°C caused almost no change in the rate of production of neohexane. It is believed that at these temperatures, the lifetime of the Nptl radical is approaching the time between the collision of CH_3 radicals and Nptl radicals. Another increase of temperature will again decrease the lifetime of the Nptl radical, and

the rate of neohexane production is expected to decrease with increase of temperature.

Decomposition of Neopentyl Radicals

Up to now there have been only a few studies dealing with decomposition of Nptl radicals. Anderson and Benson (16) investigated the reaction in a study of the pyrolysis of Nptn in the presence of HCl. In this system the Nptl radical is produced in the course of hydrogen abstraction from Nptn by a Cl atom. The rate constant for the decomposition of a Nptl radical into i-C_4H_8 and the CH_3 radical at 742°K was found to be $10^{3.3\pm0.3}$ sec^{-1}. For the activation energy and the pre-exponential factor the following value was assigned:

$$\log A = 13\pm1 \quad \text{and} \quad E = 34\pm3.5 \text{ kcal/mole.}$$

It would appear that the activation energy is overestimated; the upper limit is almost in the region of the activation energies for the decomposition of an alkyl radical into olefin and H atom. The low limit should therefore be taken as more probable.

Sato and Tsunashima (13) studied the mercury-photosensitized decomposition of Nptn. On the basis of the initial rates of i-C_4H_8 and methane production they deduced for the activation energy of decomposition of the Nptl radical the value 17.0±2 kcal/mole. This value is probably too low and is comparable with the present limiting value, E^o, for decomposition at zero pressure.

In the Nptn molecule, there is only one kind of C-H bond, i.e., there are only primary hydrogens. In the initial act of photosensitization there is therefore formed only one kind of alkyl radical, i.e., Nptl radical. This avoids complications found in systems where different types of alkyl radicals are formed in the initial act. As far as decomposition is concerned, there is only one reaction that can occur, viz

$$\text{Nptl} \rightarrow \text{i-}C_4H_8 + CH_3$$

This means that at least at higher pressures this reaction is the only source of i-C_4H_8. Then, from material balance it follows that

$$v_6 = 2v_8 + v_7 + v_4$$

On the basis of this expectation the ratio

$$\frac{v_6}{2v_8 + v_7 + v_4}$$

should be equal to 1. The results in Table V show that this ratio is close to unity at all of the temperatures used. The results are taken only for pressures above 100 mm Hg, where it is assumed that the atomic cracking reaction is negligible as an additional source of CH_3 radicals.

To obtain information concerning the rate constant of the decomposition of Nptl radicals, the expression for the rates of reactions 4, 6, and 7 were taken into consideration. Thus:

TABLE V

Experimental Data for the Decomposition of Neopentyl Radicals

Temperature °C	Pressure mm Hg	$v_4 \times 10^{12}$	$v_8 \times 10^{12}$	$v_7 \times 10^{12}$	$v_6 \times 10^{12}$	$\frac{v_6}{v_4+v_7+2v_8}$
			mole cc^{-1} sec^{-1}			
230	104	1.2	-	4.5	5.88	1.04
230	240	2.47	-	4.5	6.93	1.00
256	110	6.6	0.895	11.5	20.2	1.06
256	225	10.7	0.67	11.5	22.4	0.95
286	150	36.5	3.71	26.6	75.0	1.05
286	230	41.2	3.24	26.6	80.1	1.06
310	115	68.6	11.5	33.9	120.4	0.96
310	232	115.0	10.1	33.9	163.0	0.97
335	115	158.6	26.5	33.8	237.0	0.99
335	245	272.7	24.4	33.8	353.0	1.00

$$v_4 = k_4[\text{Nptn}][CH_3]$$

$$v_6 = k_6[\text{Nptl}]$$

$$v_7 = k_7[\text{Nptl}][CH_3]$$

These rates were obtained by measuring the amounts of methane, i-C_4H_8 and neohexane respectively. Using the above expressions the following ratio can be obtained:

$$\frac{v_4 v_6}{v_7} = \frac{k_4[\text{Nptn}][CH_3] \times k_6[\text{Nptl}]}{k_7[\text{Nptl}][CH_3]} = \frac{k_4 k_6}{k_7} \times [\text{Nptn}]$$

and

$$\frac{k_4 k_6}{k_7} = \frac{v_4 v_6}{v_7} \times \frac{1}{[\text{Nptn}]}$$

To evaluate the rate constant of decomposition of an alkyl radical, the rate of decomposition is usually related to the rate of dimer formation. In the present study the rate of dimer formation was obtained only at 230°C. Another possibility is to use $v_8^{1/2}$ instead of v_4, but in the present study an unmeasurable amount of ethane was formed at 230°C and also at 256°C at pressures below 10 mm Hg; only three values are therefore available for the low pressures limiting rates.

A log-log plot of the ratio of the constants against the concentration of Nptn is shown in Figure 23. Reaction 4 is hydrogen abstraction by CH_3 radicals, and so k_4 is assumed to be pressure independent. Reaction 7 is the combination

FIGURE 23

A double logarithmic plot of k_4k_6/k_7 against the pressure of neopentane.

A	335°C
B	310°C
C	286°C
D	256°C
E	230°C

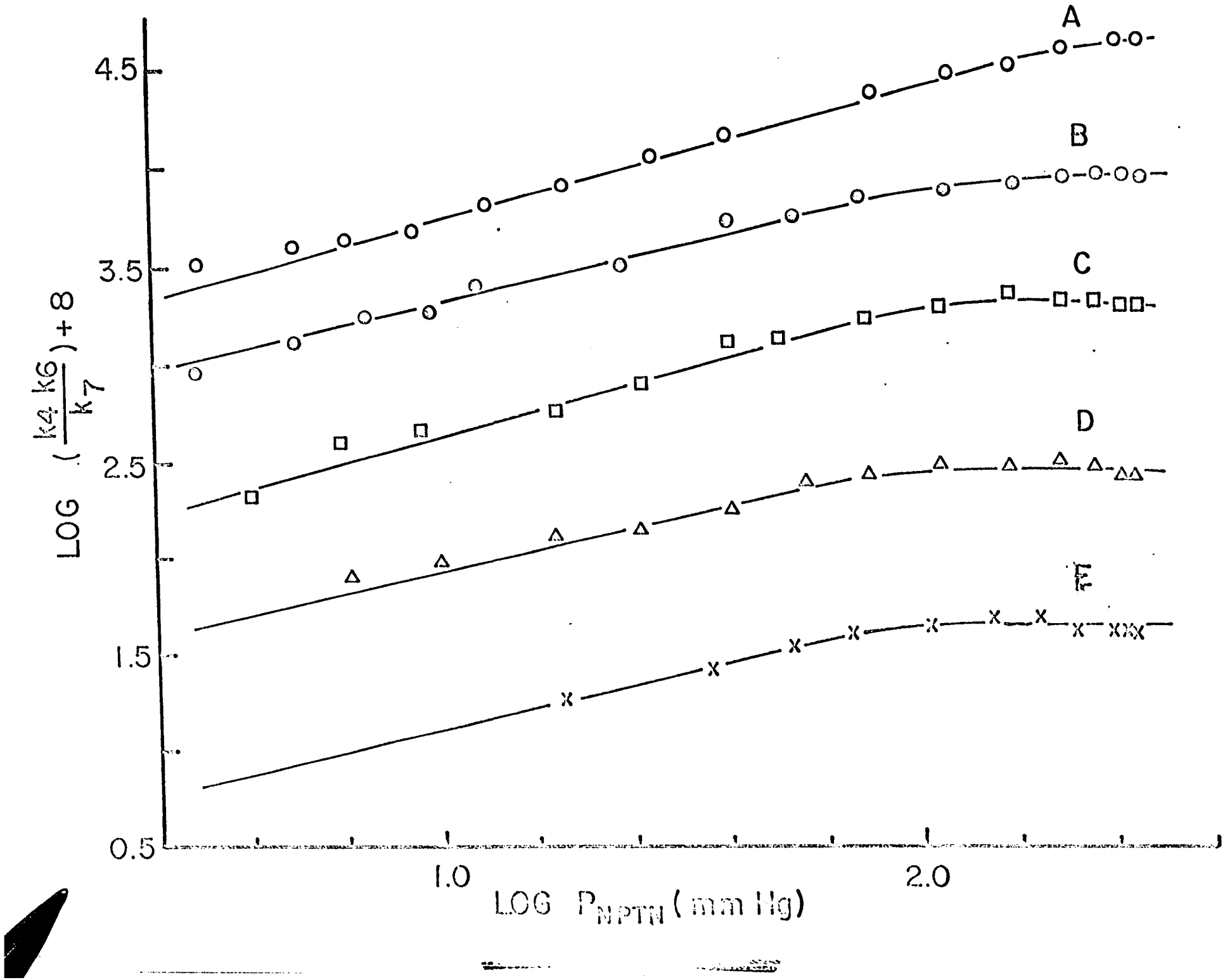
A
B
C
D
E
4.5
3.5
2.5
1.5
0.5
1.0
2.0
LOG $\left(\frac{k_4 k_6}{k_7}\right)+8$
LOG P_{NPTN} (mm Hg)

reaction of Nptl radicals with CH_3 radicals. In view of calculations of Rabinovitch and Setser (29) that the fall-off pressure of the CH_3 with C_2H_5 radical recombinations will be shifted to lower pressures by a factor of 300 with respect to the combination of two CH_3 radicals, we can assume that the combination of Nptl and CH_3 radicals is independent of pressure over the whole pressure range employed. This means that the observed pressure dependence must arise only from the dependence of k_6 on the concentration of the reactant.

The average values of k_6 at different temperatures and pressures are listed in Table VI. These values were calculated assuming $k_7 = 2.2 \times 10^{13}$ and taking for k_4 the values obtained in the present study.

The log-plot of k_4k_6/k_7 against the reciprocal of temperature is shown in Figure 24. The ratio is taken at pressure of 280 mm Hg. The slope gives for the total activation energy the value of 40.1 kcal/mole, i.e.,

$$E_4 + E_6 - E_7 = 40.1 \text{ kcal/mole}$$

Taking for $E_4 = 11.5$ kcal/mole as obtained in the present study, and assuming no activation energy for reaction 7,

$$E_6 = 28.6 \text{ kcal/mole}$$

From the intercept of the figure the preexponential factor is calculated assuming $A_4 = 10^{11.7}$ cc mole^{-1} sec^{-1} as obtained in the present study and $A_7 = 10^{13.34}$ cc mole^{-1} sec^{-1} (31).

TABLE VI

Rate Constants for Decomposition of Nptl

Radicals at Different Temperatures and Pressures

Pressure	Rate Constant, k_6 sec^{-1}				
mm Hg	230°C	256°C	286°C	310°C	335°C
10	0.56	2.19	6.2	18.2	29.6
20	0.76	3.15	10.02	28.7	53.3
30	1.08	3.84	13.9	36.3	74.6
50	1.36	5.20	16.8	47.6	105.5
70	1.68	6.11	23.6	58.4	133.2
90	2.12	6.80	26.8	64.2	150.1
110	2.2	6.88	30.1	70.4	173.4
175	2.2	6.88	33.6	77.4	236.7
225	2.2	6.88	33.6	79.4	265.4
280	2.2	6.88	33.6	79.4	297.8

FIGURE 24

Logarithm of k_4k_6/k_7 against the reciprocal of temperature.

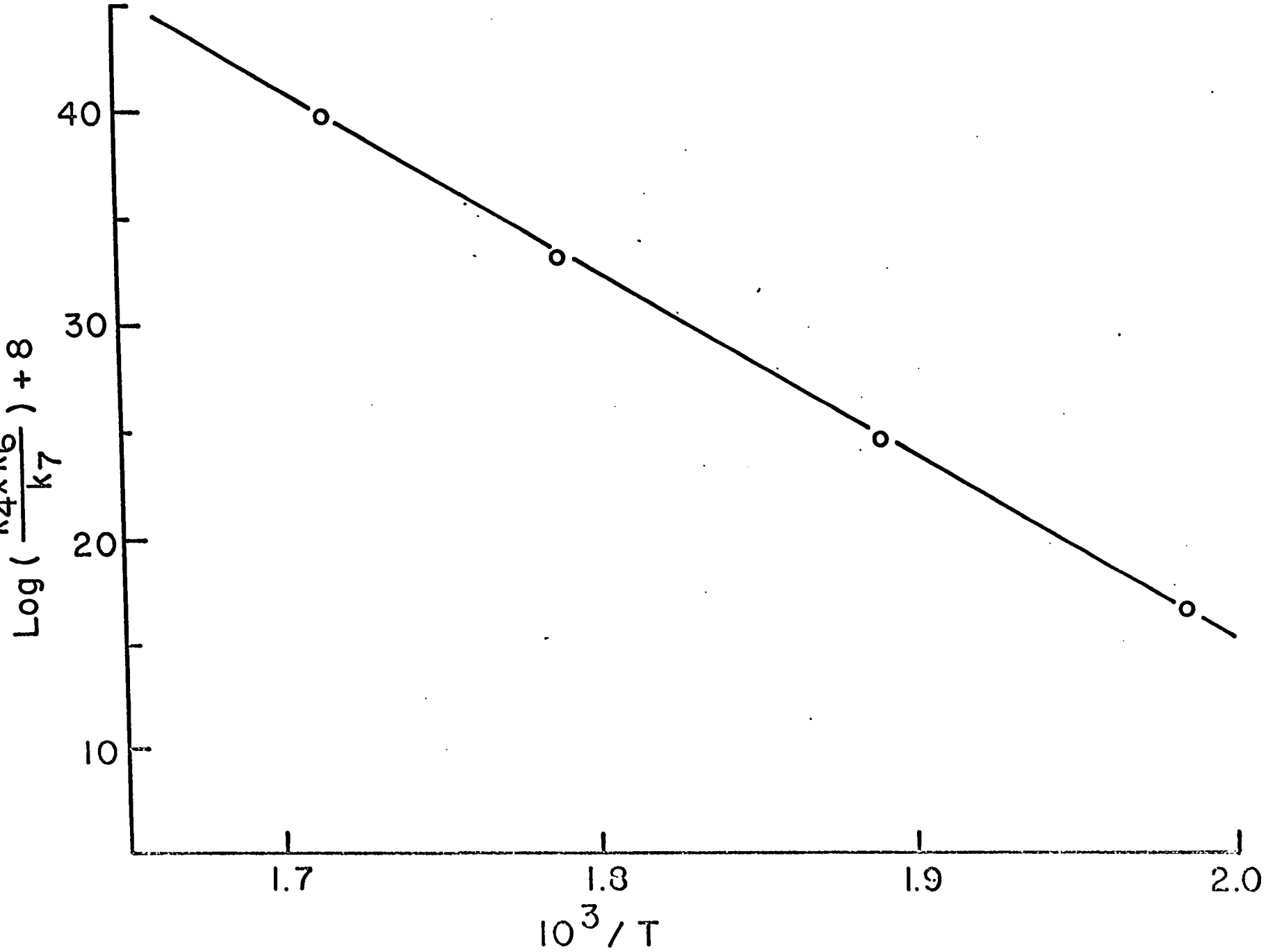
40
30
20
10
Log (k4 x k6 / k7) + 8
1.7
1.8
1.9
2.0
10^3 / T

The preexponential factor A_6 is then $10^{13.4}$ sec^{-1} and the rate constant for the decomposition of the Nptl radical k_6 is

$$k_6 = 2.3 \times 10^{13} e^{-28.6/RT} sec^{-1} .$$

To evaluate the limiting high and low pressure rates, extrapolation of the plot of k^{-1} against $[Nptn]^{-1/2}$ was used as proposed by Schlag and Rabinovitch (30). The usual extrapolation plot, k^{-1} against $[Nptn]^{-1}$ gives a good estimate of high-pressure limiting rates only for these cases where the data were extended essentially to the high-pressure limit. In this study, for reasons discussed previously, the highest pressure used was 280 mm Hg. The plot of k^{-1} against $[Nptn]^{-1/2}$ gives a more linear extrapolation. The use of this plot is illustrated in Figure 25 for the temperature of 310°C. There were some difficulties at the temperature of 230°C in evaluating the low-pressure limiting rate, because the experiments could not be carried out at low pressures as a result of inaccurate analysis; the data were adjusted to fit the Arrhenius plot.

From the intercept in Figure 25 the value of $k_7/k_4k_6^{\infty}$ is obtained, while from the slope of the linear part $k_7/k_4k_6^{o}$ is obtained. The Arrhenius plots of k_4k_6/k_7^{∞} and k_4k_6/k_7^{o} are shown in Figures 26 and 27 respectively. From the slope in Figure 24 the activation energy of 40.5 is obtained, i.e.,

$$E_6^{\infty} + E_4 - E_7 = 40.5 \text{ kcal/mole}$$

With the use of $E_7 = 0$ kcal/mole and of $E_4 = 11.5$ kcal/mole, as obtained in the present study, then $E_6^{\infty} = 29.0$ kcal/mole.

FIGURE 25

A relation of k_7/k_4k_6 against $1/[\text{Nptn}]^{1/2}$ for temperature of 310°C.

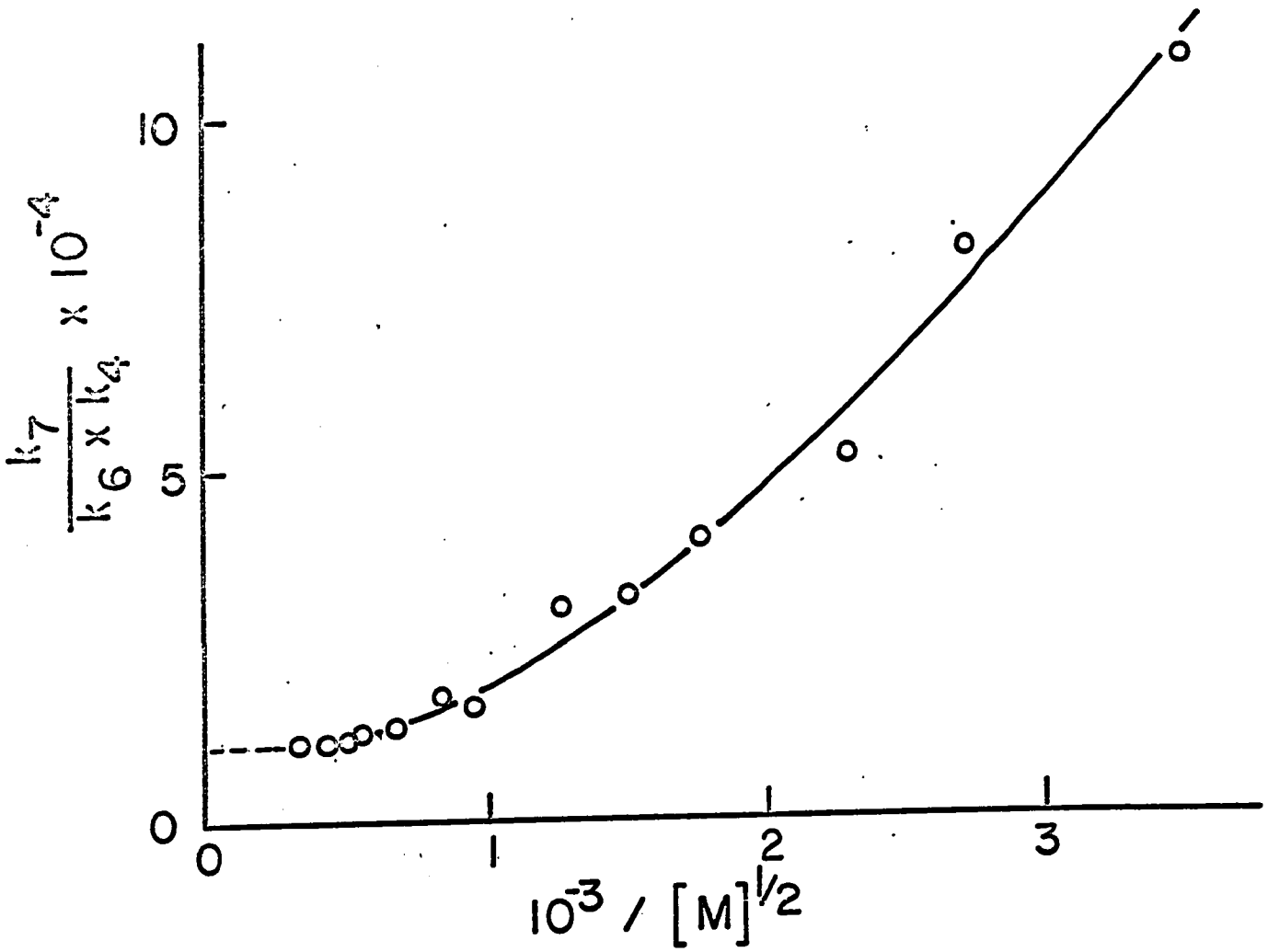
$\frac{k_7}{k_6 \times k_4} \times 10^{-4}$
10
5
0
0
1
2
3
$10^{-3} / [M]^{1/2}$

From the intercept in Figure 26, and with $A_7 = 10^{13.34}$ cc mole^{-1} sec^{-1} and $A_4 = 10^{11.7}$ cc mole^{-1} sec^{-1}, the pre-exponential factor $A_6^\infty = 2.5 \times 10^{13}$ sec^{-1} and the high-pressure limiting rate constant can be expressed as

$$k_6^\infty = 2.5 \times 10^{13} \, e^{-29.0/RT} \text{ sec}^{-1}$$

This preexponential factor, when compared with those for other decomposition reactions of alkyl radicals, falls at the lower end of the scale. This means that the entropy of the transition state is also low. In the case of the Nptl radical it is possible that there are some restrictions to free rotation of the CH_3 group which is in process of being separated from the Nptl radical; one should therefore assign for the CH_3 group much stiffer torsional motions resulting in a decrease of entropy and a much stiffer activated complex.

The preexponential factor for a unimolecular reaction is given by transition-state theory by the expression

$$A = (ekT/h) \, e^{\Delta S^\ddagger/R}$$

and so $\Delta S^\ddagger = 2.3 \times R(\log A - \log ekT/h)$ where $\Delta S^\ddagger$ is the entropy of activation, k Boltzmann's constant and h Planck's constant. The value of ekT/h at 550°K is $10^{13.5}$ and taking for $A = 10^{13.4}$ the entropy of activation $\Delta S^\ddagger = -0.46$ (standard state 1 mole/cc). The negative entropy of activation in decomposition of alkyl radicals is quite unusual and indicates a stiff activated complex.

FIGURE 26

Logarithm of $k_6^{\infty} k_4 / k_7$ against reciprocal of temperature.

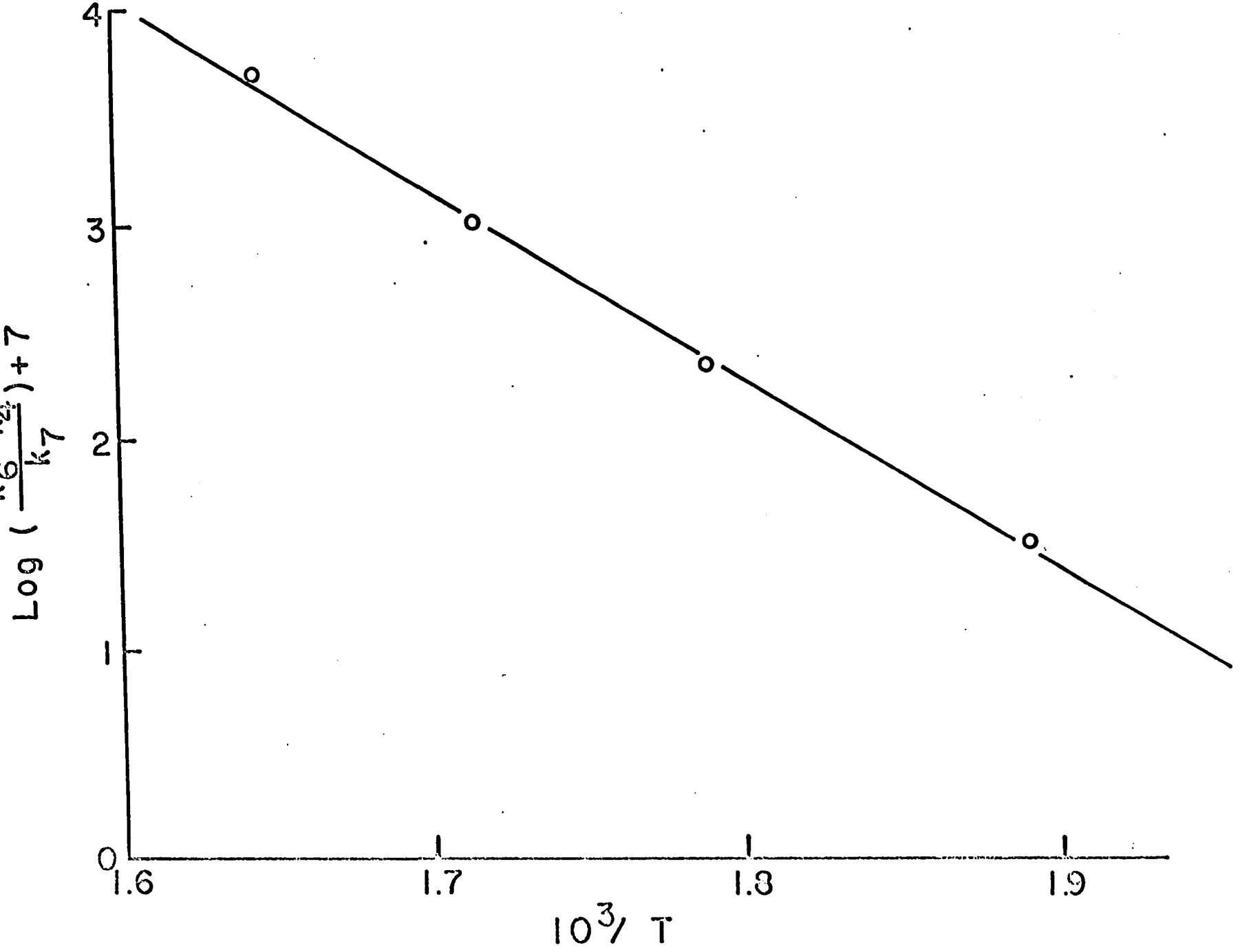
4
3
2
1
0
Log ($\frac{k_6^8 k_4}{k_7}$) + 7
1.6
1.7
1.8
1.9
$10^3/T$

The low-pressure limiting rate constant is obtained from slopes in the linear part of the plots, as for example in Figure 25 for the temperature of 310°C. The slope is equal to $k_7/k_4k_6^\circ$. An Arrhenius plot of the reciprocal of these ratios at different temperatures, i.e., $k_4k_6^\circ/k_7$, is shown in Figure 27. The slope gives an activation energy of 28.6 kcal/mole, so that

$$E_6^\circ + E_4 - E_7 = 28.6 \text{ kcal/mole}$$

Again, with $E_7 = 0$ and no pressure dependence for E_4, it is calculated that $E_6^\circ = 17.1$ kcal/mole. From the intercept of Figure 27 the preexponential factor is calculated to be

$$A_6^\circ = 5.8 \times 10^{10} \text{ cc mole}^{-1} \text{ sec}^{-1}$$

and the low-pressure limiting rate constant can be expressed as

$$k_6^\circ = 5.8 \times 10^{10} \exp(-17.1/RT) \text{ cc mole}^{-1} \text{ sec}^{-1} .$$

FIGURE 27

Logarithm of $k_6^o k_4 / k_7$ against reciprocal of temperature.

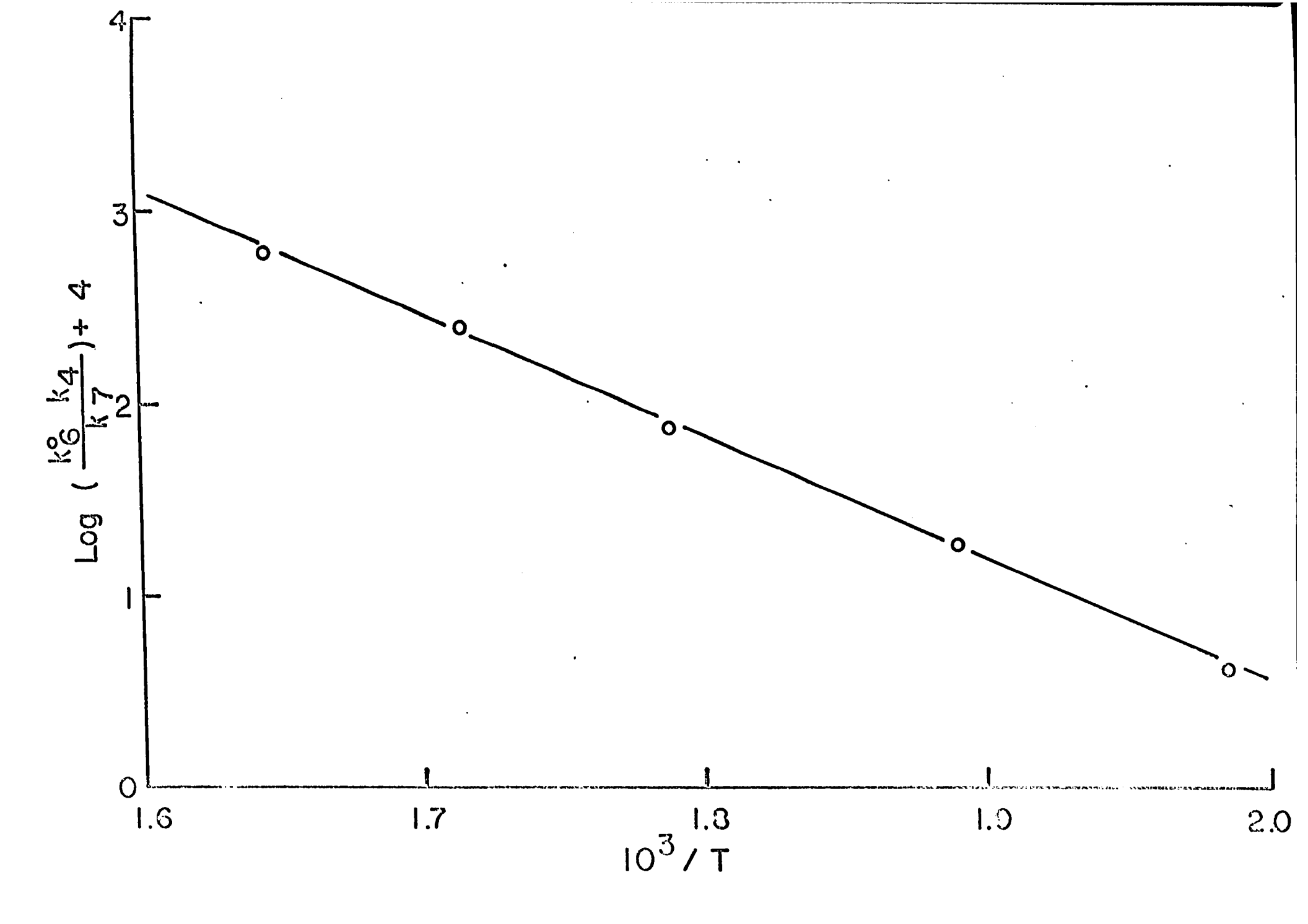
4
3
2
1
0
Log ($\frac{k_6^o k_4}{k_7}$) + 4
1.6
1.7
1.8
1.9
2.0
$10^3 / T$

THERMOCHEMISTRY

Knowledge of the value of E_6^{∞} and of the activation energy for the reverse reaction, i.e., the addition of CH_3 radicals to i-C_4H_8, enables us to calculate the heat of formation of Nptl radicals. The activation energy E_{-6} was found (32) to be 8.3 kcal/mole. These activation energies are related to the enthalpy change of the reaction

$$\text{Nptl} \rightarrow CH_3 + \text{i-}C_4H_8$$

by the expression

$$\Delta H_6(T) = E_6 - E_{-6} + \Delta nRT$$

The coefficient Δn is in this case equal to unity because two species are formed from one in the decomposition reaction.

Enthalpy changes at other temperatures can be obtained by use of the relationship

$$\Delta H_6(T) = \Delta H_6(0^{\circ}K) + \int_0^T \Delta Cp \, dT$$

where $\Delta H_6(0^{\circ}K)$ is the enthalpy change of the reaction at $0^{\circ}K$. The integral $\int \Delta Cp \, dT$ shows the change of ΔH° in changing the temperature of the system from $0^{\circ}K$ to $T^{\circ}K$. There are some complications in evaluating this integral because of lack of heat capacities as a function of temperature. Another possibility is to use heats of formation of the Nptl radical, the CH_3 radical and i-C_4H_8; however, the heat of formation of Nptl is not available. To obtain at least some approximate

value of the integral, it is usual to take, instead of the radical, some compound which is assumed to have a similar change of heat capacities to the radical concerned. In the present work, instead of the Nptl radical Nptn was used; the values of the integral at different temperatures are summarized in Table VII. The enthalpy change obtained from the experimental results is related to a temperature of 550°K, which is considered to be the middle of the temperature range used. The heats of formation at 550°K for Nptn, CH_3 and i-C_4H_8 were obtained by extrapolation of the data of Rossini et al (35).

Taking into consideration both expressions for enthalpy change and the values of the integral, the enthalpy change of the reaction at 0°K is obtained from the expression

$$\Delta H_6(0^\circ K) = E_6 - E_{-6} + RT - \int_0^T \Delta Cp \, dT$$

With the value of 1.1 kcal/mole for RT, with E_6 = 29.0 kcal/mole, E_{-6} = 8.3 kcal/mole, and the integral = 2.8 kcal/mole, the enthalpy change at 0°K, i.e., $\Delta H_6(0^\circ K)$ is calculated to be 19.0 kcal/mole.

From the enthalpy change $\Delta H_6(T)$, it is possible to calculate at various temperatures the heat of formation of the Nptl radical,

$$\Delta H_T^\circ(\text{Nptl}) = \Delta H_T^\circ(CH_3) + \Delta H_T^\circ(\text{i-}C_4H_8) - \Delta H_6^\circ(T)$$

The heats of formation of the Nptl radical at different temperatures are listed in the fourth column of Table VII.

TABLE VII

Thermodynamic Quantities at Different Temperatures

Temp. ^{o}K	$\int_{o}^{T} \Delta CpdT$ kcal/mole	ΔH_6 kcal/mole	ΔH_f(Nptl) kcal/mole	ΔH_f(Nptl-H) kcal/mole
0	0	19.0	14.7	97.6
298.2	2.3	21.3	6.7	98.5
550	2.8	21.8	2.2	98.9

In the literature (33) there is listed the heat of formation of the Nptl radical only at a temperature of 298.2°K, and this agrees with the value obtained in the present study.

In the last column of Table VII there is listed the enthalpy change for the reaction

$$\text{Nptn} \rightarrow \text{Nptl} + \text{H}$$

i.e., the bond dissociation energy of the C-H bond in Nptn at different temperatures. These values were calculated using the expression

$$\Delta H_f(\text{Nptl-H}) = \Delta H_f(\text{Nptl}) - \Delta H_f(\text{Nptn}) + \Delta H_f(\text{H})$$

A previous value of the bond dissociation energy of the C-H bond in Nptn at 298.2°K is 99.0 kcal/mole (33), in good agreement with the present value.

The rate constants for the forward and the reverse reactions, i.e., the unimolecular decomposition of Nptl radicals and the addition of CH_3 radicals to i-C_4H_8, are related by the equilibrium constant

$$k_6/k_{-6} = A_6/A_{-6}\ e^{-(E_6 - E_{-6})/RT}$$

and so

$$\Delta S_6 = R\ln(A_6/A_{-6})$$

Knowledge of both preexponential factors enables us to calculate the entropy change of the reaction. With $A_6 = 10^{13.4}$ and $A_{-6} = 10^{11.4}$ (34)

$$\Delta S_6 = 2.3 \times R \log(10^{13.4}/10^{11.4}) = 8.8 \text{ cal deg}^{-1}\text{mole}^{-1}$$

for standard state 1 mole cc^{-1}, or 28.0 cal deg^{-1} $mole^{-1}$ for standard state 1 atm. With use of the entropy change and entropies of CH_3 radicals and i-C_4H_8 (35), the entropy of Nptl radicals at 550°K is calculated from the expression

$$\Delta S_6 = S\ (CH_3) + S\ (i\text{-}C_4H_8) - S\ (\text{Nptl})$$

and S (Nptl) = 109.5 cal deg^{-1} $mole^{-1}$ (standard state 1 atm). The entropies of i-C_4H_8 and CH_3 radicals at 550°K were obtained from the data (35) by extrapolation.

The thermochemical data obtained in this study are approximate owing to the fact that there is no experimental value of E_{-6} available.

As far as the values of activation energies obtained in this work are concerned, the errors in calculating these values result from errors in the measured initial rates used for calculating the ratios of rate constants. It is believed that the errors in the rate measurements to some extent cancel in the ratios of rate constants, and that the expected accuracy is better than within 1 kcal/mole.

CHAPTER IV

SECONDARY REACTIONS

In this chapter are considered those products of the photosensitized decomposition of Nptn whose yield-time plots show induction periods. These products are: ethylene, propylene, propane, i-C_4H_{10}, 2,2,3,3-tetramethylbutane (2,2,3,3-TMB) and 2,2,4,4-tetramethylpentane (2,2,4,4-TMP). Because of the simplicity of the primary reactions, it was possible to analyze these secondary products and so to obtain information concerning their origin. As was shown in the preceding chapter, the yield-time plots of the primary products were linear only in the early stages; there were later deviations from linearity because of secondary reactions occurring.

Because of the very high quenching cross sections of the hydrogen molecule with respect to $Hg(^3P_1)$ atoms (3), it is expected that hydrogen formed in the early stages of the experiments, after reaching a certain concentration, will effectively quench the mercury atoms and consequently decompose. Hydrogen atoms present react with olefins (37), in this case i-C_4H_8, which is produced in the course of the decomposition of Nptl radicals. The rate of scavenging of H atoms by an olefin increases with decrease of the ratio alkane/olefin (38). Addition of H atoms to olefin leads to the formation of so-

called "hot" radicals having some excess of energy with respect to both C-C and C-H bond rupture; however, the excess is much higher with respect to C-C than to C-H split. In certain pressure regions the activated radicals are deactivated by collisions with molecules and then undergo their usual reactions (39,40) such as combination, disproportionation and hydrogen abstraction.

In an early study on the photosensitized hydrogenation of i-C_4H_8 (41) at 23°C, the following products were analyzed: i-C_4H_{10} (52.2%), CH_4 (15.2%), 2,2,3,3-TMB (12.2%), neopentane (11.7%); as minor products were observed ethylene, ethane, propylene and propane. It was believed that the sole product of the addition of H atoms to i-C_4H_8 are t-C_4H_9 radicals; i-C_4H_9 radicals are either not formed at all or they decompose or isomerize before reacting. At 300°C a small amount of 2,4,4-trimethyl pentene-1 was detected. The photosensitized hydrogenation of i-C_4H_8 was also studied with the object of obtaining information concerning the disproportionation/combination ratio of t-C_4H_9 radicals (42). As far as the product composition is concerned, qualitative agreement was obtained with previous work (41). The value obtained for k_d/k_c was 2.2±0.3.

MECHANISM AND DISCUSSION

The most likely reactions leading to the secondary products are as follows:

$H + i\text{-}C_4H_8$	→	$t\text{-}C_4H_9^*$	1
	→	$i\text{-}C_4H_9^*$	2
$t\text{-}C_4H_9^* + M$	→	$t\text{-}C_4H_9 + M$	3
$i\text{-}C_4H_9^* + M$	→	$i\text{-}C_4H_9 + M$	4
$t\text{-}C_4H_9^*$	→	$i\text{-}C_4H_8 + H$	5
	→	$CH_3 + C_3H_6$	6
$i\text{-}C_4H_9^*$	→	$i\text{-}C_4H_8 + H$	7
	→	$CH_3 + C_3H_6$	8

As was seen in the preceding chapter, extensive scavenging of H atoms by $i\text{-}C_4H_8$ begins only after a sufficient amount of the olefin has been produced. In the addition of H to $i\text{-}C_4H_8$ two kinds of alkyl radicals are formed, $t\text{-}C_4H_9^*$ and $i\text{-}C_4H_9^*$. The formation of excited $i\text{-}C_4H_9^*$ radicals is proved by the presence of propylene which arises only from decomposition of the radical. The assumption is sometimes made of isomerization of the $t\text{-}C_4H_9$ radical into the $i\text{-}C_4H_9$ radical (13), as the origin of C_3H_6 formation. However, in studies of $sec\text{-}C_4H_9$, $i\text{-}C_4H_9$ and C_3H_7 radicals (43,44,45,46) the isomerization of alkyl radicals was negligible and the evidence now available (34) is against the isomerization of

C_3 and C_4 alkyl radicals. In the present case it is also assumed that isomerization does not occur or at least is negligible. All $i\text{-}C_4H_9^*$ radicals then arise from the quenching of H atoms by $i\text{-}C_4H_8$, and the origin of C_3H_6 is decomposition of the radicals. Iso-$C_4H_9^*$ radicals will decompose predominantly by reaction 8. Nesby and co-workers (43) found that even up to 540°C the decomposition of $i\text{-}C_4H_9$ radicals occurs mostly by elimination of CH_3 radicals. If the isomerization of $t\text{-}C_4H_9^*$ radicals into $i\text{-}C_4H_9^*$ radicals is neglected it is expected that $t\text{-}C_4H_9^*$ will decompose by C-H bond split.

The predominant mode of decomposition of $n\text{-}C_3H_7$ radicals is C-C bond rupture leading to the formation of C_2H_4 and CH_3 radicals; for $i\text{-}C_3H_7$ radicals the decomposition occurs mostly by C-H bond split, as is the case with $i\text{-}C_4H_9$ and $t\text{-}C_4H_9$ radicals. It was found that the rate of decomposition of the "hot" $n\text{-}C_3H_7$ radical is about 100 times as fast as that of the "hot" $i\text{-}C_3H_7$ radical, if $n\text{-}C_3H_7$ decompose by C-C split and $i\text{-}C_3H_7$ by C-H bond split (47). It is also expected that decomposition of $i\text{-}C_4H_9^*$ radicals will be much faster than that of $t\text{-}C_4H_9^*$ radicals, so that there is a much greater possibility for $t\text{-}C_4H_9^*$ to be stabilized than for $i\text{-}C_4H_9^*$ radicals. It can then be assumed that the most of the $i\text{-}C_4H_9^*$ radicals will decompose before being stabilized by a collision with a molecule.

If the observed products are taken into account it is possible to propose other reaction steps involving stabilized radicals:

$2\ t\text{-}C_4H_9$	→	C_8H_{18} (2,2,3,3-TMB)	9
	→	$i\text{-}C_4H_8 + i\text{-}C_4H_{10}$	10
$t\text{-}C_4H_9 + Nptn$	→	$i\text{-}C_4H_{10} + Nptl$	11
$t\text{-}C_4H_9 + Nptl$	→	C_9H_{20} (2,2,4,4-TMP)	12
$t\text{-}C_4H_9 + CH_3$	→	Nptn	13
$t\text{-}C_4H_9 + CH_3$	→	$CH_4 + i\text{-}C_4H_8$	14

It is expected that reaction of H atoms with $t\text{-}C_4H_9$ radicals will also taken place in this system. However, no qualitative evidence can be obtained from the present results and so these reactions are not included in the scheme.

As minor products analyzed were: ethylene, propylene and propane. As was shown above, propylene arises from the decomposition of "hot" $i\text{-}C_4H_9^*$ radicals in reaction 6. The propylene produced is consequently scavenged by H atoms leading to the formation of "hot" propyl radicals. According to Bradley and co-workers (48), more than 93% of the addition of H atoms to propylene leads to i-propyl radical. Addition leading to $n\text{-}C_3H_7$ radicals is suggested by the presence of C_2H_4 which arises from decomposition of the "hot" n-propyl radicals. The following scheme for reactions of propyl radicals can be proposed:

$C_3H_6 + H$	→	$i\text{-}C_3H_7^*$	15
	→	$n\text{-}C_3H_7^*$	16

$i\text{-}C_3H_7^*$	→	$C_3H_6 + H$	17
$n\text{-}C_3H_7^*$	→	$CH_3 + C_2H_4$	18
$i\text{-}C_3H_7^* + M$	→	$i\text{-}C_3H_7 + M$	19
$n\text{-}C_3H_7^* + M$	→	$n\text{-}C_3H_7 + M$	20
$2\ C_3H_7$	→	$C_3H_8 + C_3H_6$	21
	→	C_6H_{14}	22
$C_3H_7 + Nptn$	→	$C_3H_8 + Nptl$	23

where M is as previously the parent neopentane molecule.

On the assumption that isomerization of $i\text{-}C_3H_7^*$ radicals to $n\text{-}C_3H_7^*$ radicals does not occur, it is believed that the ethylene observed arose only from decomposition of "hot" $n\text{-}C_3H_7^*$ radicals formed by addition of H atoms to C_3H_6. The amount of ethylene produced accounts for 11 to 14% of all C_2 and C_3 secondary products analyzed. This indicates that addition of H atoms to C_3H_6, leading to $n\text{-}C_3H_7$ radicals, occurs to a greater extent than was observed (48). However, it is necessary to take into consideration the fact that some of the C_3H_7 radicals were removed in combination reactions, the products of which it was not possible to analyze; the amount will then be smaller.

From the present results it is possible, with some assumptions, to obtain at least approximate information concerning the relative rates of addition of H atoms to $i\text{-}C_4H_8$ with the formation of $i\text{-}C_4H_9^*$ and $t\text{-}C_4H_9^*$ radicals. As was

shown above, all of the ethylene, propylene and propane have their origin in "hot" i-$C_4H_9^*$ radicals. In Table VIII it is seen that all these products account for about 3% of all the C_4H_9 radicals removed in the secondary reactions at 310°C. At lower temperatures the analyses are inaccurate because only small amounts of these products are formed. As was said before, some of the C_3H_7 radicals are removed in combination reactions the products of which were not analyzed. On the other hand, in the calculation are not included the t-C_4H_9 radicals removed in reactions 13 and 14. From the present results it is not possible to get quantitative information concerning these two effects, which compensate each other; the calculated ratio of i-C_4H_9 and t-C_4H_9 radicals formed by addition of H atoms to i-C_4H_8 should be considered as approximate.

Production of Iso-Butane and 2,2,3,3-TMB

Typical yield-time plots for i-C_4H_{10} production are shown in Figures 28 and 29 for temperatures 256°C and 310°C respectively. The plots show an induction period which decreases with increase of temperature. It was only possible to obtain the maximal rate of i-C_4H_{10} production, from the slopes in the linear region. In Figure 29 it is shown that the maximal rate is constant at pressures above 54 mm Hg at 310°C. The dependence of the maximal rate of i-C_4H_{10} production, calculated from the slopes of the linear portions of Figure 29, on pressure is shown in Figure 30. The pressure dependence of lower pressures can be attributed to decrease of deactivation of "hot" t-C_4H_9 radicals, i.e., an increasing fraction of the t-$C_4H_9^*$ radicals

TABLE VIII

The yields of secondary products

Temperature °C	Pressure mm Hg	Time sec.	C_2H_4	C_3H_6	C_3H_8	i-C_4H_{10}	2,2,3,3-TMB
			moles per reaction vessel x 10^7				
310	40	1000	n.m.	0.52	n.m.	4.4	n.m.
310	40	2000	0.12	0.76	0.23	11.3	3.4
310	40	3000	0.20	0.83	0.38	14.8	6.1
310	115	1000	n.m.	0.55	n.m.	4.9	n.m.
310	115	2000	0.11	0.80	0.20	12.1	3.2
310	115	2500	0.18	0.88	0.28	13.8	4.8

FIGURE 28

Yield-time plot for iso-butane production at 256°C and at different pressures.

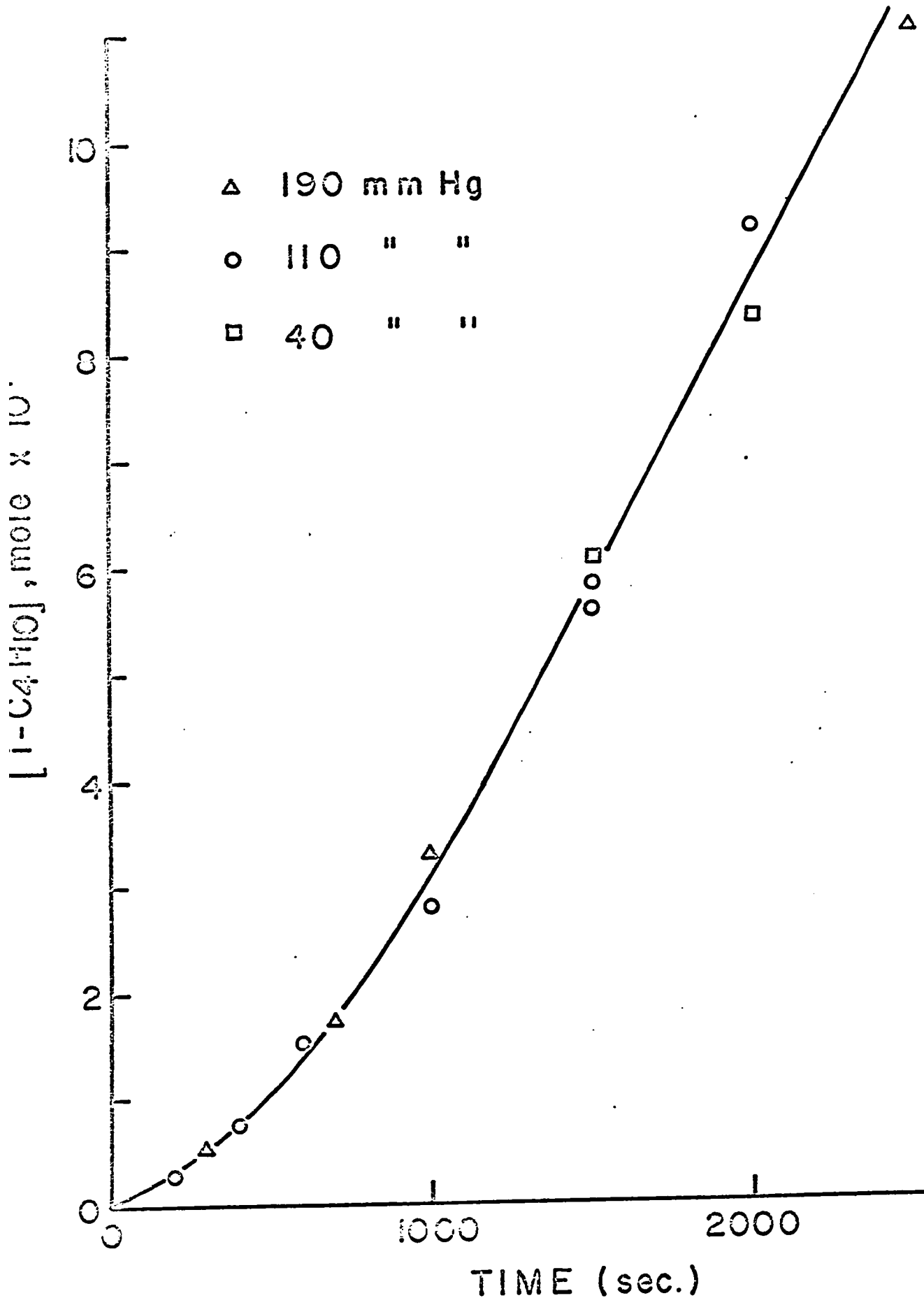
△ 190 mm Hg
○ 110 " "
□ 40 " "
[i-C4H10], mole x 10
0
2
4
6
8
10
0
1000
2000
TIME (sec.)

FIGURE 29

Yield-time plot for iso-butane production at 310°C and at different pressures.

A higher than 54 mm Hg

B 40 mm Hg

C 24 mm Hg

D 16 mm Hg

E 7 mm Hg

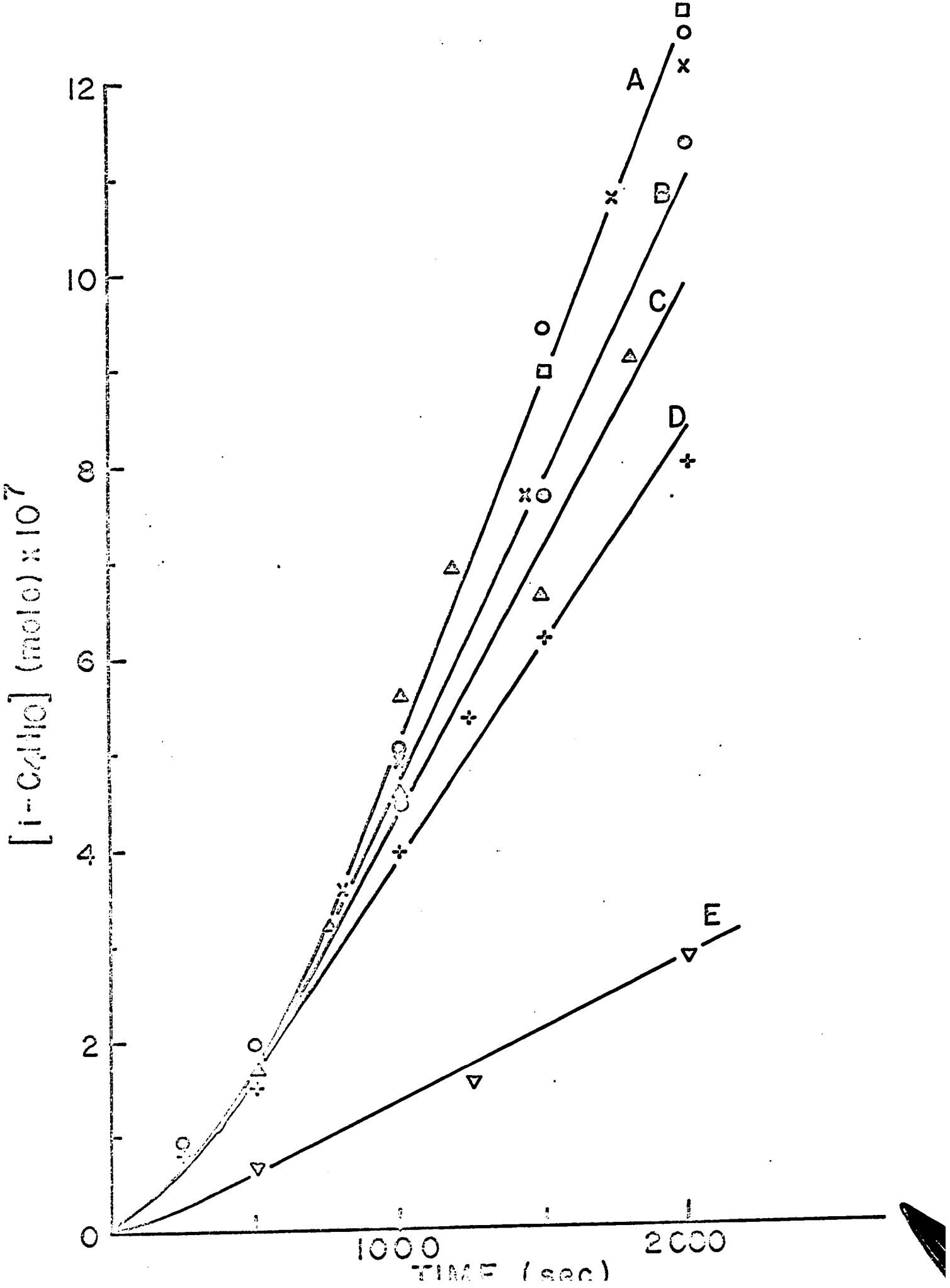
[i-C4H10] (mole) x 10^7
TIME (sec)
0
2
4
6
8
10
12
1000
2000
A
B
C
D
E

FIGURE 30

The maximal rate of iso-butane production against pressure at temperature of 310°C.

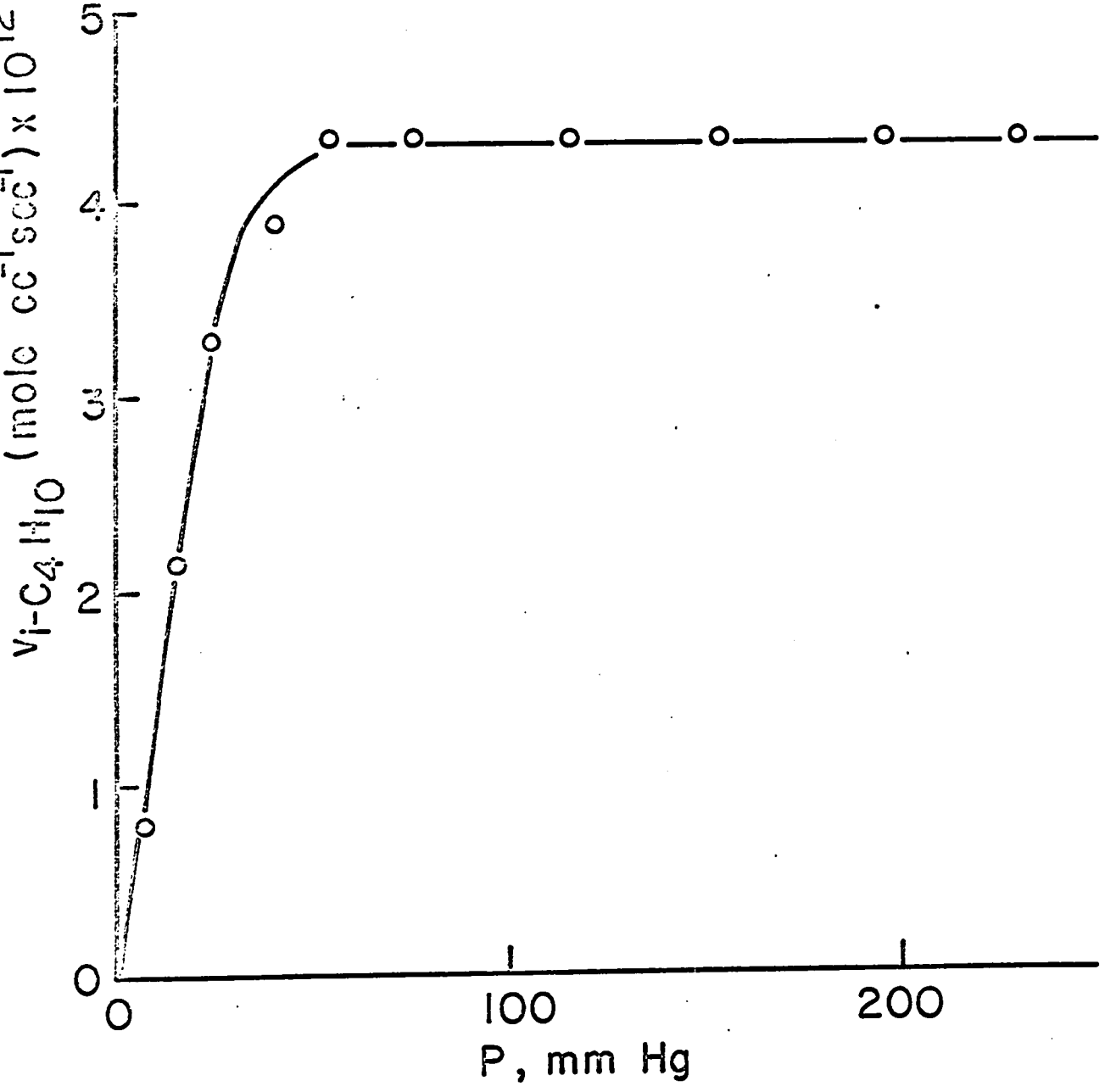
v_i-C_4H_{10} (mole $cc^{-1}sec^{-1}$) x 10^{12}
0
1
2
3
4
5
0
100
200
P, mm Hg

will decompose as the pressure is lowered. The maximal rates in regions of pressure independence for different temperatures are listed in Table IX. Plots of the logarithms of the maximal rates against the reciprocal of the temperature are shown in Figure 31. From the slope the activation energy is found to be 3.6 kcal/mole.

Typical yield-time plots for 2,2,3,3-TMB production are shown in Figure 32 for 256°C, and in Figure 33 for 310°C. The induction periods are increasing with decrease of temperature. Comparison with i-C_4H_{10} shows that in the case of 2,2,3,3-TMB the induction periods are longer at the same temperature. It was here only possible to obtain maximal rates, from the slopes in the linear regions of the yield-time plots. As is seen in Figure 33, at 310°C the decrease of the slope is observed at 24 mm Hg. The maximal rates in the region of pressure independence are listed in Table IX. A plot of the logarithm of the maximal rates against the reciprocal of the temperature is shown in Figure 34. The activation energy obtained is 2.8 kcal/mole.

Both of the values of the activation energy obtained, i.e., from the maximal rates i-C_4H_{10} and 2,2,3,3-TMB production, are in the region of activation energies of H atom additions to olefins. The higher values in the case of i-C_4H_{10} is probably caused by the fact that some of the i-C_4H_{10} is produced by an H abstraction reaction by t-C_4H_9 radicals from neopentane molecule.

TABLE IX

The maximal rates of iso-butane and 2,2,3,3-TMB production, and the k_d/k_c ratio at different temperatures

Temperature °C	iso-C_4H_{10} max. rate (mole cc^{-1} sec^{-1}) x 10^{12}	2,2,3,3-TMB	k_d/k_c
230	2.82	1.2	2.4
256	3.31	1.3	2.5
286	4.15	1.6	2.6
310	4.45	1.7	2.6

FIGURE 31

Plot of logarithm of maximal rate of i-C_4H_{10} production against reciprocal of temperature.

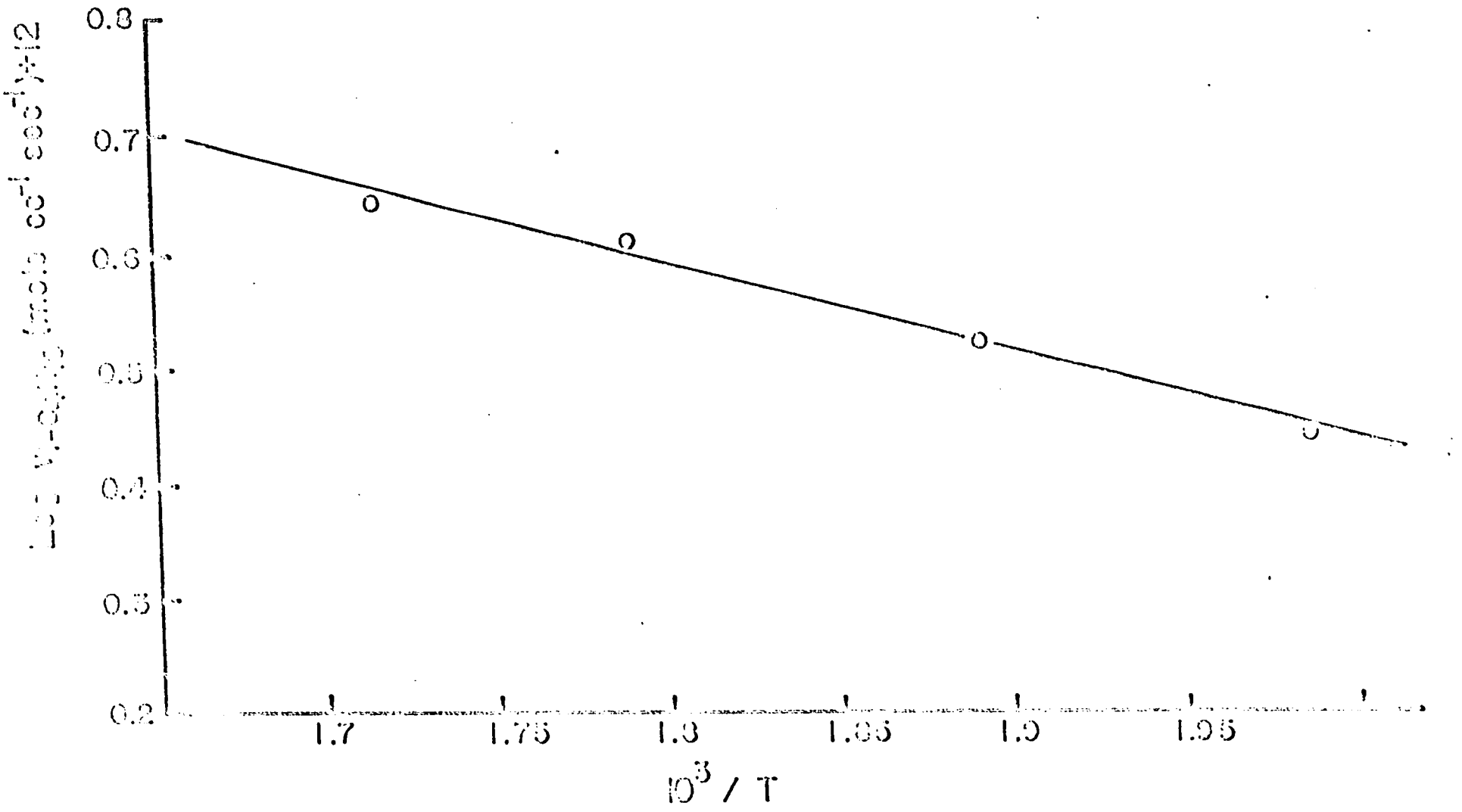
0.8
0.7
0.6
0.5
0.4
0.3
0.2
1.7
1.75
1.8
1.85
1.9
1.95
10^3 / T

FIGURE 32

Yield-time plot of 2,2,3,3-TMB at 256°C.

ooo 40 mm Hg

xxx 115 mm Hg

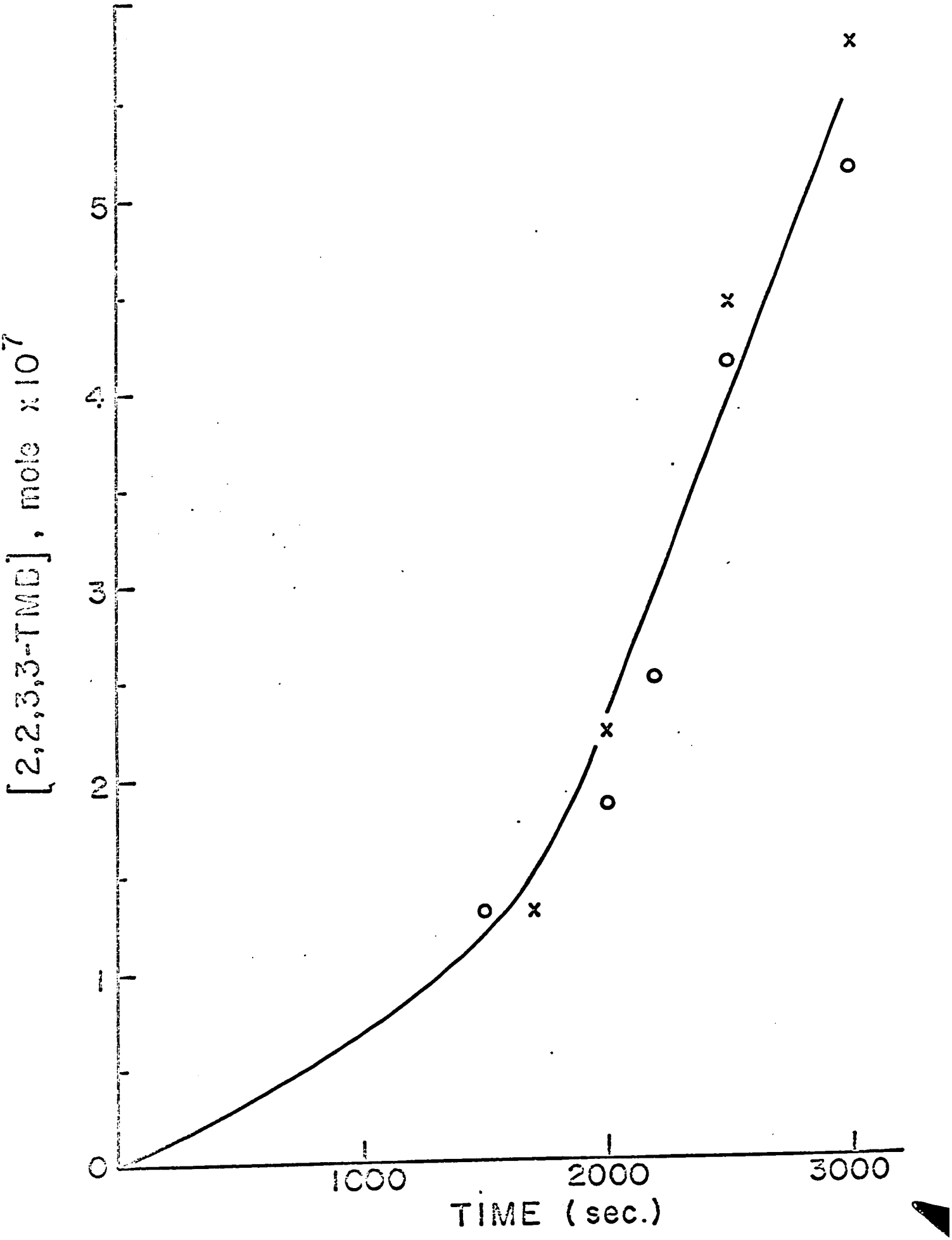
[2,2,3,3-TMB], mole x 10^7
0
1
2
3
4
5
1000
2000
3000
TIME (sec.)

FIGURE 33

Yield-time plot of 2,2,3,3-TMB production at different pressures and at 310°C.

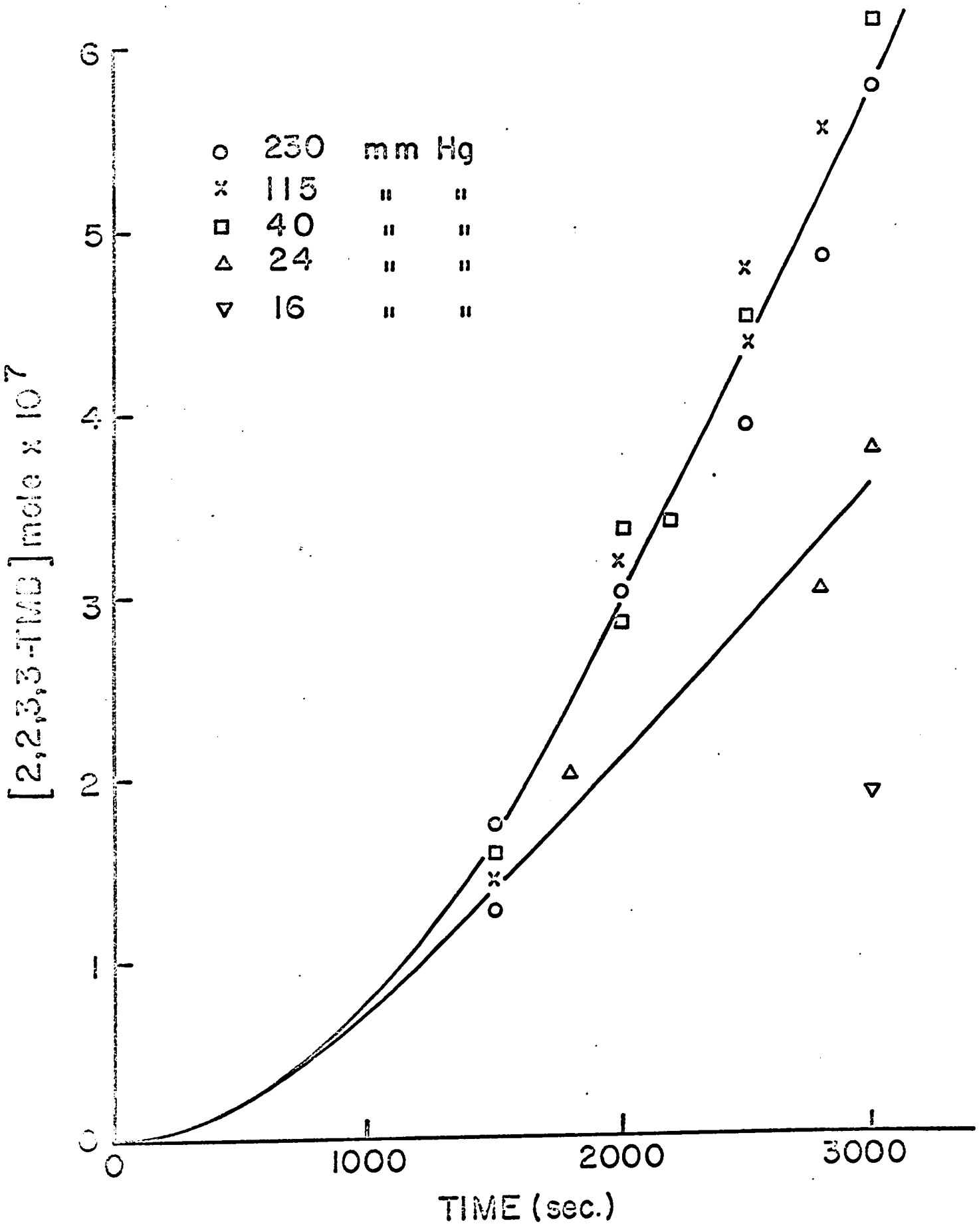
o 230 mm Hg
× 115 " "
□ 40 " "
△ 24 " "
▽ 16 " "
[2,2,3,3-TMB] mole x 10^7
0
1
2
3
4
5
6
1000
2000
3000
TIME (sec.)

FIGURE 34

Plot of logarithm of maximal rate of 2,2,3,3-TMB production against reciprocal of temperature.

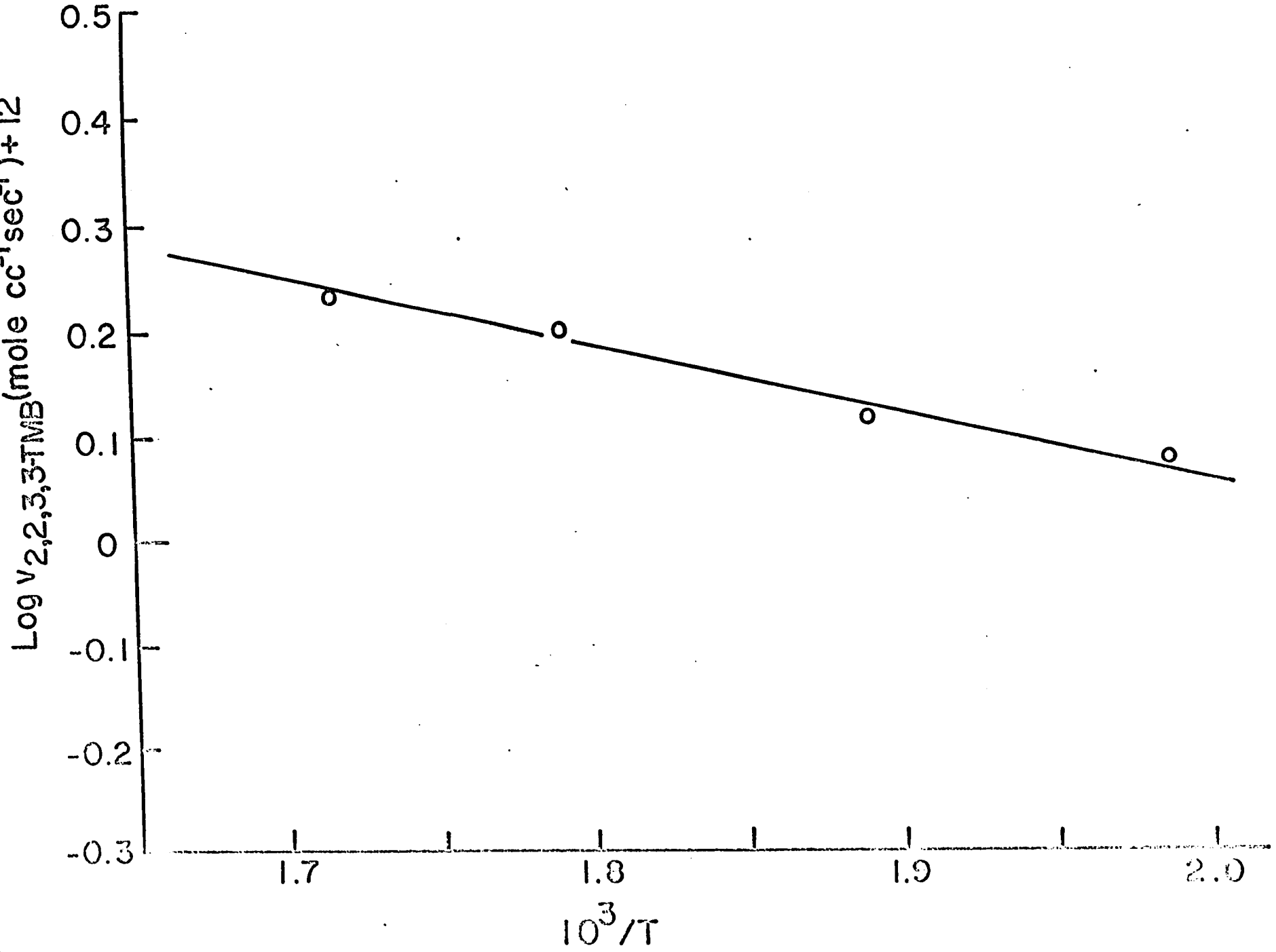
0.5
0.4
0.3
0.2
0.1
0
-0.1
-0.2
-0.3
Log $V_{2,2,3,3\text{-TMB}}$(mole $cc^{-1}sec^{-1}$)+ 12
1.7
1.8
1.9
2.0
$10^3/T$

From the maximal rates for i-C_4H_{10} and 2,2,3,3-TMB production it is possible to obtain some information concerning the disproportionation/combination ratio (k_d/k_c) of t-C_4H_9 radicals:

$$\frac{v_{i\text{-}C_4H_{10}}}{v_{2,2,3,3\text{-TMB}}} = \frac{k_d}{k_c}$$

The ratios for different temperatures are summarized in Table IX. The values are affected by H abstraction of t-C_4H_9 radicals. As was discussed previously, a limited accuracy of analysis of 2,2,3,3-TMB can be also responsible for a certain error in the determination of the ratio. Listed values of the k_d/k_c ratio for t-C_4H_9 radicals in the literature (27) are in the region of 2 to 7.4; thus the present values agree better with the low values previously obtained.

Production of 2,2,4,4-TMP

A typical yield-time plot for the production of 2,2,4,4-TMP is shown in Figure 35. The yield decreases with increase of temperature, the maximal yield being observed at 230°C. Little 2,2,4,4-TMP was found at 286°C and none at 310°C. As was seen in the preceding chapter, qualitatively the same behaviour was also noticed with dineopentyl.

Production of Ethylene, Propylene and Propane

Typical yield-time plots for ethylene, propylene and propane are shown in Figures 36, 37 and 38. The plots for

FIGURE 35

Yield-time plot of 2,2,4,4-tetramethyl pentane production at different pressures and temperature..

A 230°C

B 286°C

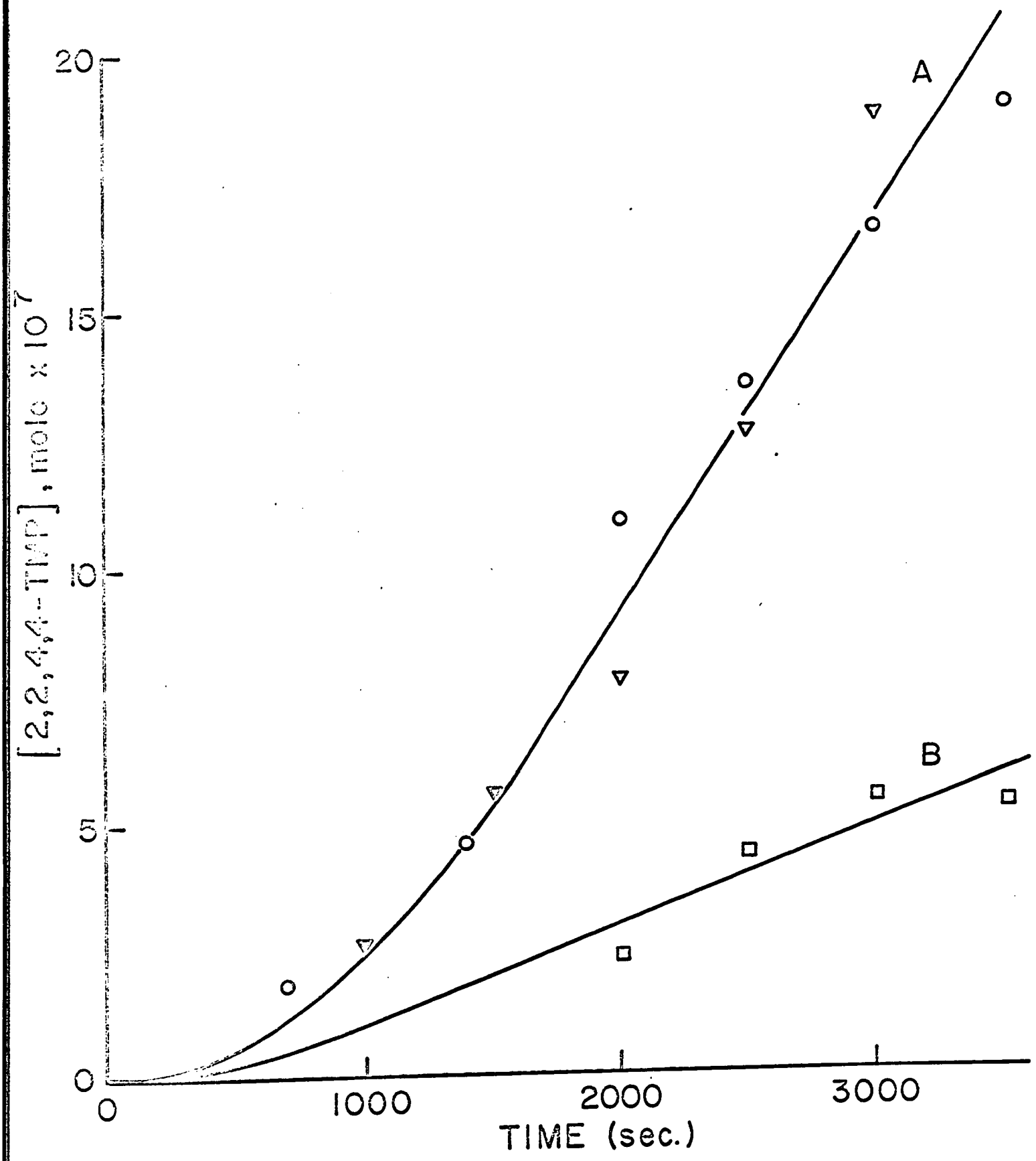
20
15
10
5
0
0
1000
2000
3000
TIME (sec.)
[2,2,4,4-TMP], mole x 10⁷
A
B

FIGURE 36

Yield-time plot for ethylene production at 310°C and pressures of 40 and 115 mm Hg.

ooo 40 mm Hg

xxx 115 mm Hg

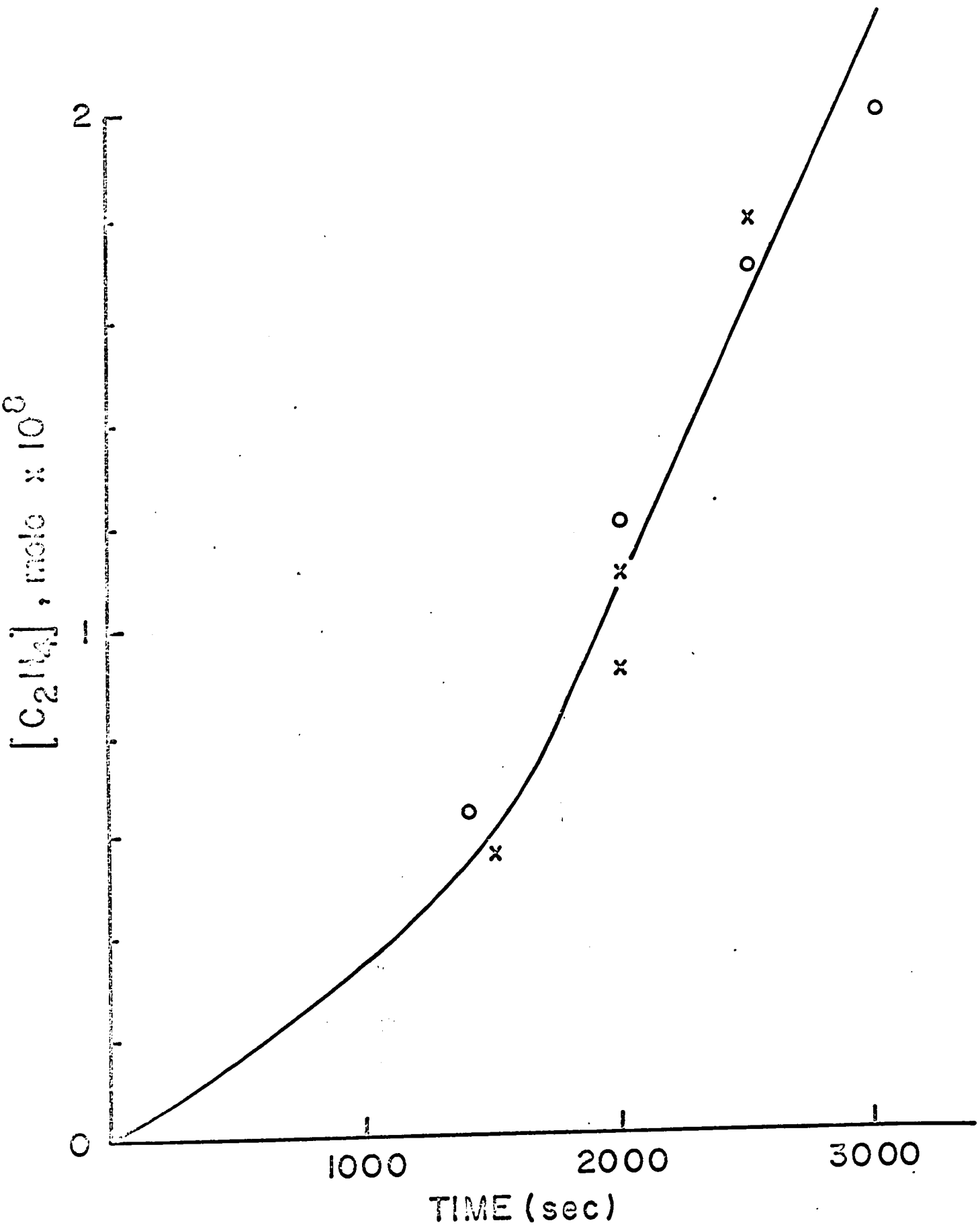
2
1
0
$[C_2H_4]$, mole $\times 10^3$
1000
2000
3000
TIME (sec)

FIGURE 37

Yield-time plot for propane production at 310°C and pressures of 40 and 115 mm Hg.

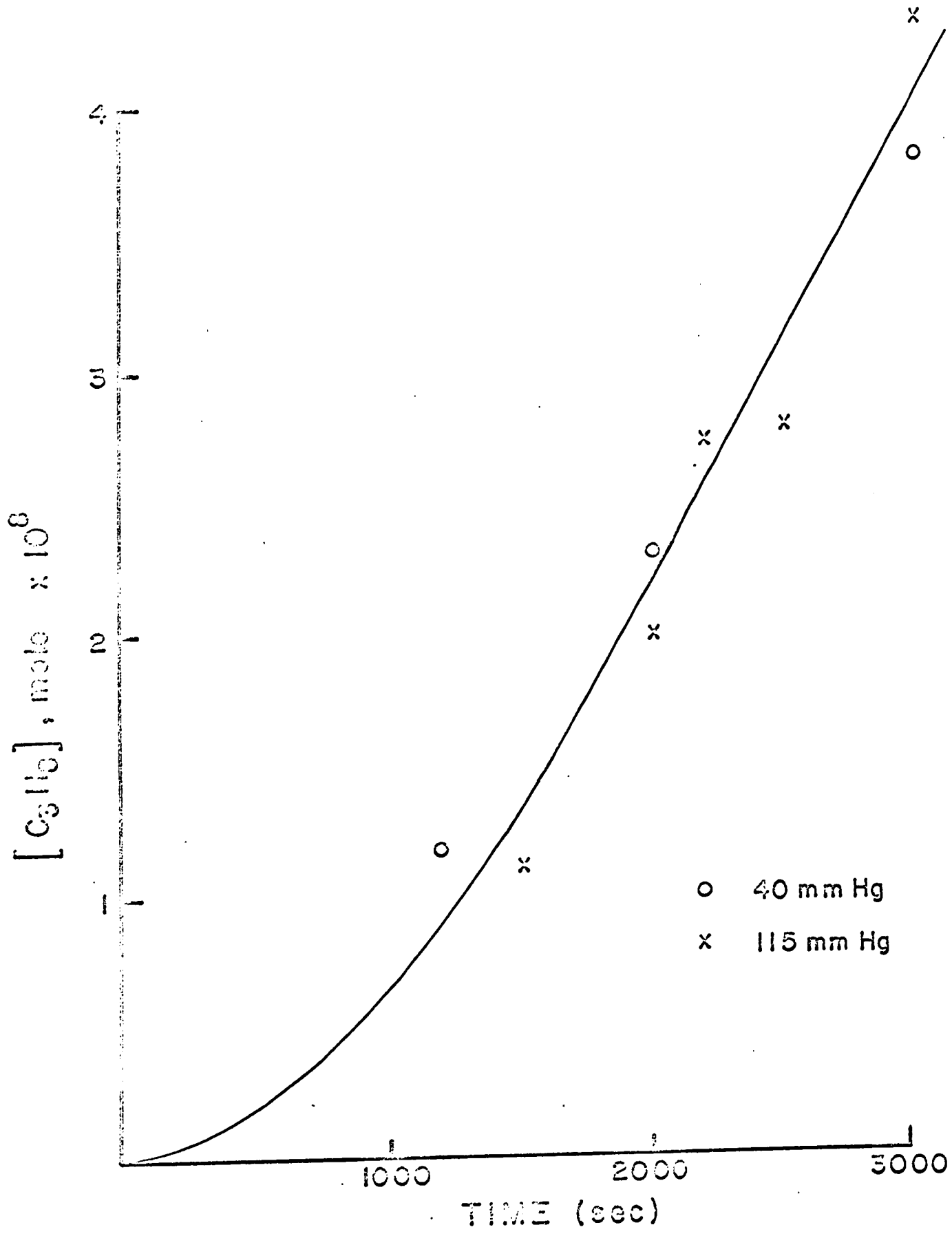
$[C_3H_8]$, mole $\times 10^3$
4
3
2
1
1000
2000
3000
TIME (sec)
o 40 mm Hg
x 115 mm Hg

FIGURE 38

Yield-time plot for propylene production at 310°C and pressures of 40 and 115 mm Hg.

ooo 40 mm Hg

xxx 115 mm Hg

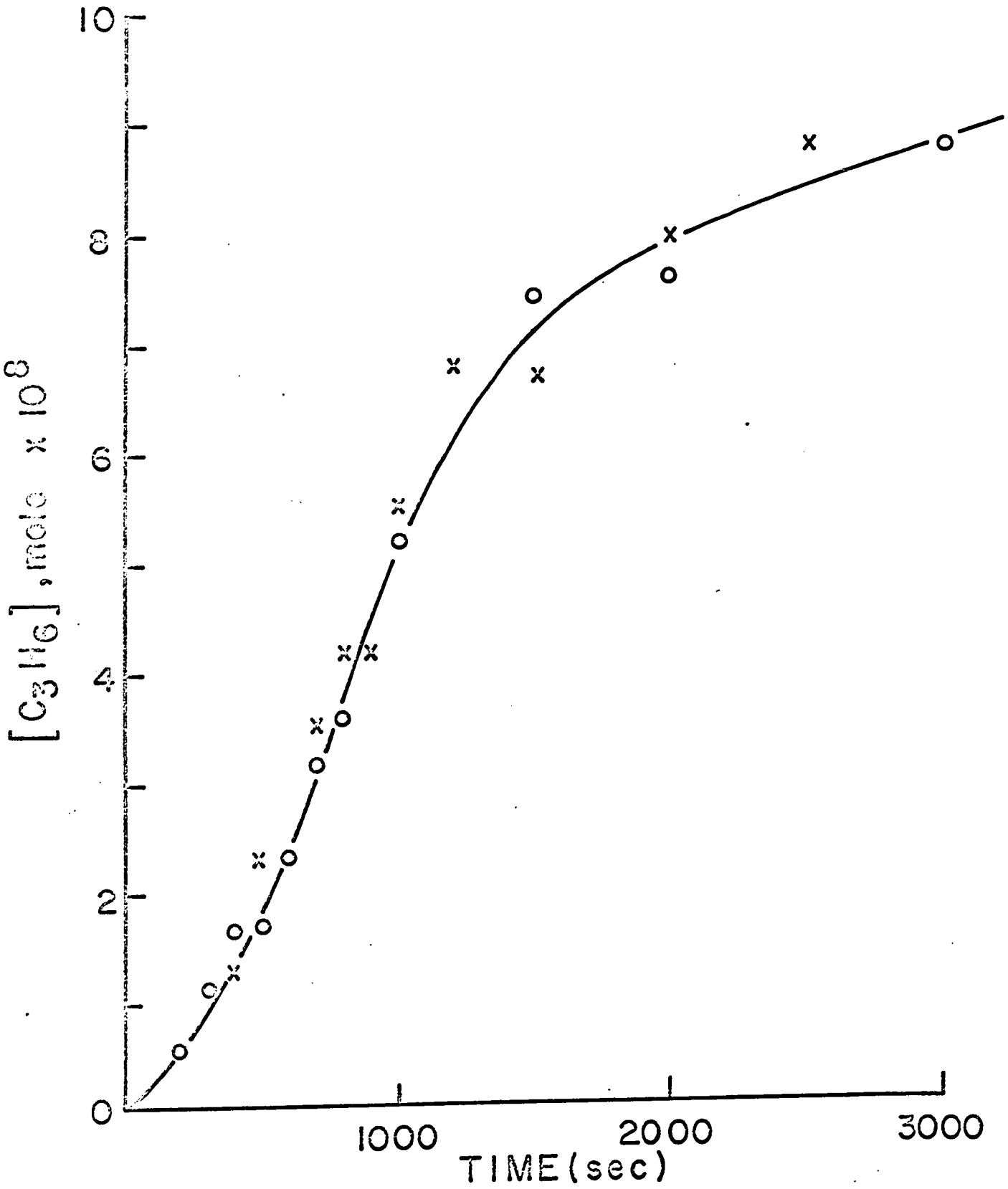
10
8
6
4
2
0
$[C_3H_6]$, mole x 10^8
1000
2000
3000
TIME (sec)

ethylene and propane are for 310°C, because only small amounts of these products were formed at lower temperatures, and the results were not reproducible. Induction periods for these are well established at this temperature. For C_3H_6 it was possible to obtain the plot also at lower temperatures. The plot is S-shaped owing to the fact that C_3H_6 is at first formed in a secondary reaction and later undergoes another reaction (addition of H atoms), resulting in its removal.

In high conversion experiments several very small peaks were observed for C_5 and C_6 hydrocarbons. Analyses of these peaks were not reproducible.

CLAIMS TO ORIGINAL RESEARCH

1. The kinetics of the mercury-photosensitized decomposition of neopentane were studied over the pressure range up to 280 mm Hg and at temperatures of 320°, 256°, 286°, 310° and 335°C.

2. The pressure dependence of the first-order coefficient for the unimolecular decomposition of neopentyl radicals was studied over the pressure range.

3. The limiting high-pressure and low-pressure Arrhenius parameters and activation energies for the decomposition of the neopentyl radicals were obtained from the temperature and pressure studies.

4. The pressure dependence of the rate coefficient for the combination of methyl radicals was examined in the study of the mercury-photosensitized decomposition of neopentane.

5. The frequency factor and the activation energy for the hydrogen abstraction from neopentane by methyl radicals was obtained from the present study.

6. By the use of the present results the C-C bond dissociation energy in the neopentyl radical was calculated. The standard enthalpy of formation of the neopentyl radical, and the C-H bond dissociation energy in the neopentane molecule, have been obtained. The entropy

change of the decomposition of the neopentyl radical into CH_3 and i-C_4H_8 was derived. The entropy of activation for the unimolecular decomposition of neopentyl radicals was estimated, and showed that there is a stiff activated state.

7. The formation of the energized radicals and the mechanism of the secondary reactions occurring in the system were investigated.

8. On the basis of the secondary reactions occurring, some approximate information concerning the disproportionation/combination ratio of t-C_4H_9 radicals was obtained. Also, the approximate relative amount of addition of hydrogen atoms to i-C_4H_8 leading to t-C_4H_9, with respect to that of i-C_4H_9 radicals, was calculated.

REFERENCES

1. E. W. R. Steacie, Atomic and Free Radical Reactions, Reinhold Publishing Corp., New York, 1954.
2. J. G. Calvert and J. N. Pitts, Jr., Photochemistry, John Wiley and Sons, N.Y., 1966.
3. R. J. Cvetanovic, Mercury Photosensitized Reactions, In Progr. Reaction Kinetics, Vol. 2, Ed. G. Porter, Pergamon Press, 1964.
4. H. E. Gunning and O. P. Strausz, Advances in Photochemistry, Vol. 1, 209, Ed. W. A. Noyes, Jr., G. S. Hammond and J. N. Pitts, Intersci. Publ., John Wiley and Sons, N.Y., 1963.
5. L. F. Loucks and K. J. Laidler, Can. J. Chem., 45, 2763 (1967).
6. L. F. Loucks and K. J. Laidler, Can. J. Chem., 45, 2767 (1967).
7. L. F. Loucks, Can. J. Chem., 45, 2775 (1967).
8. L. F. Loucks and K. J. Laidler, Can. J. Chem., 45, 2795 (1967).
9. M. M. Papic and K. J. Laidler, Can. J. Chem., 49, 535 (1971).
10. M. M. Papic and K. J. Laidler, Can. J. Chem., 49, 549 (1971).
11. B. de B. Darwent and E. W. R. Steacie, Can. J. Res., B 27, 181 (1949).
12. R. J. Norstrom, O. P. Strausz and H. E. Gunning, Can. J. Chem., 42, 2140 (1964).
13. S. Sato and S. Tsunashima, Bull. Chem. Soc., Japan, 37, 543 (1964).

14. R. A. Holroyd and G. W. Klein, J. Phys. Chem., 67, 2273 (1963).

15. S. G. Lias and P. Ausloos, J. Chem. Phys., 43, 2748 (1965).

16. K. H. Anderson and S. W. Benson, J. Chem. Phys., 43, 3747 (1964).

17. J. Engel, A. Combe, M. Letort and M. Niclause, Compt. Rend., 244, 453 (1957).

18. F. Baronnet, M. Dzierzynski, G. M. Come, R. Martin and M. Niclause, Int. J. Chem. Kin., 3, 197 (1971).

19. W. Tsang, J. Chem. Phys., 44, 4282 (1966).

20. M. M. Papic, Ph.D. Thesis, University of Ottawa, 1970.

21. G. B. Kistiakowsky and E. K. Roberts, J. Chem. Phys., 21, 1637 (1953).

22. R. E. Dodd and E. W. R. Steacie, Proc. Roy. Soc. (London), A 223, 283 (1954).

23. S. Toby and B. H. Weiss, J. Phys. Chem., 68, 2492 (1964).

24. J. Grotewold, E. A. Lissi and M. G. Neumann, J. Chem. Soc. (A), 375 (1968).

25. F. Casas, C. Previtali, J. Grotewold and E. A. Lissi, J. Chem. Soc. (A), 7, 1001 (1970).

26. L. F. Loucks, Ph.D. Thesis, University of Ottawa, 1967.

27. A. F. Trotman-Dickenson and G. S. Milne, Tables of Bimolecular Gas Reactions, NSRDS-NBS9, 42, 1967.

28. J. A. Kerr and D. Timlin, J. Chem. Soc. (A), 1241 (1969).

29. B. S. Rabinovitch and D. W. Setser, Advances in Photochemistry, Vol. 3, 1964.

30. E. W. Schlag and B. S. Rabinovitch, J. Am. Chem. Soc., 82, 5996 (1960).

31. A. Shepp, J. Chem. Phys., 24, 939 (1956).

32. H. E. O'Neal and S. W. Benson, Kinetic Data on Gas-Phase Unimolecular Reactions, NSRDS-NBB, U.S.

33. J. G. Calvert and J. N. Pitts, Jr., Photochemistry, p.815-820.

34. J. A. Kerr and A. C. Lloyd, Quarterly Reviews, 22, 549 (1968).

35. F. D. Rossini et al., Selected Values of Physical and Thermodynamic Properties of Hydrocarbons and Related Compounds, API, Carnegie Press, Pittsburg, 1953.

36. J A N A F Interim Thermochemical Tables, Dow Chemical Company, Midland, Michigan.

37. R. J. Cvetanovic, W. E. Falconer and K. R. Jennings, J. Chem. Phys., 33, 1225 (1961).

38. K. R. Jennings and R. J. Cvetanovic, J. Chem. Phys., 35, 1233 (1961).

39. B. S. Rabinovitch and R. W. Diesen, J. Chem. Phys., 30, 735 (1959).

40. B. S. Rabinovitch, D. H. Dills, W. H. McLain and J. H. Current, J. Chem. Phys., 32, 493 (1960).

41. W. J. Moore and L. A. Wall, J. Chem. Phys., 17, 1325 (1949).

42. P. J. Boddy and J. C. Robb, Proc. Roy. Soc., A 249, 233 (1959).

43. W. M. Jackson, J. R. Nesby and B. deB. Darwent, J. Chem. Phys., 37, 2256 (1962).

44. A. S. Gordon and J. R. Nesby, J. Chem. Phys., 33, 1882 (1960).

45. M. C. Lin and K. J. Laidler, Can. J. Chem., 44, 2927 (1966).

46. M. C. Lin and K. J. Laidler, Can. J. Chem., 45, 1315 (1967).

47. R. J. Cvetanovic, Addition of Atoms to Olefines in the Gas Phase, in Advances in Photochemistry, Vol. 1, 115, (1963).

48. J. N. Bradley, H. W. Melville and J. C. Robb, Proc. Roy. Soc. (London), A 236, 339 (1956).

END O

REEL